International
Progress Report

IPR-05-05

Äspö Hard Rock Laboratory

The MICROBE framework

Site descriptions, instrumentation, and characterisation

Karsten Pedersen

Göteborg University

February 2005

Svensk Kärnbränslehantering AB
Swedish Nuclear Fuel
and Waste Management Co
Box 5864
SE-102 40 Stockholm Sweden
Tel 08-459 84 00
+46 8 459 84 00
Fax 08-661 57 19
+46 8 661 57 19

Äspö Hard Rock
Laboratory

Report no.
IPR-05-05

No.
F82K

Author
Karsten Pedersen

Date
2005-02-25

Checked by

Date

Approved
Anders Sjöland

Date
2005-03-02

Äspö Hard Rock Laboratory

The MICROBE framework

Site descriptions, instrumentation, and characterisation

Karsten Pedersen

Göteborg University

February 2005

Keywords: Biofilm, Laboratory, Microorganisms, Gas, Hydrogeology, Biocorrosion, Redox, immobilisation, Mobilization

Abstract

Micro-organisms interact with their surroundings, and commonly have a significant effect on the geochemical record. Microbial processes could thus significantly influence the functioning of any future high-level radioactive waste repository. The limitations of investigations of this matter carried out at ground surface level have motivated the establishment of sites for microbiological investigation in the Äspö Hard Rock Laboratory (HRL) tunnel. The multi-disciplinary research conducted at sites operating within the MICROBE framework combines microbial physiology, ecology, and molecular biology with nuclear chemistry, geochemistry, and geology in exploring how microbial processes may influence the repository and migration of radionuclides. The main site connected with the MICROBE framework is a laboratory situated at the 450-m level of the HRL; at this site three boreholes have been drilled, equipped with packers, and connected to the tunnel with tubing. Several other sites along the tunnel have also been in use since start of the framework. This report describes the sites, as well as their instrumentation and characterization. Scientific results will be published separately. The major objectives for the MICROBE framework are to provide *in situ* conditions for studying the bio-mobilization of radionuclides, to present a range of conditions relevant to the study of the bio-immobilization of radionuclides, to provide the proper circumstances for research into the effect of microbial activity on the long-term geochemical stability of the repository environment, and to enable investigations of bio-corrosion of copper under conditions relevant to a high-level radioactive waste repository. Finally, the main site at the 450-m level is an excellent reference for the site investigations.

Seven activities have been carried out within the MICROBE framework. The first concerned the development and installation of circulation systems for the study of microbial biofilm processes. In support of this activity, the hydrological characteristics of the packed-off sections, KJ0050F01, KJ0052F01 and KJ0052F03, were determined. Research into the immobilization of trace elements on biological iron oxides (BIOS) and on microbial biofilms is ongoing as well. A system for the extraction and analysis of gases dissolved in groundwater has been developed and installed. The influence of micro-organisms on the reducing capacity of granitic rock environments is being studied, mainly at the 450-m level, as is the microbial mobilization of trace elements from mineral surfaces.

Sammanfattning

Mikroorganismer samverkar med sin omgivning, och de har ofta en stor inverkan på geokemiska parametrar. Mikrobiella processer kan således på ett betydande vis påverka funktionen i ett framtida förvar för högaktivt radioaktivt avfall. Konceptuella begränsningar i undersökningar av sådana processer på markytan har motiverat etablering av forskningsplatser under jord i Äspölaboratoriets tunnlar. Multi-disiplinärt forskningsarbete utförs på flera platser inom det ramverk som utgörs av MICROBE. Där kombineras forskning om mikrobiell fysiologi, ekologi och molekylär biologi med kärnkemi, geokemi och geologi. Forskningen inriktas på hur mikrobiella processer kan påverka ett slutförvar och migration av radionuklider. Huvudplatsen inom MICROBE är ett laboratorium som ligger på 450 m djup. Här har tre borrhål tagits upp in till vattenförande sprickor som utrustats med packers och förbundits via rör med tunneln. Ytterligare tre andra platser i Äspötunneln utnyttjas, eller har utnyttjats, inom MICROBE sedan start. Rapporten beskriver forskningsplatserna samt deras instrumentering och karaktärisering. De vetenskapliga resultaten publiceras separat.

Huvudmålen för MICROBE är att skapa *in situ* förhållanden för forskning om bio-mobilisering av radionuklider, att erbjuda en serie möjligheter relevanta för undersökningar kring bio-immobilisering av radionuklider, att skapa relevanta förhållanden för forskning om vilka effekter mikrobiella processer kan ha på förvarets långsiktiga geokemiska stabilitet, samt att möjliggöra experiment kring bio-korrosion av koppar under förvarsrelevanta förhållanden. Slutligen utgör huvudplatsen inom MICROBE på 450 m djup en utmärkt referens för platsundersökningarna, där metoder och koncept först utprovas.

Sju aktiviteter genomförs inom MICROBEs ramverk. Den första var utveckling och installation av cirkulationssystem för undersökningar av mikrobiella biofilmprocesser. Som stöd till denna aktivitet genomfördes en hydrologisk karakterisering av de avpackade formationerna, KJ0050F01, KJ0052F01 and KJ0052F03. Forskning om immobilisering av spårelement på biologiska järnoxider (BIOS) och på mikrobiella biofilmer pågår. Ett system för analys av lösta gaser i grundvatten har installerats på 450 m nivån. Mikrobiell påverkan på den reducerande kapaciteten i grantiska akviferer studeras också på 450 m nivån. Där undersöks samtidigt om mikrobiella processer kan mobilisera spårmetaller från mineralytor.

Contents

1 The MICROBE framework 9
1.1 Introduction 9
1.2 Background 9
1.3 Microbial processes 10
1.3.1 Bio-immobilization of radionuclides 11
1.3.2 Bio-mobilization of radionuclides 12
1.3.3 Microbial effects on the chemical stability of deep groundwater environments 12
1.3.4 Microbial corrosion of copper 13
1.4 Objectives 13
1.5 Site locations in the Äspö Hard Rock Laboratory 14
1.6 Aim of this report 15

2 Site descriptions and instrumentation 17
2.1 The sulphur sites 17
2.1.1 The 1127B pond 17
2.2 The BIOS sites 19
2.2.1 The 907A ditch 19
2.2.2 The 2200-m BIOS site 19
2.3 The MICROBE 450 m site and laboratory 21
2.3.1 Drilling and instrumentation of the MICROBE 450-m boreholes 22
2.3.2 Instrumentation of the MICROBE 450-m boreholes 24
2.3.3 The laboratory container 26
2.3.4 Circulation systems for *in situ* investigations 26
2.3.5 Hydrological characteristics of the intersected and circulated fractures 30
2.3.6 Anaerobic box 35
2.3.7 Gas chromatograph 35
2.3.8 Gas extractor 35
2.3.9 ATP analysis 37
2.3.10 Remote monitoring and control 38
2.4 Groundwater characterization 38
2.4.1 Groundwater chemistry and stable isotopes 38
2.4.2 Gas composition 42
2.4.3 Stable isotopes 42

3 Evaluation of the MICROBE-450 site characteristics 43
3.1 Geochemistry 43
3.1.1 Principal component analysis 43
3.1.2 Physical and chemical parameters 45
3.1.3 Laboratory analysis of dissolved gases 45
3.1.4 Calibration of the gas chromatograph 50
3.1.5 *In situ* measurements of carbon-containing gases and hydrogen 50
3.2 Microbiology 57
3.2.1 Total number of micro-organisms in groundwater 57
3.2.2 Biomass-ATP 57
3.2.3 Total number of micro-organisms on flow-cell surfaces 57
3.2.4 Most probable number of metabolic groups 64

4 References 71

5 Appendix 1: Expansion vessel 73
5.1 Schematic drawing 73
5.2 Construction drawing, dimensions in mm. 74

6 Appendix 2: Flow cell 75
6.1 The flow-cell tube and diffusers, dimensions in mm. 75
6.2 Holders for diffusers, dimensions in mm. 76
6.3 Diffusers, dimensions in mm. 77
6.4 Inlet/outlet of flow cell, dimensions in mm. 78
6.5 Test pile with the u-shaped lock tool for sampling (lower right) , dimensions in mm. 79
6.6 Check list for sampling cabinet flow cells at MICROBE 80

7 Appendix 3: Gas extractor 81
7.1 Schematic drawing 81
7.2 Extractor cylinder, dimensions in mm. 82
7.3 Extractor piston, dimensions in mm. 83
7.4 Cryo trap, CO_2 container. 84
7.5 Cryo trap, lid, dimensions in mm. 85

1 The MICROBE framework

1.1 Introduction

The MICROBE framework comprises seven activities of various scopes, as indicated by the following activity plan titles:

AP-TD-F82-02-013: Development and installation of a circulation system (in Swedish)

AP-TD-F82-02-014: Determination of the hydrological characteristics of the packed-off sections, KJ0050F01, KJ0052F01 and KJ0052F03 (in Swedish)

AP-TD-F82-02-015: Immobilization of trace elements on biological iron oxides (BIOS) (in Swedish)

AP-TD-F82-02-016: Immobilization of trace elements on microbial biofilms (in Swedish)

AP-TD-F82-02-017: Development and installation of a system for the extraction and measurement of gases (in Swedish)

AP-TD-F82-02-018: The influence of micro-organisms on the reducing capacity of granitic rock environments (in Swedish)

AP-TD-F82-02-019: Microbial mobilization of trace elements from surfaces and minerals (in Swedish)

Activities 13, 14, and 17 have been finalized and are reported here; activities 15 and 16 will be completed and published separately in 2005. Activities 18 and 19 will take the longest to complete, running until mid 2007.

1.2 Background

Micro-organisms interact with their surroundings, and commonly have a significant effect on the geochemical record. Microbial processes could thus significantly influence the functioning of any future high-level radioactive waste repository (Pedersen, 2002). The study of microbial processes in the laboratory can yield valuable information about possible microbial effects on such a repository. However, the effects suggested by laboratory studies must be tested in a repository-like environment for several reasons. First, at repository depth, hydrostatic pressure approaches 50 bars, a level that is very difficult to reproduce in the microbiology laboratory. Such high pressure influences chemical equilibria and the amount of gas that can be dissolved. Second, the geochemical environment of deep groundwater, on which microbial life depends, is complex. Dissolved salts and trace elements, and in particular the redox chemistry and carbonate system, are characteristics that are very difficult to mimic in a research laboratory located on the ground surface level. Third, natural ecosystems, such as those in deep groundwater, comprise many different species in various mixes (Pedersen, 2001); the surface-level laboratory, however, is best suited for studies of pure cultures. Therefore, the effect of processes arising from many contributing species in natural ecosystems cannot easily be investigated there.

The aforementioned limitations of surface-level investigations motivated the establishment of microbiological investigation sites in the Äspö Hard Rock Laboratory (HRL) tunnel. The main site is the MICROBE laboratory at the 450-m level, but several other sites along the tunnel have been in use since start of MICROBE.

1.3 Microbial processes

Microbial processes can significantly alter the mobility of radionuclides in the environment. The multi-disciplinary research conducted at sites operating within the MICROBE framework combines microbial physiology, ecology, and molecular biology with nuclear chemistry, geochemistry, and geology in exploring how microbial processes may influence the repository and migration of radionuclides.

Table 1-1. Microbial processes can directly or indirectly influence retention of radionuclides in several ways. The most important variables in such processes are the state of attachment (i.e. whether the microbes are attached or unattached) and whether the microbes are metabolically active or dormant and inactive.

Microbial processes that influence radionuclide migration	Microbes in this process are in the following state(s):		This action of this microbial process on radionuclides is:		This process requires an active microbial energy-driven metabolism:	
	Planktonic	Biofilm	Direct	Indirect	Yes	No
Immobilization processes						
Biosorption		X	X			X
Bioaccumulation		X	X		X	
Biotransformation	X	X	X		X	
Biomineralization	X	X		X	X	
Metabolic redox reactions	X	X		X	X	
Mobilization processes						
Biosorption	X		X			X
Bioaccumulation	X		X		X	
Production of complexing agents	X	X	X		X	

Table 1-1 and Figure 1-1 summarise the microbial processes that can influence the speciation and thereby the migration behaviour of radionuclides. Microbial processes can have either immobilizing or mobilizing action, depending on the type of process and the state of the microbes involved. Microbes in biofilms will, with the exception of those which produce complexing agents, be immobilizing. Planktonic cells that biosorb or bioaccumulate radionuclides will have a mobilizing effect on radionuclides. These processes can act directly or indirectly in affecting radionuclide transport in the geosphere. Direct action involves contact between a microbe and the radionuclide, with a resulting change in radionuclide speciation. Indirect action is caused by changes in the environment generated by microbial metabolism, which in turn influence radionuclide behaviour. Finally, all microbial processes except biosorption require an active, energy-driven metabolism. The modelling of microbial processes, therefore, must include a

proper understanding of microbial energy turnover rates in deep rock aquifers. All processes presented in Table 1 are being or will be investigated to various degrees of detail within the framework of the MICROBE research project. The emphasis is on their importance for understanding geosphere mobilization and immobilization phenomena in the safety assessment of radioactive waste disposal. They are briefly introduced below.

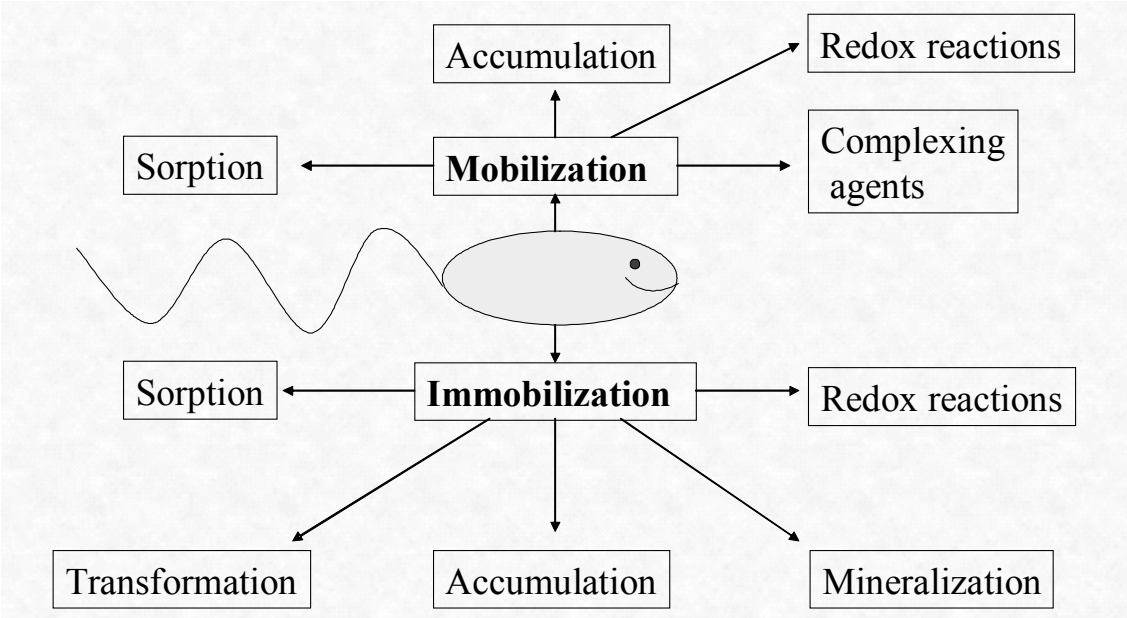

Figure 1-1. *Schematic representation of microbial processes that may influence radionuclide migration.*

1.3.1 Bio-immobilization of radionuclides

Biosorption

The term biosorption (Table 1-1) is used to describe the metabolism-independent sorption of heavy metals and radionuclides to biomass, i.e. microbial cells. Biosorption can be summarized as the sorption and accumulation of trace elements to the surface of microbial cells. Both living and dead biomass are capable of biosorption, and the ligands involved in metal binding include carboxyl, amine, hydroxyl, phosphate, and sulphydryl reactive groups on the cell wall.

Microbe numbers as high as 10^{11} cells/m^2 have been reported in biofilms in Fennoscandian shield rock groundwater (Pedersen, 2001). Biofilm micro-organisms commonly excrete extra-cellular material supporting attachment, and this material also creates the three-dimensional shape of a growing biofilm. As this extra-cellular material is organic in nature, it adds a biosorption capacity to the cell's surfaces. In conclusion, biosorption to attached microbes in biofilms can have an immobilizing effect on radionuclides (Table 1-1). Very few *in situ* experimental data exist regarding the importance of biofilm biosorption processes in understanding geosphere retention phenomena in the safety assessment of radioactive waste disposal. In response to this lack, ongoing experiments (AP-TD-F82-02-016) within the MICROBE framework are attempting to elucidate these processes.

Bioaccumulation and biomineralization

A large group of microbes catalyse the formation of iron oxides from dissolved ferrous iron in groundwater that reaches an oxidizing environment (Ferris et al., 1999, 2000). Such biological iron oxides (BIOS) will have a retardation effect on many radionuclides. Typically, those microbes form stalks and sheaths that increase the volume of the iron oxides from densely packed inorganic oxides to a fluffy, rust-like material with a water content of up to 99%. The microbes contribute to the exposure of a large oxide area to trace elements flowing past in the groundwater; as well, the organic biological material has a strong retention capacity of its own, in addition to that of the iron oxides. The retention effect of BIOS (bioaccumulation and mineralization, Table 1-1) is being studied in the MICROBE framework (AP-TD-F82-02-015).

1.3.2 Bio-mobilization of radionuclides

Microbes need metals for their metabolism, as do multicellular living organisms, and both bacteria and microscopic fungi share this need. Such metals are often available only in small quantities or, as with iron in surface waters, are not bio-available at all due to low solubility under aerobic conditions. Therefore, microbes produce various kinds of chelating compounds to increase the bioavailability of essential elements needed for metabolism. These ligands are not always highly specific, and several of them will also mobilize other elements such as heavy metals and radionuclides. In the process of capturing the metal–ligand complex, microbes sort toxic metals from essential ones and expel the toxic elements back to the environment. The potential for the mobilization of radionuclides from repository environments by bacterially produced ligands is unknown; it is thus a concern in safety analysis that warrants exploration. This process has been investigated in the laboratory using micro-organisms isolated from the deep groundwaters of the Äspö Hard Rock Laboratory; *in situ* experiments (AP-TD-F82-02-019) will follow the laboratory experiments. Fungi have the ability to produce large amounts of complexing agents, for example, via fermentation processes. The presence of fungi in deep groundwaters has been noted in earlier work: a detailed survey of fungi found in Äspö groundwaters was performed by Ekendahl et al. (2003).

1.3.3 Microbial effects on the chemical stability of deep groundwater environments

Micro-organisms can have an important influence on the chemical conditions in groundwater (Haveman and Pedersen, 2002). In particular, they may execute reactions that stabilize the redox potential of groundwater at a low and thus beneficial level for the repository. It is hypothesized that hydrogen from deep geological processes contributes to the redox stability of deep groundwater via microbial turnover of this gas. Energy metabolisms of hydrogen, and possibly also of carbon monoxide and methane, generate secondary metabolites such as ferrous iron, sulphide, and organic carbon. The metabolic activity of these species lowers the redox potential and they will act so as to reduce possibly introduced oxygen. Circulation systems and analytical instrumentation for studying gas dissolved in groundwater have been installed at the deepest (450 m) MICROBE site (AP-TD-F82-02-018).

Microbial energy metabolism requires a reduced electron and energy donor and an oxidized electron acceptor (Table 1-2). The energy donor can be an organic or an inorganic compound. The electron acceptor is generally an inorganic compound, except in fermentation, where both the electron donor and electron acceptor are the same organic compound. Electron donors and acceptors can be combined in redox couples according to the difference in free energy. Any redox couple that releases energy via a reaction is a possible source of energy for microbes. The result of microbial harvesting of energy from redox couples is an oxidized donor and a reduced acceptor. Notably, microbial metabolism generally lowers the redox potential of the environment.

Table 1-2. The most common energy and electron donors and electron acceptors in microbial metabolism are summarized. The respective atom that donates or accepts one or several electrons is underlined.

Organic energy sources and electron donors		Inorganic energy sources and electron donors		Electron acceptors	
Reduced	**Oxidized**	**Reduced**	**Oxidized**	**Oxidized**	**Reduced**
Carbohydrates	$\underline{C}O_2$			$\underline{O_2}$	$H_2\underline{O}$
Amino acids	$\underline{C}O_2$	$\underline{N}H_4^+$	$\underline{N}O_3$	$\underline{N}O_3$	$\underline{N_2}$
Organic acids	$\underline{C}O_2$	$\underline{Mn}^{2+}$	$\underline{Mn}^{4+}$	$\underline{Mn}^{4+}$	$\underline{Mn}^{2+}$
Fat	$\underline{C}O_2$	$\underline{Fe}^{2+}$	$\underline{Fe}^{3+}$	$\underline{Fe}^{3+}$	$\underline{Fe}^{2+}$
		$H_2\underline{S}$	$\underline{S}O_4^{2-}$	$\underline{S}O_4^{2-}$	$H_2\underline{S}$
		$\underline{C}H_4$	$\underline{C}O_2$	$\underline{S}^0$	$H_2\underline{S}$
		$\underline{C}O$	$\underline{C}O_2$	$\underline{U}^{6+}$	$\underline{U}^{4+}$
		$\underline{H_2}$	$\underline{H_2}O$	$\underline{C}O_2$	$\underline{C}H_4$

1.3.4 Microbial corrosion of copper

The bio-corrosion, if any, of copper canisters can result from microbial sulphide production. Two important questions have been identified and studied within the MICROBE framework. Can sulphide-producing microbes survive and produce sulphide in the bentonite that surrounds the canisters? Can microbial sulphide production in the neighbouring rock exceed a performance safety limit? A series of laboratory and field experiments has indicated that the answers to both these questions are negative (Pedersen et al., 2000a-b). However, the results have been criticized for not accounting for natural conditions, such as high pressure and the natural population of sulphate-reducing bacteria in deep groundwater. This issue has now been studied under *in situ* conditions.

1.4 Objectives

The major objectives for the MICROBE sites are:

- To provide *in situ* conditions for studying the bio-mobilization of radionuclides,
- To present a range of conditions relevant for studying the bio-immobilization of radionuclides,
- To provide the proper conditions for research into the effect of microbial activity on the long-term chemical stability of the repository environment, and
- To enable investigation of the bio-corrosion of copper under conditions similar to those of a high-level radioactive waste repository.

1.5 Site locations in the Äspö Hard Rock Laboratory

To fulfil the objectives of the MICROBE framwork, four sites along the Äspö HRL tunnel at different depths (Figure 1-2) have been selected for various research purposes. They are situated at 907 m, 1127 m, and 2200 m along the tunnel from the entrance. The main site is located in the F tunnel at a depth of 450 m. The sites are briefly described below. Detailed characterization and evaluation follows in sections 2 and 3 of this report, respectively.

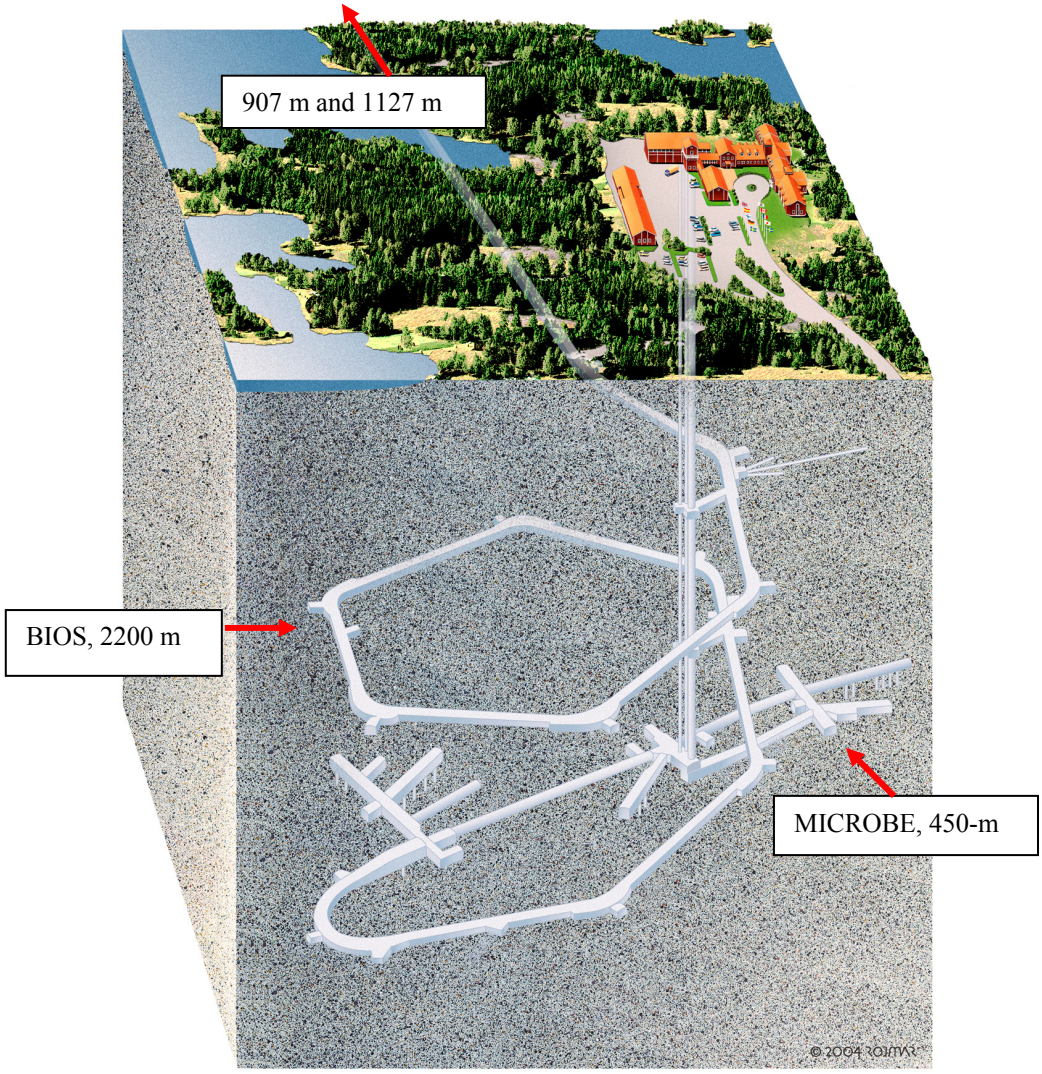

***Figure 1-2**. Location of the sites used within the MICROBE framework*

At 907 m along the tunnel from the entrance, on the A side, a small vault with a rescue chamber supports a ditch with groundwater that is rich in ferrous oxides and iron-oxidizing bacteria. This ditch was used as a natural site for investigations of BIOS formation. A unique ecosystem of sulphur-oxidizing bacteria was found at 1127 m along the tunnel, on the B side; the microbes there oxidized sulphide to elemental sulphur and sulphate. Apart from being an intriguing site from a microbiological perspective, it also allowed the investigation of microbial effects on the sulphur cycle in underground environments. Unfortunately, the pool dried out in fall 2002. An attempt in 2003 to open up the site by digging out the pond down to the rock was unsuccessful. One particularly good site for investigating BIOS has been identified at 2200 m along the tunnel, on the A side. A vault reaches approximately 10 m into the host rock perpendicular to the tunnel, and has a borehole in its face that delivers groundwater rich in ferrous iron and iron-oxidizing bacteria. The borehole has been connected to two $2000 \times 300 \times 250$ mm artificial channels that mimic ditches in the tunnel. The main MICROBE project site is at the 450-m level of the F tunnel. At this site three core-drilled boreholes, KJ0050F01, KJ0052F01, and KJ0052F03, intersect water-conducting fractures. A well-equipped laboratory container has been installed at this site.

1.6 Aim of this report

The drilling, instrumentation, and characterization of the 450-m level site was reported on at the end of year 2000 (Pedersen, 2000). Since then, more sites have been added to the MICROBE framwork, and all sites have been characterized in detail. This framework includes several experiments and investigations. These are at various stages of completion: some are still in progress, while others have been completed and have had their results published. This report describes the sites and their instrumentation in detail and reviews the status of the experiments conducted within the MICROBE framwork.

2 Site descriptions and instrumentation

The sites used in the MICROBE framework have very different characteristics, depending on the purpose of the investigations. Two of the sites, denoted 907A and 1127B, have been used without adaptation, as they occur in the tunnel. The vault at 2200 m from the tunnel entrance has been installed with artificial channels for BIOS growth, and an existing borehole was packed off. Finally, the main MICROBE project site at the 450-m level has been installed with three boreholes and an advanced laboratory. The following is a detailed technical description of the sites and their respective instrumentation installations.

2.1 The sulphur sites

Sulphur is an important element which must be considered in the safety analysis of any future high-level radioactive waste (HLW) repository. First, sulphide is corrosive to copper. Second, sulphide production reduces the redox potential and may act as a scavenger for oxygen. Finally, sulphide forms solid phases with many metals, and may immobilize certain radionuclides under various conditions. Microbial processes interact with the sulphur cycle. Some transformations involved in this cycle, such as sulphate reduction, only occur under anaerobic conditions, such as those resulting from microbial respiration at the temperature and pressure intervals found in a repository. It is thus important to understand the influence of microbial processes on the cycling of sulphur in repository environments. Apart from the sulphide copper corrosion that is investigated at the MICROBE 450-m site, some other processes involved in the sulphur cycle can be investigated along the tunnel. There are many sites along the Äspö HRL tunnel where sulphur-oxidizing bacteria (SOB) oxidize sulphur with the concomitant consumption of oxygen. Two such sites have been or are being investigated: the first is a pond system on the B side of the tunnel, 1127 m from the entrance; the second coincides with the BIOS site 2200 m from the tunnel entrance. These sites are described in more detail below.

2.1.1 The 1127B pond

Investigations conducted from 1991 to 1994, during construction of the Äspö HRL tunnel, found that sulphate reduction (to sulphide) was most vigorous at places where the influx of organic carbon was high combined with a high mixing ratio of Baltic or modified Baltic seawater (Laaksoharju et al., 1995). One dominant site for sulphate reduction was located about 1100 to 1300 m along the tunnel from the entrance, where the tunnel runs under the sea floor. Here, the smell of sulphide was strong. A very distinct SOB ecosystem emerged 1127 m along the tunnel, where sulphide-rich water trickled into the tunnel (Figure 2-1). This system has been under observation for more than a decade, and it has changed significantly in structure. Slowly and steadily, the inflow of sulphide into the groundwater has decreased, stopping completely in 2003.

Attempts were made to deepen the pool system, first by hand digging and then by machine, but in vain. The sulphur pond at 1127B is gone and cannot serve as a sulphur research site anymore. Fortunately, sulphur communities have developed at another MICROBE site, in the artificial channels at the site 2200 m along the tunnel, as described below.

While SOB were active in the 1127B pond, some investigations were undertaken. Sulphur fractionation patterns and SOB diversity were investigated in spring 2003; the results were presented as an M.Sc. thesis in fall 2003. The conclusions from those investigations were as follows:

- SOB could have contributed significantly to an isotopic fractionation effect observed in sedimentary sulphides; and
- Judging by microscopy and molecular analysis, the dominant SOB groups in the 1127B pond were an SOB species that deposits filamentous sulphur (Taylor and Wirsen, 1997) and *Thiothrix* which deposits intracellular sulphur globules.

Figure 2-1. *The 1 × 2-m sulphur pond at the 1127B site. The image was taken 17 January 2002. The cloud-like white structures are colonies of filamentous sulphur-forming SOB and the filamentous structures are strings of Thiothrix.*

2.2 The BIOS sites

Organic surfaces and iron oxides have been identified as important factors in radionuclide transport modelling. Several micro-organisms oxidize ferrous iron to ferric iron, resulting in a mix of organic material (microbes) and iron oxides – here denoted BIOS (biological iron oxides). BIOS can be found everywhere along the Äspö HRL tunnel system. BIOS in the Äspö HRL are mainly produced by the stalk-forming bacterium, *Gallionella ferruginea* (Hallbeck and Pedersen, 1990, 1991, 1995; Hallbeck, Ståhl, and Pedersen, 1993). Two particularly good sites for investigating BIOS have been identified on the A side at 907 and 2200 m along the tunnel from the entrance.

2.2.1 The 907A ditch

At 907 m along the tunnel from the entrance, on the A side, a small vault with a rescue chamber supports a ditch containing groundwater rich in ferrous oxides and iron-oxidizing bacteria (Figure 2-2). This ditch was used as a natural analogue to the artificial BIOS channels at 2200 m. The growth characteristics of the BIOS of this site were compared with those growing at the 2200 m site (2.2.2.).

This site was flooded with sand and water in fall 2003 due to a blockage in a drainage tube above the site. It slowly recovered in 2004, but there are currently no plans to continue work at this site.

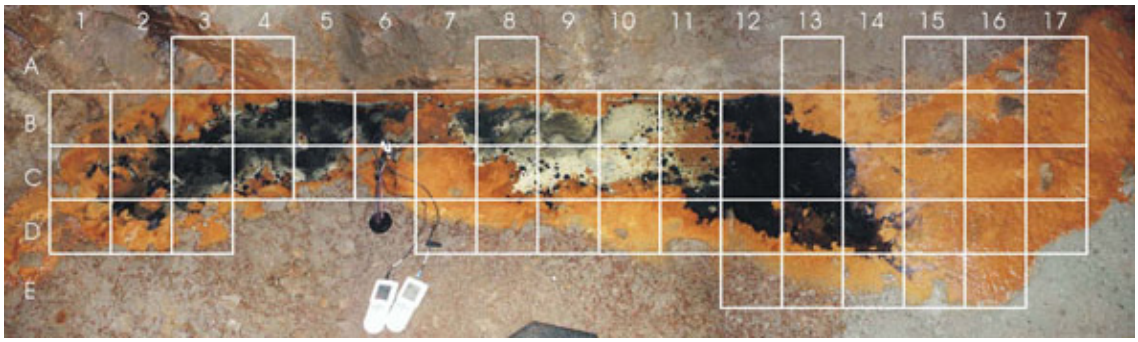

Figure 2-2. *The 907-m ditch site is located at a depth of about 130 m and is characterized by a shallow, elongated pond that overflows into the main tunnel ditch to the right in the image. The brown material is BIOS. The black colour results from iron sulphide precipitates and the white material is calcium carbonate. The overlaid grid created an organized environment and enabled pH, oxygen, and redox measurements to be made in three dimensions. Field instruments are shown at the bottom of the figure. Grid size is about 20 × 20 cm.*

2.2.2 The 2200-m BIOS site

During 1998 the entire Äspö HRL tunnel was searched for sites with dense growth of iron-oxidizing bacteria that produce BIOS (Ferris et al., 1999). A ditch in a side vault located 2200 m along the tunnel from the entrance, and four additional sites were identified. This ditch received anaerobic and reduced groundwater from a borehole in the face of the vault, denoted KA2198A. The 2200-m BIOS was found to be of good and reproducible quality, and this, together with the protected character of the site (an undisturbed side vault), qualified it for continued examination within the MICROBE framwork.

Borehole KA2198A

This borehole was core drilled on November 15, 1993 in the face of a 10-m side vault on the A side of the Äspö HRL tunnel, 2200 m along the tunnel from the entrance (corresponding to a depth of about 296 m). The borehole has a diameter of 86 mm and extends about 14.68 m. It was used for rock tension measurements in 1993 and was thereafter abandoned. In 2001 it was chosen for use in the MICROBE project, and a packer was installed in the orifice of the borehole. The flow from this fully opened borehole was 0.8 L per minute in June 2002; this flow rate dropped somewhat to about 0.6 L per minute by June 2004.

The BRIC systems

To culture BIOS, two plexiglass boxes of dimensions 2000 × 300 × 250 mm (length/width/height) were constructed (Figure 2-3). They are denoted BRIC (BIOS reactor, *in situ*, continuous flow) systems.

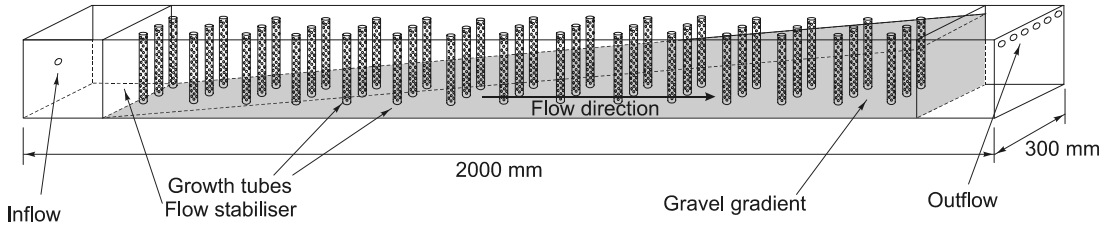

Figure 2-3. *Schematic diagram of a BRIC installed at the 2200 site. See text for details.*

Figure 2-4. *Microbiologists working with BRICs at the BIOS site, making redox, pH, and oxygen measurements along the flow line.*

Water flow stabilizers were mounted 200 mm from each end with 5-mm holes drilled every 20 mm in a two-dimensional grid pattern. Water enters the BRIC at the centre on the left and exits via six 14-mm drainage holes at the top of the right-hand end. Later, the outflow was modified to become a brim drainage system. Inside each BRIC there is a gradient of gravel derived from local Äspö rock to provide the organisms with a stable base for stalk adhesion and community development. Three rows of 15 growth tubes were placed at 100-mm intervals in the gravel. Each tube has a 36-mm inside diameter with 96 (eight sets of twelve), 8-mm holes to allow water to flow through. The BRICs had removable lids to reduce the amount of oxygen diffusion if needed.

Water was supplied from borehole KA2198A through 6-mm stainless steel tubing. The borehole was cleaned and fitted with a packer system to isolate the fracture and had a main water shut-off valve close to the rock face. The conduit system had two additional Swagelok® (SVAFAB, Stockholm, Sweden) valves and a 1-bar pressure gauge installed to control water flow and allow sampling of inflow water.

2.3 The MICROBE 450 m site and laboratory

The main MICROBE site is at the 450-m depth level in the F tunnel (Figure 2-5). A laboratory container has been installed at this site, complete with laboratory benches, a chamber with an anaerobic environment, and an advanced climate control system. A gas chromatograph and a gas extraction system are installed (AP-TD-F82-02-017), which can analyse the following gases (detection limit): hydrogen (1 ppb), carbon mono-oxide (1 ppb), carbon dioxide (1 ppm), methane (1 ppm), ethane (1 ppm), and ethylene (1 ppm). Three core-drilled boreholes, KJ0050F01, KJ0052F01, and KJ0052F03, that intersect water-conducting fractures are connected to the MICROBE laboratory via 1/8" poly-ether-ether-ketone (PEEK) tubing. The boreholes are equipped with metal-free packer systems that allow controlled circulation of groundwater via each respective fracture. Each borehole has been equipped with a circulation system offering a total of 0.21 m^2 of test surface for biofilm growth experiments under *in situ* pressure, temperature, and chemistry conditions (AP-TD-F82-02-013). Detailed descriptions of drilling and instrumentation at this site are given next.

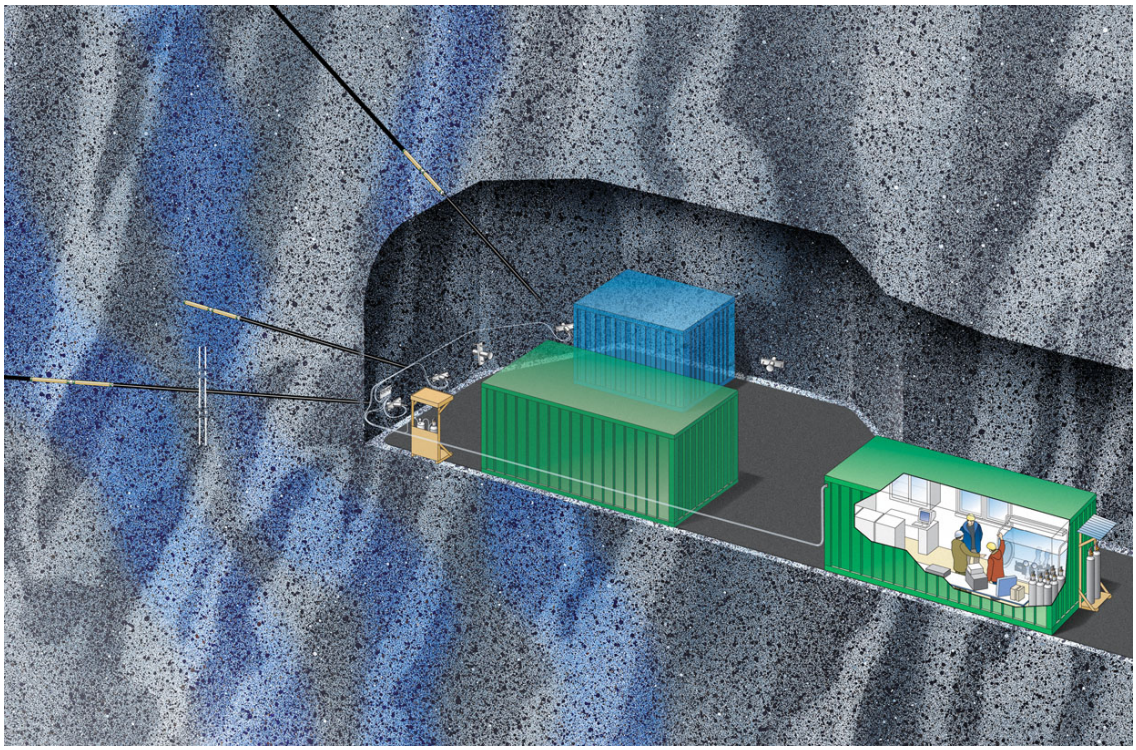

Figure 2-5. *Artist's conception of the MICROBE framework's 450-m site and the metal-free packer configuration. The laboratory (to the right) is situated in a steel container and connected to three discrete fractures in the rock matrix. PEEK tubing connects the systems in the lab with the groundwater (see 2.3.2 for details).*

2.3.1 Drilling and instrumentation of the MICROBE 450-m boreholes

A quality plan was established for drilling the MICROBE boreholes. The CHEMLAB boreholes (KJ0044F01, KJ0052F02) were drilled as part of the same programme, namely, drilling of KJ0052F01, KJ0052F02, KJ0050F01, KJ0044F01 for the RNR experiments and microbiology sampling in the J-niche quality plan (QP) TD F58-99-015. KJ0052F03 was added to the campaign after the QP was written, but the drilling procedures followed what had been decided for the other two MICROBE project boreholes. Triple-tube drilling was applied (Figure 2-6). This drilling technique, which uses a core retriever, was used so as to minimise the exposure of the core to drill water and to deliver the core intact, even when multifractured rock was penetrated. The drill tube protected the drill core from contact with aquifer systems intersected during drilling. The split tube kept the intersected fractures intact, and even kept small pieces of rock in their original positions. Steam and alcohol cleaning was applied to minimize potential contamination, as described in the QP. These MICROBE boreholes are described in detail below.

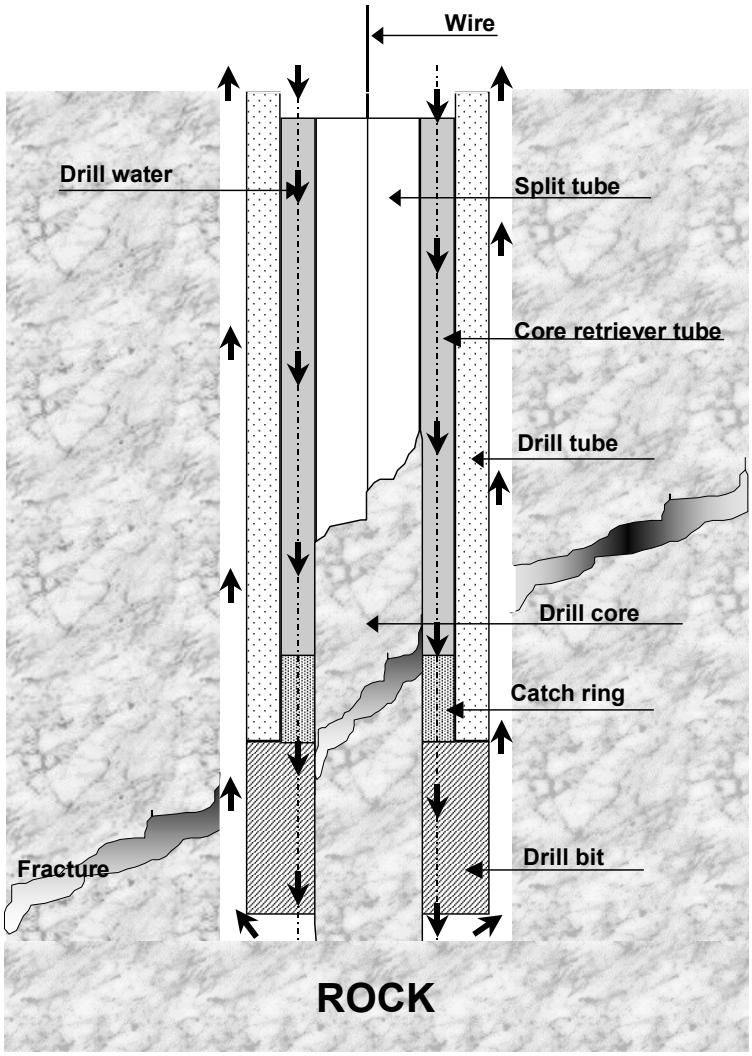

Figure 2-6. *The triple-tube drilling principle.*

KJ0050F01

This borehole, drilled in May 1999 in the J tunnel of the MICROBE 450-m site, reaches a length of approximately 50 m and has a diameter of 76 mm (Figure 2-7). One water-conducting feature was found at a depth of 12.7 m. It has a flow of 0.4 L per minute and the formation pressure was 26 kg cm^2 as of December 2004 (Table 2-1).

KJ0052F01

This borehole, drilled in May 1999 in the J tunnel of the MICROBE 450-m site, reaches a length of approximately 50 m and has a diameter of 76 mm (Figure 2-7). One water-conducting feature was found at a depth of 43.8 m. It has a flow of 0.9 L per minute and the formation pressure was 31.5 kg cm^2 as of December 2004 (Table 2-1).

KJ0052F03

This borehole, drilled in May 1999 in the J tunnel of the MICROBE 450-m site, reaches a length of approximately 10 m and has a diameter of 76 mm (Figure 2-7). One water-conducting feature was found at a depth of 9.3 m. It has flow of 1.5 L per minute and the formation pressure was 26 kg cm^2 as of December 2004 (Table 2-1). The borehole intersects the fracture at 9.3 m, about 20 cm below where KJ0052F02 intersects the same fracture. The KJ0052F01 and KJ0052F03 boreholes are consequently connected via a conductive fracture.

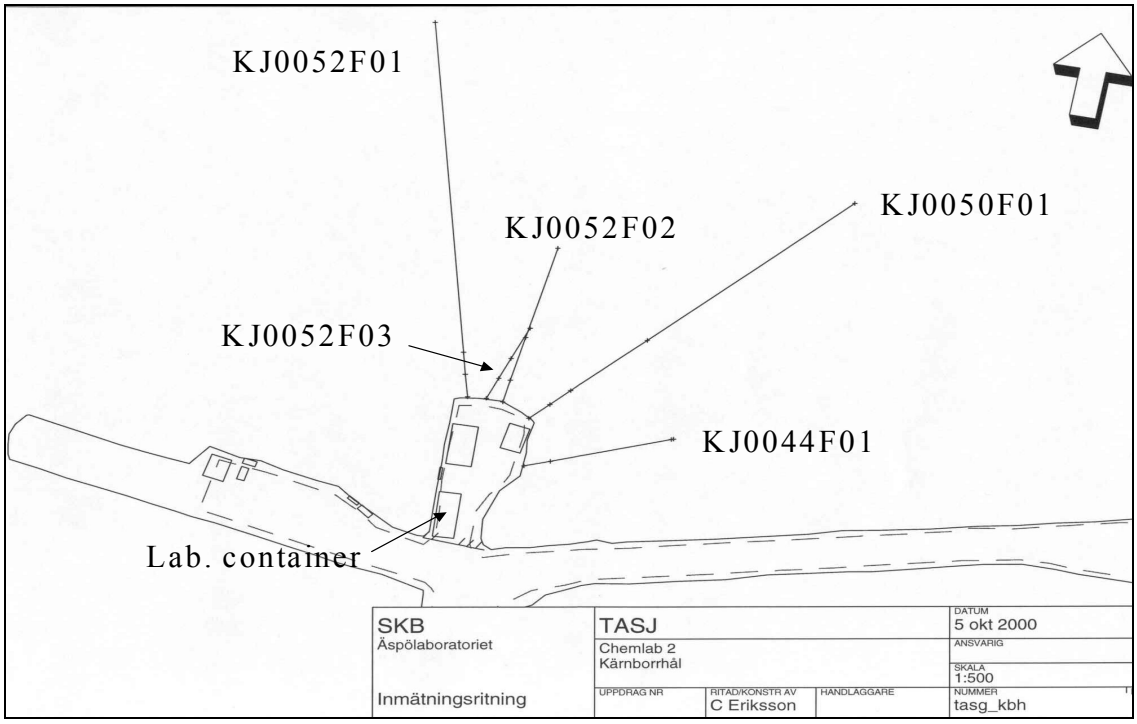

Figure 2-7. *The J niche with MICROBE boreholes KJ0050F01, KJ0052F01, and KJ0052F03, and CHEMLAB boreholes KJ0044F01 and KJ0052F02.*

2.3.2 Instrumentation of the MICROBE 450-m boreholes

The MICROBE 450-m boreholes are instrumented with packers that do not expose the groundwater to metal. It was deemed important to have the smallest possible void volume in the systems.

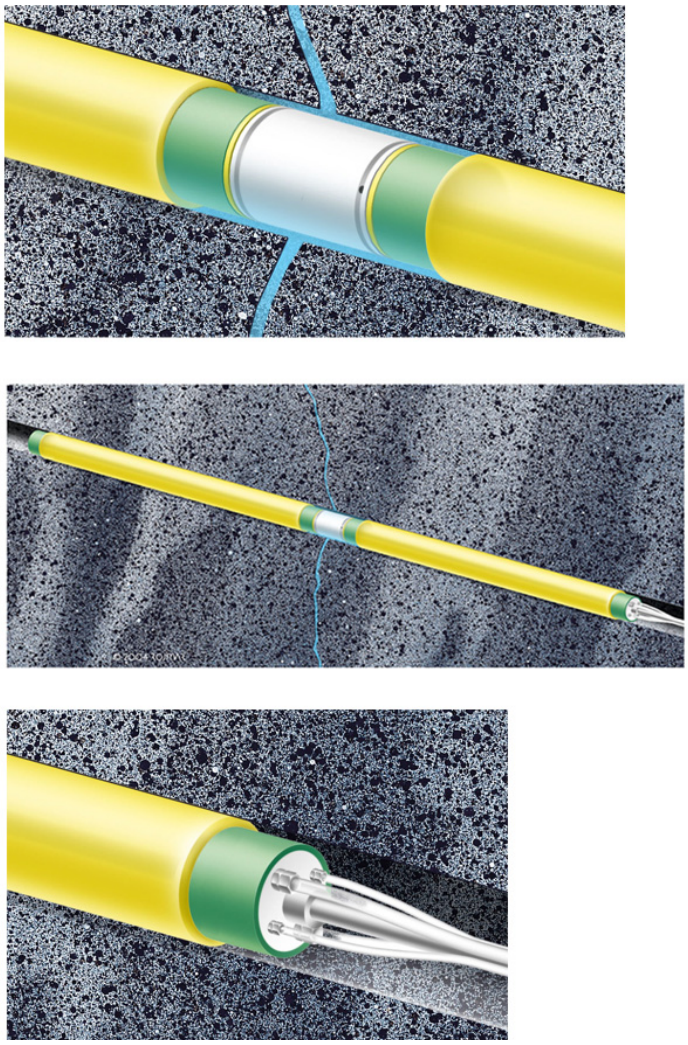

Figure 2-8. *The packer system. The yellow sections are expandable polyurethane packers, while the green rings are the Teflon-coated stainless steel casings. The grey parts are made of PEEK. The sampling tubes are made of 1/8" (outer diameter) PEEK. Sampling and circulation of groundwater is mediated via two small holes made opposite each other in the grey portion in the middle of the packer assembly (dark spot in the top drawing).*

One water-conducting feature was found in each of the MICROBE boreholes. They were sectioned off with a double packer having a sealing length of 1000 mm per packer. The material chosen for the hard body parts was PEEK. Polyurethane rubber (Shore 90) with a thickness of 6 mm was used for the expansion part. Teflon-coated (green in the figure) stainless steel casings were used to attach the rubber to the PEEK bodies (Figure 2-8). A dummy body was installed between the packers to minimize the borehole void volume. This body has an outer diameter of 73 mm, leaving a 1.5-mm slot between the borehole wall and the dummy. Two pieces of PEEK tubing (outer diameter: 1/8" / inner dimension: 2 mm) were installed so that water can be circulated, if needed, through the packed-off section. The sections inside and outside the packers were connected by polyamide tubing to manometers and valves on the outside. Guard packers, and expansion systems for the packers were also installed. One common expansion vessel was installed for all three packer systems.

2.3.3 The laboratory container

A steel container measuring 6.0 × 2.5 × 2.7 m (length, width, height) was installed in the F tunnel at the 450-m level (Figure 2-5, 2-7). The lab environment is kept stable by a climate control system that maintains the temperature at the chosen level, about 22°C, within ± 0.5°C, and the humidity at 40 ‰ ± 5 ‰. The container is equipped with laboratory benches, and with instrumentation for microbiological research (Figure 2-9). The instrumentation is described in detail below and in Appendices 1–3.

Figure 2-9. *The interior of the laboratory container.*

2.3.4 Circulation systems for *in situ* investigations

The sections packed off in respective boreholes (2.3.1) are connected to the MICROBE laboratory via two pieces of 1/8" PEEK tubing, allowing circulation of water from the respective fractures via the laboratory and back again under *in situ* pressure.

Each borehole has been equipped with a flow-cell cabinet exposing a total of 2112 cm^2 of test surface to the circulation of each borehole. This surface area allows biofilm formation under *in situ* pressure, temperature, and chemistry conditions. The systems operate under the parameters listed in Table 2-1. Remote alarms have been installed for the monitoring of pressure, flow rate, and temperature; the alarms are connected via the ALFA system to the ground surface at Äspö HRL (2.3.10).

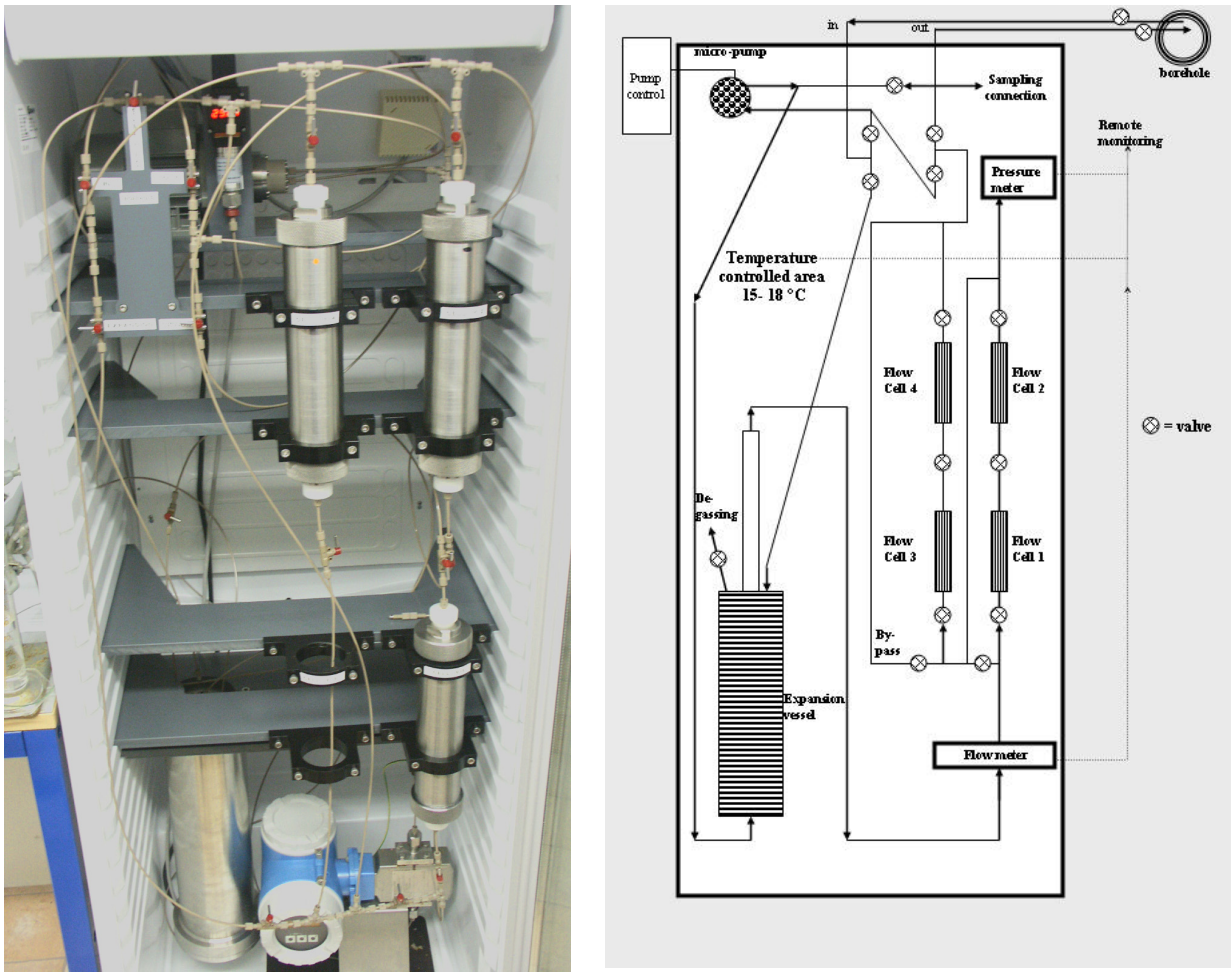

A B

Figure 2-10. A. *Image of one of the three installed flow-cell cabinets* (lower left flow cell has been removed for sampling). ***B.*** *Schematic view* of the cabinet depicted in A.

Table 2-1. Operation parameters for the flow-cell, circulating systems at MICROBE. The tube lengths given represent the combined lengths of ingoing and outgoing tubing. Volumes exclude expansion vessel volume.

Borehole	Pressure (kg/cm^2)	Temperature range (°C)	Flow rate range (mL/min.)	Idle flow rate (mL/min.)	Total length of circulation (m)	Volume of circulation (ml)
KJ0050F01	26.1	15–18	0–100	25–30	100.6	316
KJ0052F01	31.5	15–18	0–100	25–30	145.4	457
KJ0052F03	25.6	15–18	0–100	25–30	83.6	262

	Volume of one flow cell (ml)	Total volume with 4 flow cells (ml)	Tube length to borehole (m)	Tube length in borehole (m)	Tube length in cupboard (m)
KJ0050F01	150	916	65.2	25.4	10
KJ0052F01	150	1057	47.8	87.6	10
KJ0052F03	150	862	55.0	18.6	10

The flow-cell cabinets can either be open and connected to the packed-off borehole section via two pieces of 1/8" PEEK tubing or closed for internal circulation. In the open mode, groundwater with microbes is continuously circulated from the borehole section through the flow cells and back again to the borehole. In the closed mode, the same groundwater and unattached microbes are circulated within the cabinet.

The flow cell has a volume of 530 mL without inserts. This set-up was used during tests of the hydraulic character of the intersected fractures (2.3.5).

Expansion vessel

When the flow-cell cabinet is in the open mode and connected to a fracture in the rock, pressure is maintained by the actual groundwater pressure. When the flow-cell cabinet is in the closed mode, this pressure control is lost. Any sampling of groundwater will immediately reduce the pressure to atmospheric pressure. This is avoided by introducing an expansion vessel into the circulation (lower left in Figure 2-10). The vessel has a maximum volume of 4000 mL which can be reduced to 0 ml. It is operated using the *in situ* pressure of the fracture from which the circulation is drawn by means of simple valve technology. By decreasing the pressure outside or inside the circulation system, total circulating volume increases or decreases, respectively. Detailed drawings of the vessel can be found in Appendix 1.

Pumps and pump rate interval

One micro, cogwheel pump is installed in each circulation system (top left in Figure 2-10A). The pump head is made of PEEK by the Geosigma AB workshop, so metal is not in contact with the medium being pumped. The pump can take a maximum pressure of 50 bars. The maximum speed is 2800 rpm, which renders a maximum flow of about 100 mL/min and a maximum pump pressure of about 3 bars in the circulation systems. The pumps are controlled by Telemecanique Altivar 08 frequency transducers (ATV-08E**M2), which are displayed on top of the cabinet in Figure 2-9.

The flow range is continuous, ranging from 0 to the maximum rate in the respective circulation systems. The differences in maximum flow occurring between the circulation systems are due to the varied lengths of tubing leading to the packed-off fractures, which result in related pressure drops. The cogwheels become worn over time, which eventually reduces the maximum flow rate and pump pressure obtained. This process has, however, been found to be slow and the pump rates remain stable for several months at a time.

Flow meters

One flow meter is installed in each circulation system (lower right in Figure 2-10A). They are Endress+Hauser Promag 50 meters with flow chambers made of PEEK. Metal is not in contact with the medium; however, a small titanium chamber is installed in the flow path and is needed for electrically grounding the instrument. The flow meters have a calibrated precision of 0.5% and the installed measuring range is from 1 to 500 mL/min.

Pressure transmitters

One pressure transmitter is installed in each circulation system (top centre in Figure 2-10A); these are of Druck PTX 1400 type, with a maximum pressure of 60 bars. Each pressure transmitter has a digital display attached of the AUF-1000 type.

Flow cells

Each cabinet is equipped with four flow cells. Those cells are intended for the attachment and growth of micro-organisms in the groundwater. In-depth theory and previous results pertaining to this method can be found elsewhere (Pedersen, 2001, 2003). The flow-cell construction is based on a concept that has been used for research since 1980. The first model was a double-flow channel cell (Pedersen, 1982), later redesigned to form a single-channel flow cell (Pedersen et al., 1986). Based on the single-channel flow cell, a pressure-resistant flow cell was constructed for the purpose of the MICROBE experiments (Figure 2-11). Detailed drawings can be found in Appendix 2, which also gives a detailed description of the sampling procedure.

The flow cells are sterilized with 70 % alcohol before start. After sterilization, the test surfaces are installed. They can be made of different materials, such as, glass, copper, rock, or minerals produced in the laboratory. There is room for 10 surfaces of 120 × 24 × 1 mm (length × width × thickness). One mm on each side lies inside the test pile holder slots and is not exposed to the flow. The distance between the test surfaces is 2 mm. The total surface exposed to flowing groundwater and micro-organisms is thus 120 × 22 × 10 × 2 = 52800 mm^2 or 528 cm^2. With four flow cells in a cabinet, 2112 cm^2 (0.21 m^2) is offered for attachment and growth. Each cabinet consequently mimics 0.21 m^2 fracture surface. There is also an option to remove the surfaces and fill the flow cells with porous material when such a set-up is needed.

Figure 2-11. *The pressure-resistant flow cell with a shell of stainless steel. The interior is made of a polymer material called polyvinylidene fluoride (PVDF). Three flow diffusers distribute the flow evenly over all test surfaces in the test pile. The steel is not in contact with the groundwater.*

2.3.5 Hydrological characteristics of the intersected and circulated fractures

The circulation systems are based on the assumption that hydraulic gradients exist across the fractures in the boreholes, generating a flow of groundwater over the fracture. The systems will thus assume the characteristics and properties of a chemostat. The characteristics of the intersected fractures have been determined and interpreted as presented below (AP-TD-F82-02-014).

The interior apparatus of the flow cells was removed and then the cells were filled with distilled water. Each flow cell takes 530 mL without the test pile and the diffusers. The total volume of the circulation system then approximates 2400 mL (Table 2.2). The water was then circulated via the packed-off section, and samples were withdrawn for analysis of conductivity, sulphate, and bromide. The hypothesis was that the fracture flow would replace the distilled water with groundwater, thereby increasing conductivity and the concentrations of the analysed ions; the results are presented in Figure 2-12. The pump rate was 1200 mL/hr, which means that the circulation volume was turned over in a little over 2 h. This may have caused some deviation in the early data, as the sampling point is located after the flow cells. All distilled water had to pass before the diluted groundwater could be sampled. Therefore, the first two measurements, obtained within three hours, were not included in the calculation of the dilution rates.

The most common type of continuous culture device in microbiology is the chemostat, which permits control of both the population density and the growth rate of a culture. Two elements are used in the control of a chemostat: the dilution rate (d) and the concentration of a limiting nutrient. In a chemostat there is a steady-state relationship between the flow rate and the volume of the culture vessel. Thus, with a vessel of 1000 mL and a flow rate through the vessel of 500 mL/hr, the dilution rate would be 0.5 hr^{-1}. In analogy to the chemostat, the circulation can be approximated as a vessel and the flow through the borehole section will be equivalent to the flow through the chemostat vessel. The volume of the circulation is known, and if the dilution rate is determined, the flow through the borehole section can be calculated. The replacement of distilled water in the circulation experiment will follow an exponential saturation function that asymptotically approaches the original concentration before the start of the experiment. Plotting the logarithm of the measured parameters against time ideally generates straight lines in which the inclination equals the dilution rate (the differential coefficient of the numerical saturation curve). Figure 2-12 gives the results and Table 2-2 summarizes the data.

The flow rate through the circulation system should be significantly larger than the flow through the borehole section, because chemostat theory assumes that the vessel is a thoroughly stirred tank. The results show that the circulation system flow was 20 times larger that the flow rate calculated for the borehole sections (Table 2-2). The circulation flow rate will, consequently, not affect either the dilution or borehole flow rates, if it is significantly higher than the flow in the respective borehole. A discrepancy was found between the dilution rate obtained via measuring conductivity compared to that obtained via analysing bromide and sulphate saturation. This is probably due to minor analytical variation and discrepancies.

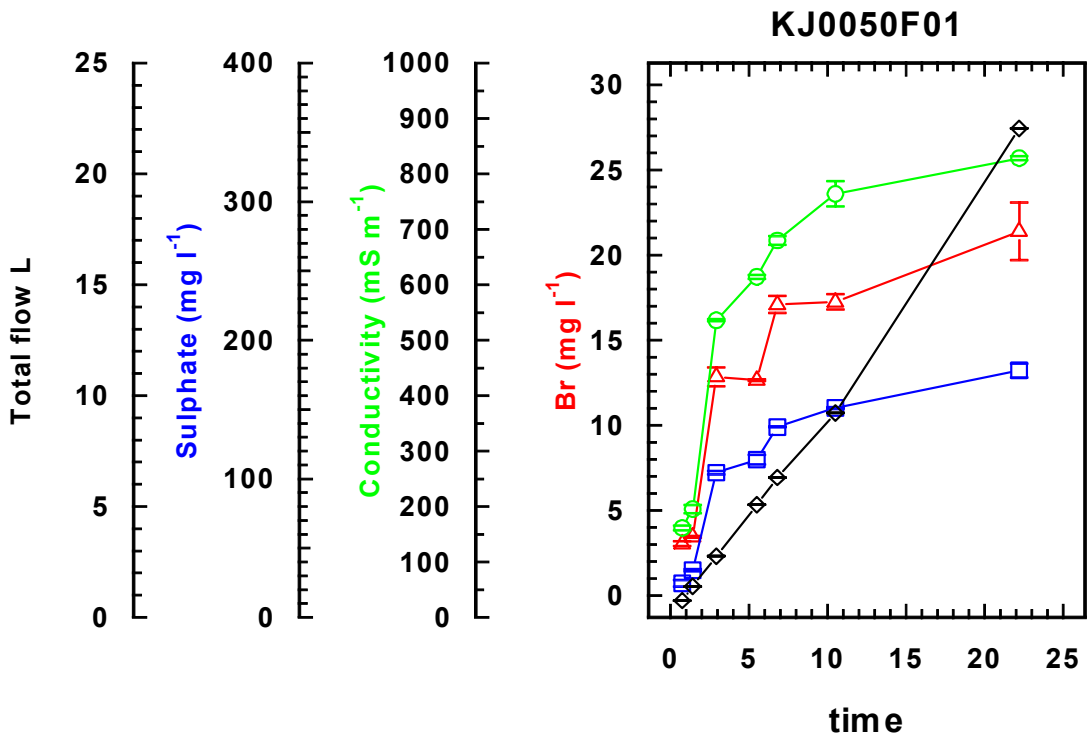

***Figure 2-12 A**. Results of the dilution rate tests. See text for details.*

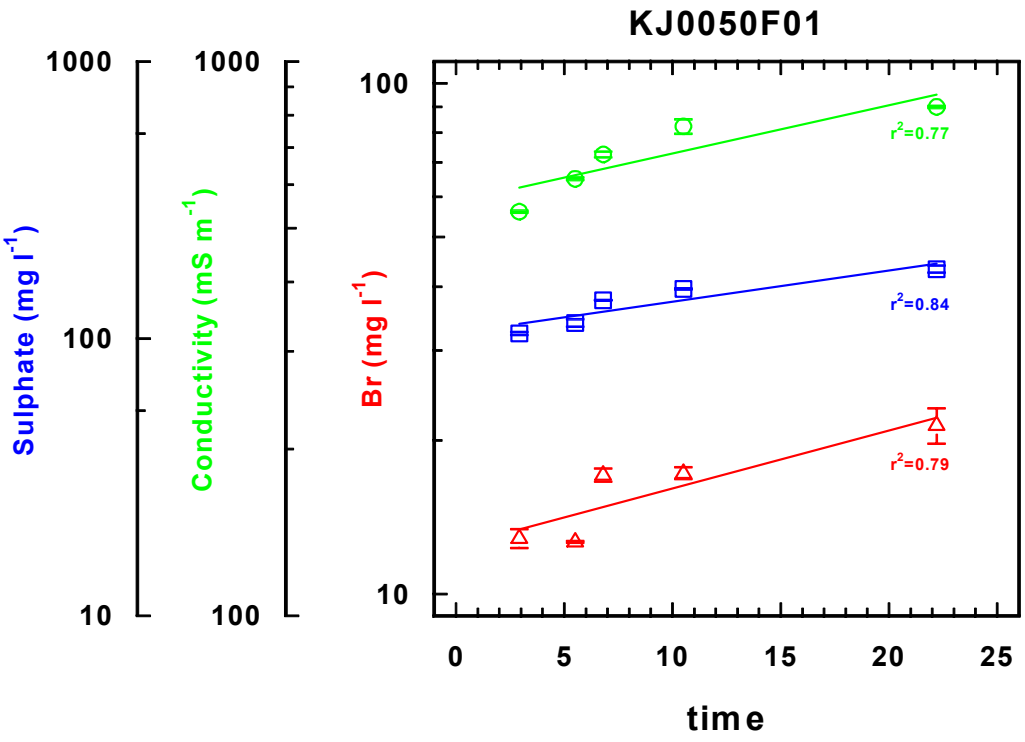

***Figure 2-12 B**. Results of the dilution rate tests. See text for details.*

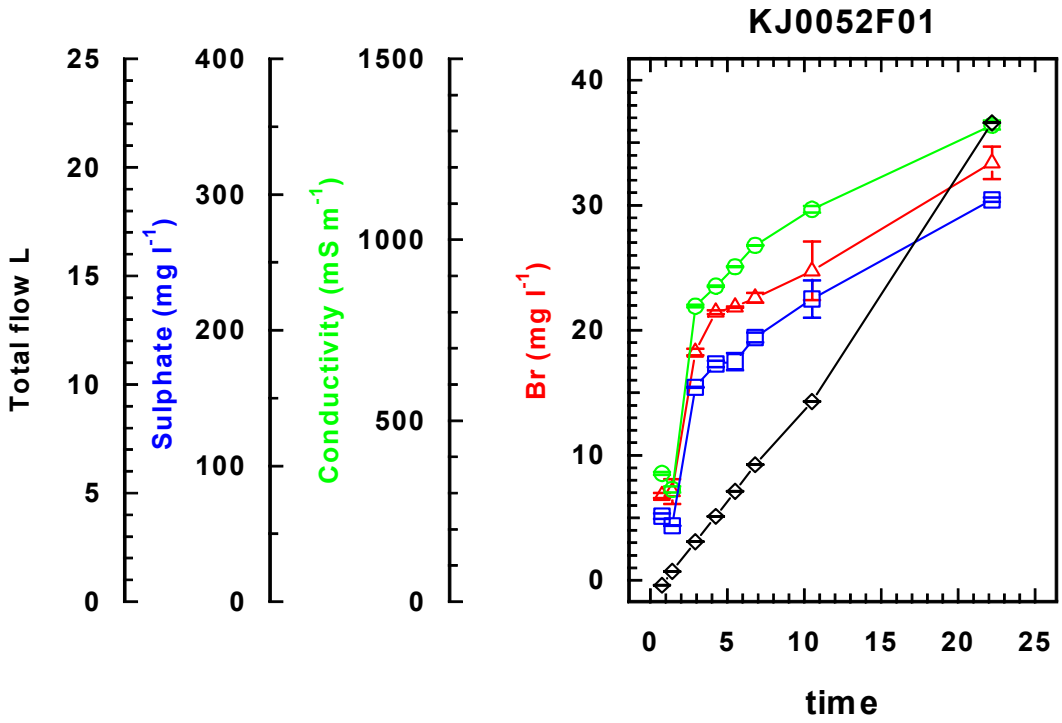

***Figure 2-12 C**. Results of the dilution rate tests. See text for details.*

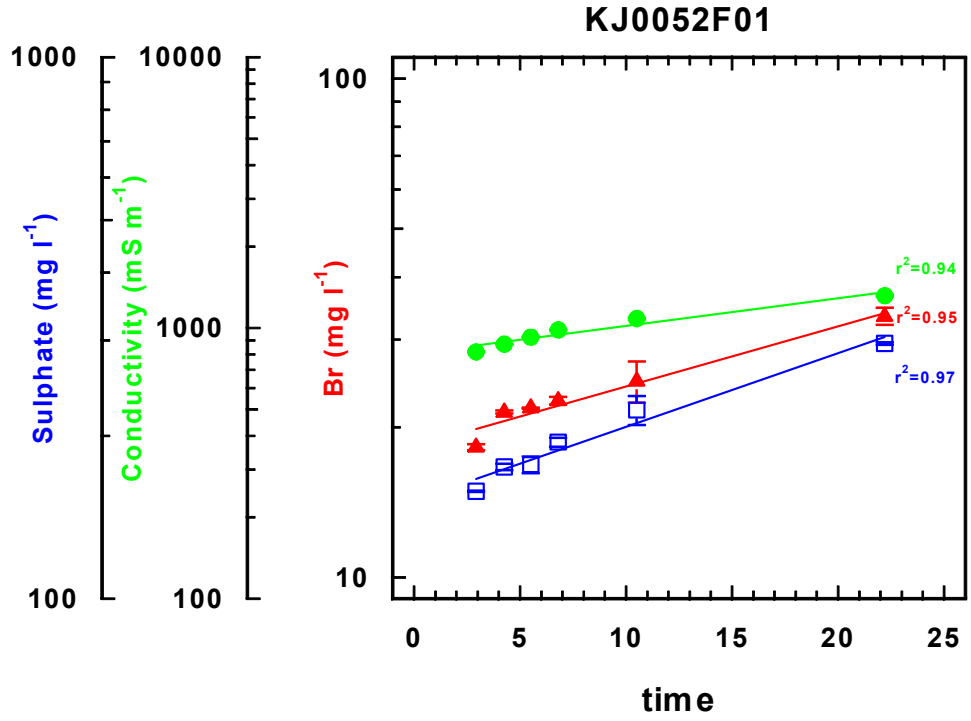

***Figure 2-12 D**. Results of the dilution rate tests. See text for details.*

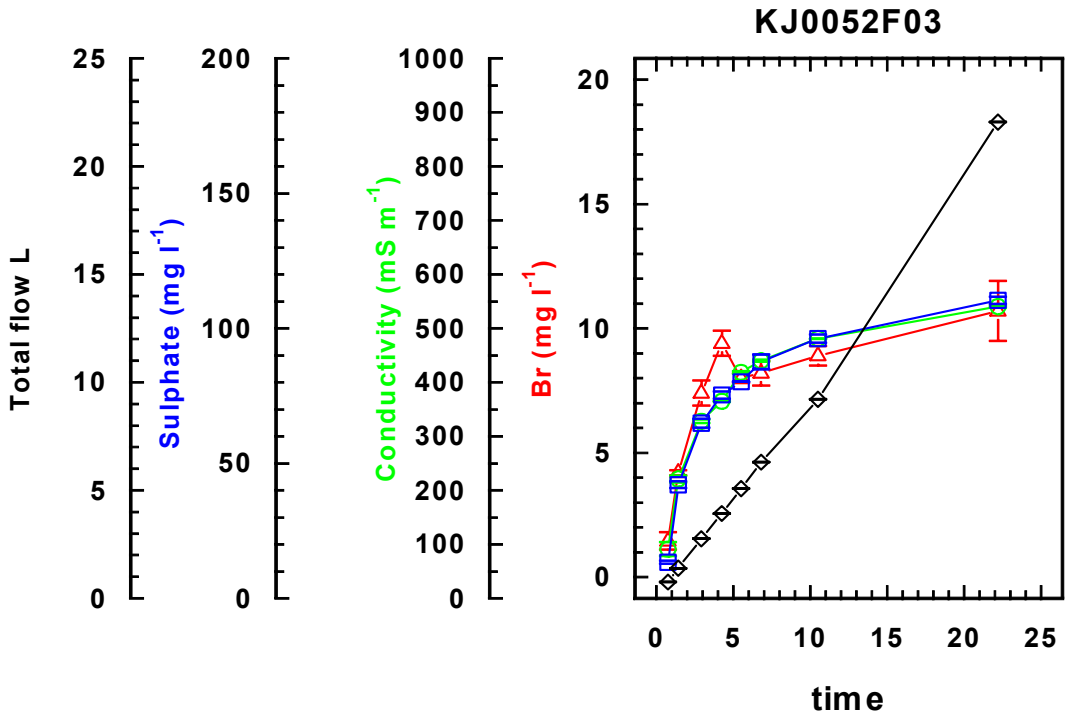

***Figure 2-12 E**. Results of the dilution rate tests. See text for details.*

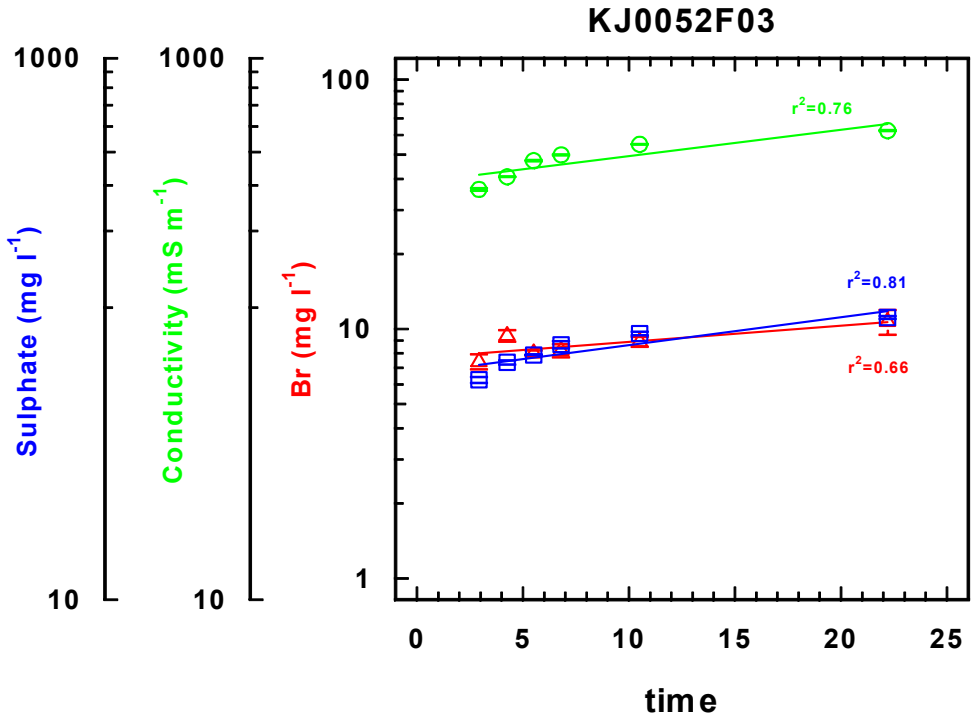

***Figure 2-12 F**. Results of the dilution rate tests. See text for details.*

Table 2-2. Calculated flow rates in the intersected fractures based on the saturation measurements depicted in Figure 2-12.

Borehole	Volume of circulation (ml)	Pump rate (mL/hr)	d (hr^{-1})			Flow in the fracture (mL/hr)	
			SO_4^{2-}	Conductivity	Br^{-1}	SO_4^{2-}/ Br^{-1}	Conductivity
KJ0050F01	2436	1200	0.026	0.020	0.026	63.3	48.7
KJ0052F01	2577	1200	0.028	0.023	0.031	76.0	59.3
KJ0052F03	2382	1200	0.017	0.014	0.017	40.5	33.3

Table 2-3. Calculated maximum dilution rates and theoretical half life of the groundwater in the respective circulation with test piles and diffusers installed.

Borehole	Volume of circulation (ml)	d_{max} (hr^{-1})		Half life (hr)	
		SO_4^{2-}/ Br^{-1}	Conductivity	SO_4^{2-}/ Br^{-1}	Conductivity
KJ0050F01	916	0.069	0.053	10	13.1
KJ0052F01	1057	0.072	0.056	9.6	12.4
KJ0052F03	862	0.047	0.039	14.7	17.8

This activity demonstrates that a significant flow of groundwater passes through the intersected fractures, ranging from about 0.5 mL/min to 1.3 mL/min (Table 2-2). Consequently, there is a continuous supply of groundwater constituents, including microbes, energy-rich gases, and organic carbon. The basic requirements for the attachment and development of microbial biofilms on surfaces in the flow cells are thus fulfilled. Inserting the test piles and diffusers reduces the circulation volumes to about 1000 ml. This does *not* influence the flow rate in the boreholes; however, the dilution rate does increase, and as chemostat theory holds that dilution rate is related to the supply of a limiting nutrient, the maximum growth rate will equal the maximum dilution rate. This rate is then controlled by the flow in each respective fracture. The relationship between dilution rate (d) and the generation time (g) of a population in a chemostat is: $d = \ln 2/g$. Table 2-3 gives the theoretical maximum half lives in the circulation systems, which equals about one to two generations per day. However, this is under the assumption that all the nutrients and trace elements needed for growth are supplied with the groundwater, such that a low concentration results in a low cell concentration. In reality, growth may be much slower if the limiting nutrient or substance is lacking, or if there are other limiting factors. Finally, it should be noted that chemostat theory is valid for microbes in suspension (unattached microbes) and can only be used as an approximation for attached cells. The theory becomes more complicated with attached microbes, but such calculations lie beyond the scope of this report.

2.3.6 Anaerobic box

A Coy type B anaerobic chamber with an automatic airlock has been installed in the laboratory container. It is 198 × 81 × 102 cm (length × width × height), and is equipped with three pairs of gloves, two on one side and one on the other. Palladium catalysts remove oxygen by reaction with hydrogen. The gas mixture used is 10% hydrogen, 5% carbon dioxide, and 85% nitrogen; the hydrogen level in the box is kept at about 3–4% for best efficiency. A Coy model 10 oxygen and hydrogen analyser is installed inside the box, and has a 0–2000 ppm range. The oxygen concentration in the chamber is generally kept at or below 1 ppm.

2.3.7 Gas chromatograph

A gas chromatograph has been installed in the laboratory container. This instrument can analyse the following gases: hydrogen, carbon monoxide, carbon dioxide, methane, ethane, and ethylene. The instrument is a KAPPA-5/E-002 analyser (http://www.traceanalytical.com). It is equipped with two parallel analysis lines with separate detectors. One line has a 156 × 1/16 inch stainless steel HayeSep A column attached to a flame ionization detector (FID). The FID line is also equipped with a methanizer that converts carbon dioxide to methane. The other line passes through a 31 × 1/8 inch stainless steel Mole sieve 5A column and attaches to a reductive gas detector (RGD). The FID system analyses the following gases (detection limits): carbon dioxide (1 ppm), methane (1 ppm), ethane (1 ppm), and ethylene (1 ppm); the RGD line analyses (detection limits) hydrogen (1 ppb) and carbon mono-oxide (1 ppb). The carrier gas tank has a pressure sensor attached to a remote ALFA alarm system; the alarm is set for low pressure.

2.3.8 Gas extractor

Various gases can be found in deep groundwater, and the analysis of such gases requires access to gas chromatographs. Prior to analysis, the gases dissolved in groundwater must be extracted. In addition, most deep groundwater is oversaturated with gases at atmospheric pressure, so the sampling container must therefore be pressure resistant and gas tight. At the MICROBE laboratory gases can be analysed on site using the chromatography system described above. To do this, a gas extractor was developed that can be attached on line between the groundwater to be sampled and the gas chromatograph. It consists of a cylinder with a piston (Figure 2-13 and Appendix 3). The piston moves downwards in the cylinder with a crank, creating a vacuum in the cylinder. Groundwater at *in situ* pressure is let into this evacuated cylinder, causing the water to boil and the dissolved gas to move into a gas phase above the water. The released gas is compressed with the piston and transferred to a glass syringe (right in Figure 2-13), the pressure is equalized to the tunnel atmospheric pressure of 1.1 atm (blue digital manometer in Figure 2-13), and the extracted volume is registered. The cycle is repeated twice, or until no more gas can be extracted. Before injection, the gas can be transferred to a second syringe (left in Figure 2-13) and diluted with carrier gas (nitrogen).

The extracted gas contains moisture that must be removed before injection. A cryo trap has been developed to carry out this task (Figure 2-14, Appendix 3.3). The gas is injected into the gas chromatograph via a stainless steel tube loop immersed in a mixture of 99% alcohol and carbon dioxide pellets, which gives a temperature of about –80 C. Moisture freezes on the tube walls. At intervals, the loop is immersed in hot water and nitrogen is used to purge the thawing moisture.

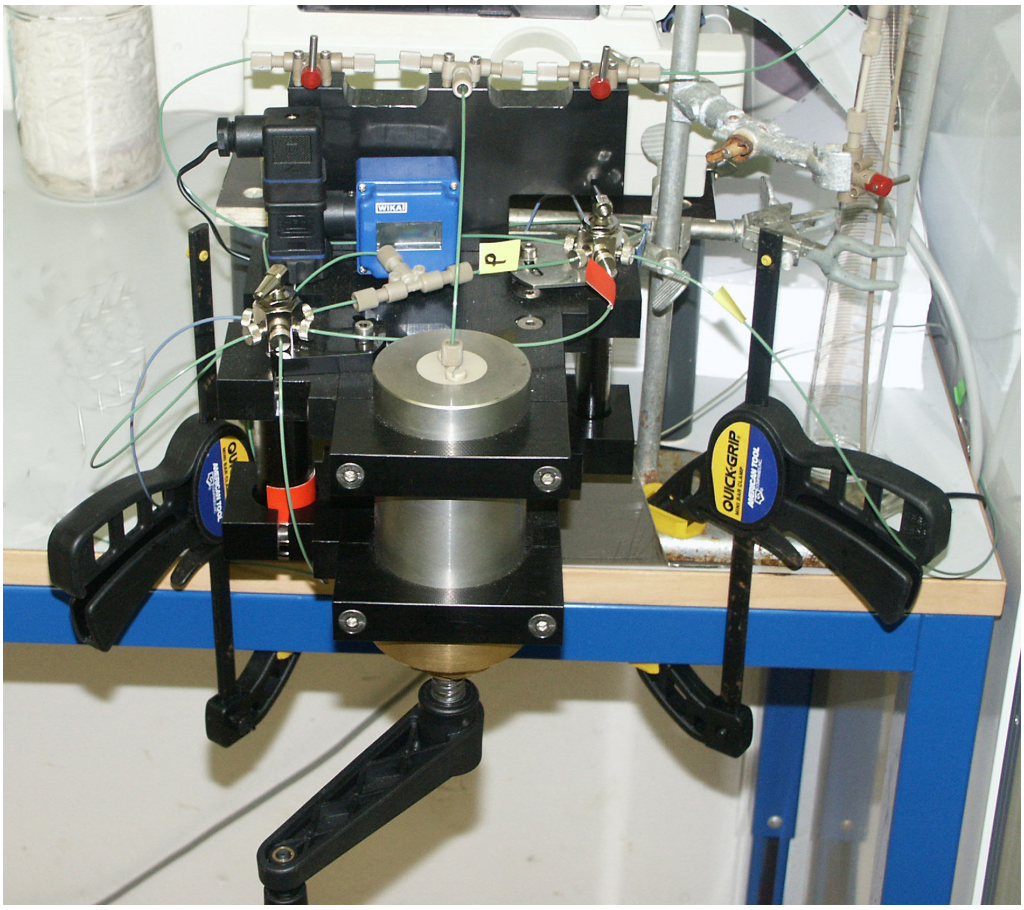

Figure 2-13. *The on-line extractor for dissolved groundwater gas.*

Figure 2-14. *The on-line cryo trap with CO_2 pellets mixed with 99% ethanol for removing moisture from gas extracted from groundwater.*

2.3.9 ATP analysis

All living organisms have an energy transportation molecule called adenosine triphosphate (ATP) in their cells. This fact has been used to develop biomass assays based on ATP measurements, a monitoring concept developed in the mid 1970s. According to this concept, the firefly luciferin–luciferase system could be added to an ATP converting reaction mixture, enabling continuous monitoring of the ATP concentration by measuring the intensity of the light emission. This is possible because certain chemical reactions result in the formation of a fluorescent molecule in its excited state. When this molecule releases its bound energy, a photon (i.e. a light particle) is emitted. The phenomenon is called chemiluminescence or, when appearing in nature, bioluminescence (fireflies provide a well-known example of this). Bioluminescence is a frequent phenomenon in the marine environment. It is catalysed by various enzymes called luciferases acting on species-specific luciferins. In luminescence analysis (or luminometry) one makes use of the fact that light is easy to measure accurately, even at very low levels. The assay is set up in such a way that the light intensity or total amount of light emitted is proportional to the analyte, i.e. the substance one wants to measure. Such assays have offer a unique combination of four characteristics:

- Low detection limits (often 10^{-18} mol or for enzymes even lower),
- Low-cost equipment – the measuring instrument is called a luminometer and is in principle much more simple than, for example, a spectrophotometer,
- Low-cost reagents (potential for miniaturized assay systems), and
- Simple and rapid analytical procedure (mix and measure).

The firefly luciferin–luciferase system is the most frequently used bioluminescent reaction for analytical purposes. It can be used for assays of ATP and any enzyme or metabolite participating in ATP-forming or degrading reactions. ATP is used in the MICROBE research for measuring biomass since the intracellular level of ATP is similar in all living cells, and is rapidly degraded when the cell dies. This gives a rapid result that otherwise may have taken days to obtain using microscopic or cultivation methods.

2.3.10 Remote monitoring and control

The flow and pressure meters and temperature sensors in each circulation cabinet are connected to the ALFA system at Äspö. These are connected to decentralized analog cards attached to a Siemens PCL via a PROFIBUS. Alarms are set on the ground surface to detect high/low values according to the experimental design.

2.4 Groundwater characterization

2.4.1 Groundwater chemistry and stable isotopes

The groundwater was twice analysed at a class-V level. The first sampling was performed on 23 February 2000; a second sampling for class-V analysis was performed 15 September 2003 (Table 2-4a). Chemical analysis was performed according to the class-V protocols. The chemical main constituents, environmental isotopes, and trace elements of the groundwater are shown in Tables 2-4, b–f.

Table 2-4a. Activity history of the groundwater chemistry analysis.

Idcode	Secup[a]	Seclow[a]	Sample No	Sampling date	Class No	Project	Northing	Easting	Elevation
	m	m					Äspö96 (m)	Äspö96 (m)	Äspö96 (m)
KJ0050F01	12.64	12.84	3153	2000-02-23	5	Microbe	7321.4	1980.7	–448.2
KJ0050F01	12.64	12.84	6151	2003-09-15	5	Microbe	7321.4	1980.7	–448.2
KJ0052F01	43.7	43.90	3155	2000-02-23	5	Microbe	7360.1	1960.7	–450.5
KJ0052F01	43.7	43.90	6206	2003-09-15	5	Microbe	7360.1	1960.7	–450.5
KJ0052F03	9.23	9.43	3156	2000-02-23	5	Microbe	7324.6	1970.3	–447.6
KJ0052F03	9.23	9.43	6150	2003-09-15	5	Microbe	7324.6	1970.3	–447.6

[a]) Secup and Seclow represent the upper and lower limits of the sampled section, respectively.

Table 2-4b. Chemical composition of the groundwater – main constituents.

Idcode	Sample	Na	K	Ca	Mg	HCO_3	Cl	SO_4	SO_4-S	Br	F	Si	Fe-ICP	Fe_{tot}	Fe^{2+}
		mg/L	mg/L	mg/L	mg/L	mg/L	mg/L	mg/L	mg/L	mg/L	mg/L	mg/L	mg/L	mg/L	mg/L
Measurement uncertainty		5%	5%	5%	5%	5%	5%	10%	5%	10%	10%	5%	5%	10%	10%
KJ0050F01	3153	2260	9.61	1890	59.3	64	6580	426	155	44.4	1.40	6.2	0.143	0.144	0.125
KJ0050F01	6151	2520	9.2	2540	51.4	30	8040	516	148	57.8	–0.2	5.6	0.095	0.109	0.105
KJ0052F01	3155	2370	7.73	2140	47.1	11	7230	485	175	47.6	1.01	5.1	0.049	0.052	0.049
KJ0052F01	6206	2730	9.26	2860	44.8	15	8590	564	164	62.5	0.9	4.8	0.052	0.109	0.096
KJ0052F03	3156	2060	8.76	1460	64.7	71	5750	388	138	34.2	1.97	6.4	0.165	0.170	0.170
KJ0052F03	6150	2100	9.77	1690	63.5	51	6110	428	129	37.5	0.8	5.9	0.183	0.221	0.215

Table 2-4c. Chemical composition of the groundwater – main constituents (continued).

Idcode	Sample	Mn	Li	Sr	pH	El. Cond.	Smpl. Flow	Drill-water	DOC	S_2	NH_4-N	I	NO_2-N	NO_3-N	PO_4-P
		mg/L	mg/L	mg/L	pH unit	mS/m	L/min.	%	mg/L	mg/L	mg/L	mg/L	mg/L	mg/L	mg/L
Measurement uncertainty		5%	5%	5%	0.1 unit	5%			0.1 mg/L	10%	20%				5%
KJ0050F01	3153	0.50	1.38	32.1	7.3	1800	0.40	0.16	3.1	0.010	0.11	n.a.	n.a.	n.a.	n.a.
KJ0050F01	6151	0.43	1.58	45.1	7.4	2140		0.44	2	0.010	0.07	0.344	0.0001	0	0.0002
KJ0050F01	6402									<0.002					
KJ0052F01	3155	0.29	1.49	36.1	7.8	1930	0.90	0.16	1.4	<0.002	0.03	n.a.	n.a.	n.a.	n.a.
KJ0052F01	6206	0.31	1.73	50.2	7.4	2231		0.05	n.a.	n.a.	0.05	0.396	0	0	0.0002
KJ0052F01	6401									0.226					
KJ0052F03	3156	0.48	1.03	25.1	7.4	1610	1.50	0.27	3.5	<0.002	0.10	n.a.	n.a.	n.a.	n.a.
KJ0052F03	6150	0.49	1.05	27	7.4	1700		0.52	2.3	n.a.	0.09	0.306	0.0002	0.0007	0.0009
KJ0052F03	6400									0.004					

Table 2-4d. Chemical composition of the groundwater – environmental isotopes.

Idcode	Secup[a]	Seclow[a]	Sample	Sampling date	δ^2H	^3H	$\delta^{18}O$
	m	m			dev SMOW	TU	dev SMOW
Measurement uncertainty:					1 unit	1 unit	0.2 unit
KJ0050F01	12.64	12.84	3153	2000-02-23	–75.1	4.4	–10.3
KJ0050F01			6151	2003-09-15	–81.5	2.9	–11.3
KJ0052F01	43.7	43.9	3155	2000-02-23	–86.2	1.0	–11.7
KJ0052F01			6206	2003-09-15	–86.1	–0.8	–12
KJ0052F03	9.23	9.43	3156	2000-02-23	–74.7	3.9	–9.70
KJ0052F03			6150	2003-09-15	–78.9	2.6	–10.8

a) Secup and Seclow represent the upper and lower limits of the sampled section, respectively.

Table 2-4e. Chemical composition of the groundwater – trace elements. Measurement uncertainty is 5–20% depending on species measured.

Idcode	Sample	U	Th	As	Sc	Cd	Hg	V	Rb	Y	Zr	In	Cs	Ba	La	Hf	Tl
		ug /L	ug /L	ug /L	ug /L	ug /L	ug /L	ug /L	ug /L	ug /L	ug /L	ug /L	ug /L	ug /L	ug /L	ug /L	ug /L
KJ0050F01	3153	0.018	–0.4	n.a.	0.412	n.a.	n.a.	n.a.	27.5	0.257	n.a.	–0.020	3.31	68.7	0.19	n.a.	0.156
KJ0050F01	6151	0.025	–0.1	–0.5	–0.5	0.0437	–0	0.056	31.7	0.373	–0.3	–0.5	3.42	65.4	0.293	–0.3	–0.3
KJ0052F01	3155	0.020	–0.4	n.a.	0.702	n.a.	n.a.	n.a.	29.1	0.415	n.a.	–0.020	4.24	68.5	0.34	n.a.	0.121
KJ0052F01	6206	0.027	–0.1	–0.5	–0.5	0.0626	–0	0.153	36.4	0.44	–0.3	–0.5	4.68	65.8	0.263	–0.3	–0.3
KJ0052F03	3156	0.040	–0.4	n.a.	0.39	n.a.	n.a.	n.a.	28.3	0.329	n.a.	0.021	3.17	60.9	0.18	n.a.	0.112
KJ0052F03	6150	0.074	–0.1	–0.5	–0.5	0.0415	–0	0.058	28.9	0.317	–0.3	–0.5	3.04	59.2	0.295	–0.3	–0.3

Table 2-4f. Chemical composition of the groundwater – trace elements.

Idcode	Sample	Ce	Pr	Nd	Sm	Eu	Gd	Tb	Dy	Ho	Er	Tm	Yb	Lu
		ug /L	ug /L	ug /L	ug /L	ug /L	ug /L	ug /L	ug /L	ug /L	ug /L	ug /L	ug /L	ug /L
KJ0050F01	3153	0.173	–0.020	0.056	–0.02	–0.02	n.a.	n.a.	n.a.	–0.02	–0.02	n.a.	–0.02	–0.02
KJ0050F01	6151	0.2	–0.05	0.052	–0.05	–0.05	–0.05	–0.05	–0.05	–0.05	–0.05	–0.05	–0.05	–0.05
KJ0052F01	3155	0.272	0.025	0.096	–0.02	–0.02	n.a.	n.a.	n.a.	–0.02	–0.02	n.a.	–0.02	–0.02
KJ0052F01	6206	0.164	–0.05	–0.05	–0.05	–0.05	–0.05	–0.05	–0.05	–0.05	–0.05	–0.05	–0.05	–0.05
KJ0052F03	3156	0.189	–0.020	0.061	–0.02	–0.02	n.a.	n.a.	n.a.	–0.02	–0.02	n.a.	–0.02	–0.02
KJ0052F03	6150	0.231	–0.05	0.074	–0.05	–0.05	–0.05	–0.05	–0.05	–0.05	–0.05	–0.05	–0.05	–0.05

2.4.2 Gas composition

The gas contents, amounts of specific gases, and volumes extracted are shown in Figures 2-5, a–b.

Table 2-5a. Content of gas in the J-niche boreholes – specific gases.

Borehole	Sample date	N_2	H_2	He	Ar	CO_2	CH_4	C_2H_2	C_2H_4	C_2H_6	C_3H_6	C_3H_8
		mL/L	µL/L	mL/L	mL/L	mL/L	mL/L	µL/L	µL/L	µL/L	µL/L	µL/L
KJ0050F01	000608	70.7	<3	7.46	0.70	0.66	0.77	<0.05	<0.05	0.3	<0.09	<0.09
KJ0052F01	000608	70.0	<3	7.42	0.80	0.20	0.63	<0.05	<0.05	0.2	<0.09	<0.09
KJ0052F03	000629	66.8	16	5.95	0.69	0.95	1.2	<0.04	<0.04	0.2	<0.08	<0.08

Table 2-5b. Content of gas in the J-niche boreholes – volume of gas and water extracted.

Borehole	Sample date	Analysis date	Volume gas	Volume water extracted
			ml	g
KJ0050F01	000608	000609	83	382
KJ0052F01	000608	000609	81	380
KJ0052F03	000629	000706	78	381

2.4.3 Stable isotopes

The stable isotopes of the carbon-containing gases were analysed. The results are shown in Table 2-6.

Table 2-6. Carbon isotope analysis of carbon dioxide and methane extracted from the J-niche boreholes.

Borehole	Sample date	IFE no GEO	CH_4 $\delta^{13}C$	CO_2 $\delta^{13}C$
			‰ PDB	‰ PDB
KJ0050F01	000608	20001393	–50.0	–21.0
KJ0052F01	000608	20001394	–50.6	–23.3
KJ0052F03	000629	20001396	–51.1	–28.1

3 Evaluation of the MICROBE-450 site characteristics

3.1 Geochemistry

The groundwater chemistry has been compared using various methods with that of other sites. First, principal component analysis (PCA) was performed. Second, data of specific interest were compared, i.e. carbonate, electron donors and acceptors for microbiological processes, and dissolved organic carbon and dissolved gases. Some of the data were compared with data obtained from site investigations pertaining to a future repository (see Table 3-1). The goal of this comparison was to assess how the conditions of the MICROBE site boreholes compare with those at the future repository site.

Table 3-1. Boreholes in igneous rock investigated for microbiology within the SKB site investigation programme, by December 2004.

Site	Borehole	Depths (m)
Forsmark	KFM01A	110–121
	KFM01A	178–184
	KFM02A	509–516
	KFM03A	448–453
	KFM03A	639–646
	KFM03A	940–946
	KFM03A	980–1002
Simpevarp	KSH01A	157–167
	KSH01A	245–262
	KSH01A	548–565

3.1.1 Principal component analysis

The evolution of groundwater is generally strongly related to present and past flow conditions. Throughout this continuous process, the type of infiltrating water as well as the existing water in the rock change in composition. The solute and isotopic content of groundwater can be interpreted as either resulting from geochemical reactions between the groundwater and the minerals it contacts, from the mixing of groundwater types of different origins (and hence different chemical signatures), or from a combination of both processes. Software tools to address these topics are under development in the international waste management community. One such tool is the multivariate mixing and mass balance (M3) model developed by SKB (Laaksoharju et al, 1999). M3 is an interpretative technique for performing cluster analysis (using multivariate principal component analysis) in order to simplify and summarize the obtained groundwater data, identify waters of different origins, infer the mixing ratio of these mixing reference waters (end members) to reproduce each sample's chemistry, identify any deviation between the chemical measurements of each sample and the theoretical chemistry from the mixing calculation, and interpret these deviations as resulting from groundwater reactions. The constituents used for the modelling are major components (Na, K, Ca, Mg, HCO_3, Cl, and SO_4), tritium (^3H), and stable isotopes (δ^2H and $\delta^{18}O$). It is known that these components contain most of the information variability in groundwater data. The boreholes analysed were KJ0050F01, KJ0052F01, and KJ0052F03.

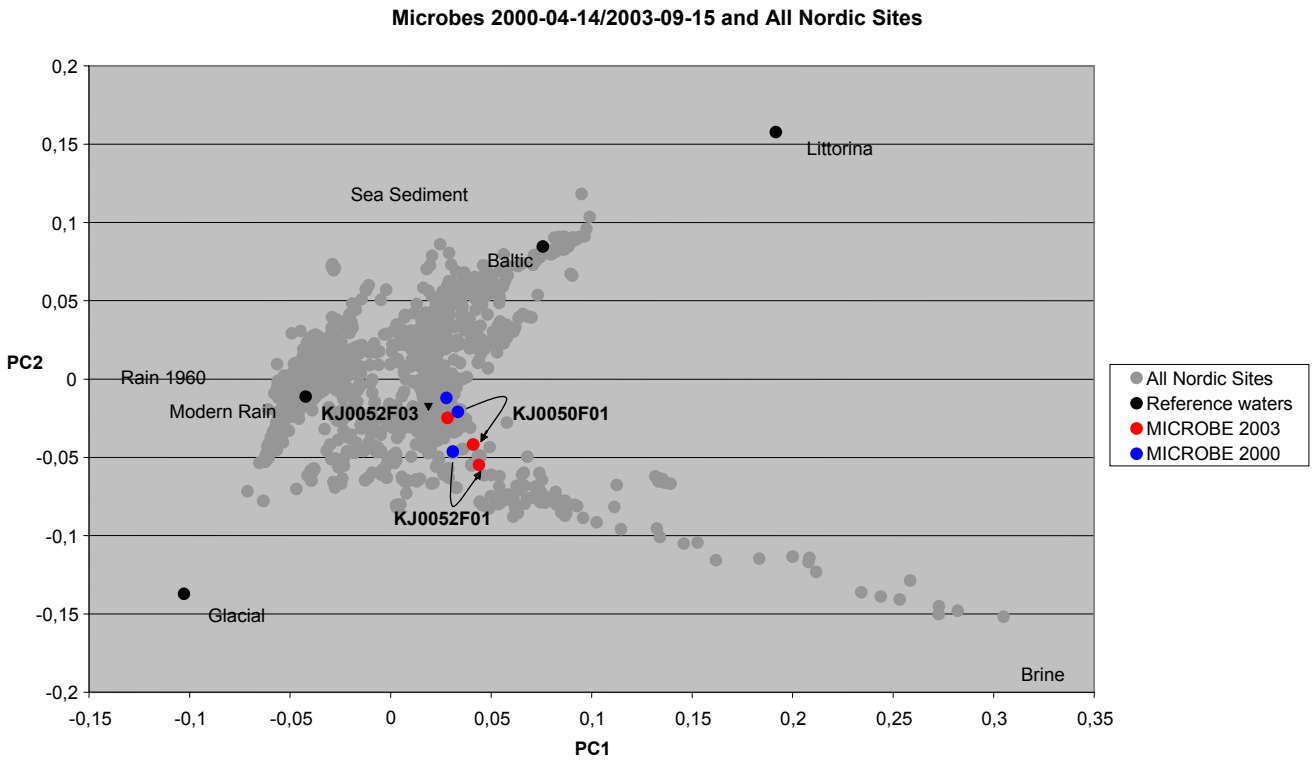

***Figure 3-1**. Principal component plot showing groundwater chemical data from the MICROBE 450-m site in comparison to data from other Nordic sites; including data from the future repository site investigations.*

The selected reference waters identified from the PCA (Figure 3-1) for the current modelling are:

Brine reference water, which represents the brine type of water found in KLX02: 1631–1681 m depth, with a measured Cl content of 47200 mg/l. Brines are waters with significantly higher salinity than ocean water (Cl content of 19800 mg/l).

Baltic Sea reference water, which represents modern Baltic Sea water, with ocean water as the saline component.

Altered marine reference water, which represents seawater altered by bacterial sulphate reduction. This water type is obtained in the HRL tunnel below marine sediments (SA0813B: 5.6–19.5 m borehole length).

Precipitation reference water, which represents dilute shallow groundwater of the type found in HLX06 (871103): 45–100 m depth.

Glacial reference water, which is a precipitation water in which the stable isotope values ($\delta^{18}O$ = –21 SMOW and $\delta^{2}H$ = –158 SMOW) are based on measured values of $\delta^{18}O$ in the calcite surface deposits, interpreted as sub-glacial precipitates, collected from various geological formations on the west coast of Sweden. The water represents a possible meltwater from the last glaciation >13000 years BP.

Principal component analysis results

The results of the PCA analysis compare the geochemical composition in April 2000 with that in September 2003. The MICROBE groundwater samples lie in the central area of the PCA plot shown in Figure 3-1. This indicates that these waters do not have an extreme groundwater composition, but rather are affected by the mixing of several reference waters. The plot shows that all three MICROBE groundwater samples have moved towards a deeper brine signature. KJ0050F01 shows the largest move and has approached the position of KJ0052F01, suggesting that deep groundwater is up-coning towards the positions of the MICROBE sites.

3.1.2 Physical and chemical parameters

The microbiological site investigations have focused on physiological groups of microbes. Their ability to use iron, manganese, sulphur, and carbon in their metabolic redox processes has been evaluated. The chemistry data from the Forsmark and Simpevarp site investigations agrees well with the MICROBE project data obtained from a depth of about 500 m, which will be the repository depth (Table 3-2). Redox of the groundwater, E_h, has been found to be important in modelling ongoing microbiological processes, but data pertaining to E_h is still lacking for the MICROBE sites. Attempts to analyse redox using a portable redox meter gave redox values that were too high to be reliable (not shown). On-line redox measurements will instead be used, as the time required to obtain stable readings has been found to be very long, often amounting to weeks (Grenthe et al., 1992).

3.1.3 Laboratory analysis of dissolved gases

Analysis of gases at the MICROBE project sites has detected gases similar to those found by the site investigation programmes (Table 3-3). However, methane levels are 10 times higher at the MICROBE sites, and hydrogen seems to be missing from two of the circulation systems. Using the on-site KAPPA-V gas chromatograph revealed hydrogen in all three circulation systems, with concentrations increasing with time; see *in situ* measurements below for details (3.1.5).

Table 3-2. Chemical composition of groundwater from the site investigations in the Forsmark area (A) and the Simpevarp area (B) compared to the MICROBE site.

A Measurement	Forsmark							MICROBE		
	KFM01	KFM01	KFM02	KFM03	KFM03	KFM03	KFM03	KJ0050F01	KJ0052F01	KJ0052F03
Depth (m)	110–121	177–184	509–516	448–453	639–646	940–947	980–1002	448.2	450.6	447.6
Date sampled (y-m-d)	03-02-24	03-03-31	03-10-20	03-10-24	04-02-23	04-03-26	03-11-11	03-09-15	03-09-15	03-09-15
Temperature (°C)	6.9	7.6	11.4	10.7	13.1	17.2	18	16.6	16.0	15.6
pH	7.47	7.60	7.18	7.49	7.55	7.67	8.26	7.4	7.4	7.4
Conductivity (mS/m)	-[a]	1481	1600	1600	1620	1890	2560	2140	2231	1700
E_h (mV)	–175	–170	–140	–250	–200	–250	–250	-	-	-
Fe^{2+} (mg/L)	0.95	0.48	1.84	0.92	0.23	0.27	0.026	0.105	0.096	0.215
Mn^{2+} (mg/L)	0.64	1.02	2.16	1.17	0.32	0.11	0.01	0.43	0.31	0.49
S^{2-} (mg/L)	<0.01	<0.01	0.01	<0.01	<0.01	<0.01	0.03	0.01	0.226[b]	0.004[b]
SO_4^{2-}(mg/L)	315	547	498	472	197	80.1	46.7	516	564	428
HCO_3 (mg/L)	61	99	125	91	22	10	6	30	15	51
DOC (mg/L)	1.5	2.3	2.1	1.2	1.6	-	1.4	2	-	2.3
Drill water (%)	4.8	0.76	6.8	0.25	4.4	8.8	7.5	0.44	0.05	0.52

[a] not analysed, [b] analysed 050117

B Measurement	Simpevarp			MICROBE		
	KSH01A	KSH01A	KSH01A	KJ0050F01	KJ0052F01	KJ0052F03
Depth (m)	157–167	245–262	548–565	448.2	450.6	447.6
Date sampled (y-m-d)	03-02-28	03-04-24	03-09-17	03-09-15	03-09-15	03-09-15
Temperature (°C)	6.3	-[a]	-	16.6	16.0	15.6
pH	7.36	7.34	7.63	7.4	7.4	7.4
Conductivity (mS/m)	1539	1718	2325	2140	2231	1700
E_h (mV)	–220	–210	–230	-	-	-
Fe^{2+} (mg/L)	1.4	1.3	0.51	0.105	0.096	0.215
Mn^{2+} (mg/L)	0.54	0.66	0.4	0.43	0.31	0.49
S^{2-} (mg/L)	<0.01	<0.01	0.05	0.01	0.226[b]	0.004[b]
SO_4^{2-}(mg/L)	31.7	51.1	230	516	564	428
HCO_3 (mg/L)	25	17	11	30	15	51
DOC (mg/L)	1.2	1.2	0.9	2	-	2.3
Drill water (%)	2.4	8.0	10.7	0.44	0.05	0.52

[a] not analysed, [b] analysed 050117

Table 3-3. Content of dissolved in groundwater from the site investigations in the Forsmark area (A) and the Simpevarp area (B) compared to the MICROBE site.

Measurement	Forsmark						MICROBE		
	KFM01	KFM02	KFM03	KFM03	KFM03	KFM03	KJ0050F01	KJ0052F01	KJ0052F03
Depth (m)	177–184	509–516	448–453	639–646	940–947	980–1002	448.2	450.6	447.6
Total gas (ml/L)	57.8	73.2	80.2	89	124.5	127.5	83	81	78
Date sampled (y-m-d)	03-03-31	03-10-20	03-10-24	04-02-23	04-03-26	03-11-11	00-06-08	00-06-08	00-06-29
He (μM)	46.4	35.7	62.5	424	750	924	333	331	266
Ar (μM)	46.0	219	38.4	45.1	62.1	71.4	31	36	31
N_2 (μM)	2420	2840	3380	3470	4710	4690	3156	3125	2982
CO_2 (μM)	4.2	179	67.0	25.4	7.1	1.3	29	9	42
H_2 (μM)	0.241	8.88	9.50	<0.17	1.96	<0.17	<0.13	<0.13	0.7
CH_4 (μM)	5.36	1.79	1.34	3.13	2.68	2.23	34	28	54
$C2H_6$ (μM)	0.062	0.011	0.0076	<0.005	0.016	0.025	0.01	0.009	0.009
C_2H_4 (μM)	0.003	0.007	0.005	0.003	0.006	<0.003	<0.004	<0.004	<0.004
C_2H_2 (μM)	<0.003	0.003	0.003	<0.003	<0.003	<0.003	<0.004	<0.004	<0.004

[a] not analysed

Measurement	Simpevarp			MICROBE		
	KSH01A	**KSH01A**	**KSH01A**	**KJ0050F01**	**KJ0052F01**	**KJ0052F03**
Depth (m)	157–167	245–262	548–565	448.2	450.6	447.6
Total gas (ml/L)	79.8	107	76.4	83	81	78
Date sampled (y-m-d)	03-02-28	03-04-24	03-09-17	00-06-08	00-06-08	00-06-29
He (µM)	98.2	67.0	335	333	331	266
Ar (µM)	57.1	49.1	62.5	31	36	31
N_2 (µM)	3370	4640	3000	3156	3125	2982
CO_2 (µM)	35.3	35.7	3.6	29	9	42
H_2 (µM)	<0.17	3.79	3.62	<0.13	<0.13	0.7
CH_4 (µM)	2.68	4.02	1.79	34	28	54
$C2H_6$ (µM)	0.045	0.039	0.031	0.01	0.009	0.009
C_2H_4 (µM)	0.010	0.042	0.032	<0.004	<0.004	<0.004
C_2H_2 (µM)	0.005	<0.003	0.016	<0.004	<0.004	<0.004

[a] not analysed

3.1.4 Calibration of the gas chromatograph

Two different gas mixtures were used to calibrate the KAPPA-V chromatograph. Gas number one contained 5 ppm each of hydrogen, carbon monoxide, carbon dioxide, methane, ethane, and ethene. Gas number two contained 50 ppm hydrogen, 1037 ppm carbon dioxide, and 985 ppm methane. Gas number 1 was used to test the precision of the chromatograph at low concentrations and the reproducibility of the gas extractor (2.3.8). Figures 3-2 and 3-3 show good reproducibility for all gases except carbon dioxide. The reason for the higher values for this gas was a small leak in the extraction cylinder. The concentration of carbon dioxide in air is about 400 ppm, and even very small leaks will immediately be evident in the analysis. The leak was mended by high quality polishing of the cylinder. Apparently, the salty groundwater leaves behind salt crystals that over time produce small scratches in the cylinder surface. However, it is easy to judge when the cylinder needs polishing from when the carbon dioxide values in the calibration procedure diverge from the expected line. Frequently flushing the system with distilled water is a standard procedure that reduces this salt problem.

The gas chromatograph detected all gases at 0.5 ppm with good reproducibility. Hydrogen and carbon monooxide are detected by the reductive gas detector with a detection limit close to 1 ppb.

Gas number two was used to investigate the linearity of the detectors for three of the gases. For methane and carbon dioxide, good linearity was found up to 700 ppm (Figures 3-4, 3-5). Hydrogen could be analysed with good linearity up to about 25 ppm (Figure 3-6); at higher concentrations, dilution must be used.

3.1.5 *In situ* measurements of carbon-containing gases and hydrogen

Variation of configurations

Gas was extracted from the circulation systems under three different configurations. The first involved extraction from the circulation systems via the boreholes, denoted *open* in Figures 3-7 to 3-9. This configuration gave the gas dissolved in the circulating groundwater. The second option was extraction from open circulation directly after the 5000 mL of groundwater was tapped off. This option is denoted *open, 5000 ml*. This was done to analyse the gas dissolved in the borehole groundwater. The third option was to analyse gas present in the circulation systems that had been closed off from the borehole section for 15 h. This configuration is denoted *closed, 15 h*. This was done to analyse gas dissolved in the groundwater circulating in the lab circulation systems. Each run in the figures represents a separate extraction.

First, it should be emphasized that the analyses presented in Figures 3-7 to 3-11 only show carbon-containing gases and hydrogen. Since the greatest amount of gas by volume comprises nitrogen and noble gases (Table 3-3), the volumes reported in Figures 3-7 to 3-9 may vary more than the analysed gases do. However, if the proportion of gases is fixed, it should nonetheless be possible to obtain information from the volume. Otherwise, all gases would have to be analysed, and that was beyond the scope of this first analysis run.

KJ0050F01 showed some discrepancy between the two *open* configuration extractions. The volume of extracted gas increased by several mL and carbon dioxide increased, while hydrogen and methane decreased somewhat. The volume of extracted gas decreased significantly in the *open, 5000 mL* configuration and levelled out in the *closed, 15 h* configuration. Methane increased and hydrogen decreased in this transition.

KJ0052F01 showed good reproducibility in the open configuration. The volume of extracted gas increased from 30 to 40 mL in the *open, 5000 mL* configuration, but the composition of major gases did not change. Carbon monoxide, ethane, and ethene did, however, decrease. In the *closed, 15 h* configuration, the volume decreased somewhat but the concentration of analysed gases, except for hydrogen, stayed at levels similar to those found in the previous configurations.

KJ0052F03 also showed an increase in volume from the *open* to the *open, 5000 mL* configuration. Methane increased in concentration, but otherwise the concentrations were not influenced to any great degree by the change in configurations. Note that ethane and ethene were below the detection threshold in this circulation system.

It is obvious that both the particular configuration used combined with the particular circulation system analysed influenced the results significantly. The reasons for this are far from obvious. Although the PEEK tubing used has a low diffusivity, some gas exchange will occur over the tube wall. KJ0052F01 and KJ0052F3 showed increased volumes when new formation water was analysed, which could indicate that gas diffused out of the system. However, KJ0050F01 showed the opposite trend, displaying a decreased volume. KJ0050F01 and KJ0052F03 had increases in methane while KJ0052F01 showed a very stable methane concentration through all the configurations. There was a general trend towards decreasing hydrogen concentrations in all circulation systems. Additional tests (not shown) have indicated a possible explanation for this seemingly random behaviour of the dissolved gases. The PEEK micropumps use small cogwheels to circulate the water. Those cogwheels were running at high speeds, close to 800 rpm, during the gas analyses. This may have caused cavitation that released gas bubbles from the groundwater. As there is a redundancy in the dissolution of gas in water, local gas phases may have been created at high points of the circulations. This possible problem has now been addressed: new cogwheels of larger dimensions have been installed, so lower pump speeds can be used. It remains to test the effects of this measure on the distributions and concentrations of dissolved gases.

Repeated analyses over time

The variability of gas concentrations in two of the circulations were analysed over a period of several months (for KJ0052F03) to more than a year (for KJ0052F01). Figures 3-10 and 3-11 show that the concentrations generally centred on borehole-specific values, with no obvious trends. The gases relate to each other in a reproducible pattern. Given the uncertainties discussed in the previous section, possibly due to cavitation caused by the pumps, the data suggest relatively stable gas concentrations over time. However, there is a significant jump in hydrogen and methane concentrations between sampling dates 021211 and 030130. The explanation could be the drilling of two new boreholes within 100 m of the MICROBE boreholes. These new boreholes, KF0066A01 and KF0069A01, are located further down the F tunnel, beyond the *Matrix borehole*, and were drilled in fall 2002. They have a deeper chemistry signature than most other

boreholes at the 500-m level, similar to that of the deepest level 860 m sampled in KAS03 during the pre-investigation stage for the rock laboratory. Possibly those boreholes connect with the MICROBE project boreholes. If so, this could explain the deeper signatures obtained in 2003 than in 2000 (Figure 3-1) and also the increase in the hydrogen and methane content; both those gases generally increase with depth (Pedersen, 2000).

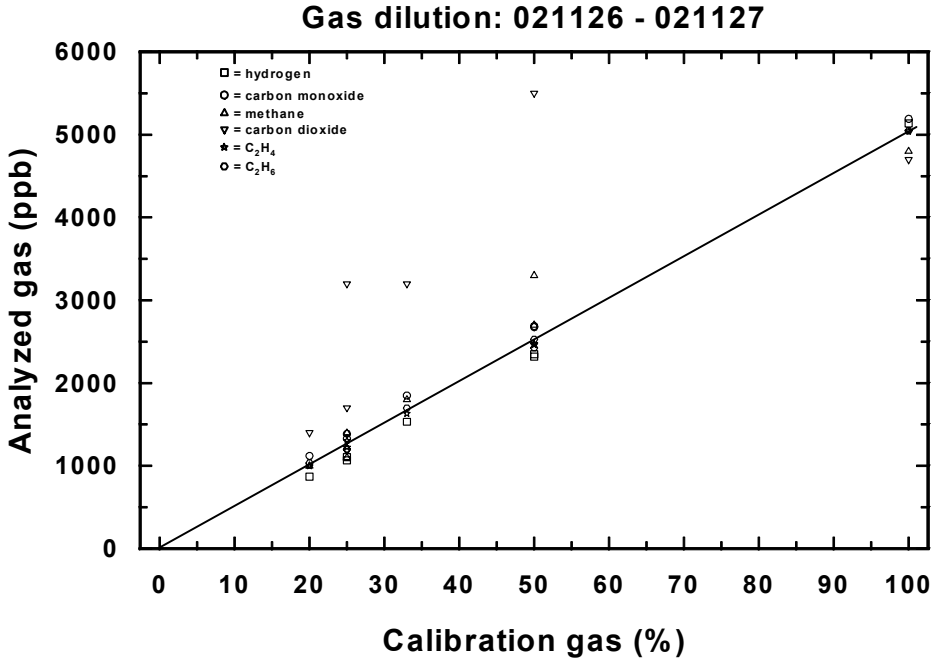

Figure 3-2. *Dilution and analysis of calibration gas in two repetitions with KAPPA-V.*

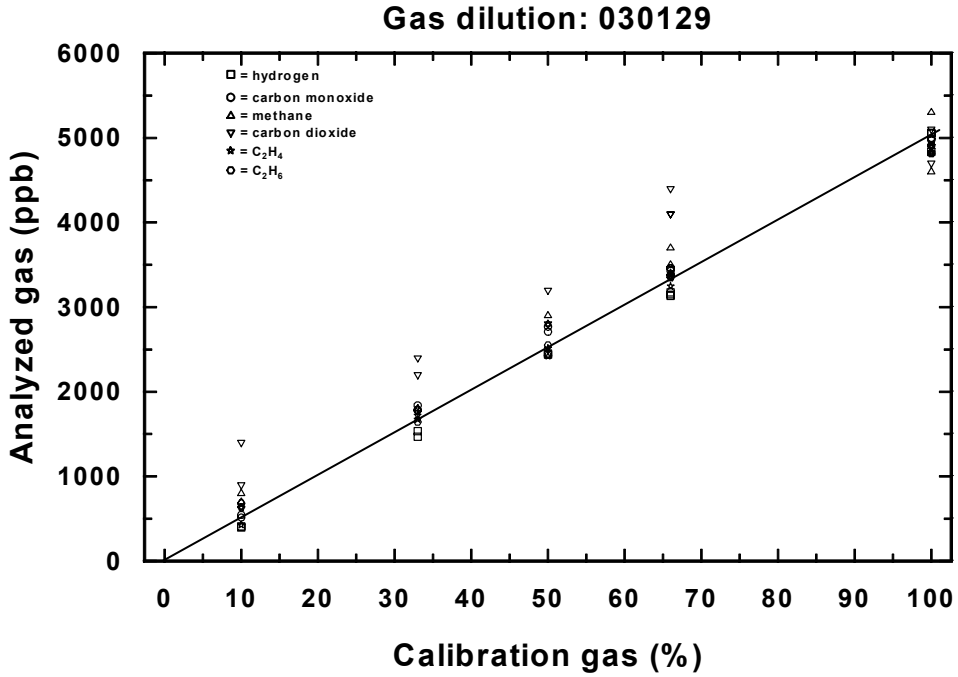

Figure 3-3. *Dilution and analysis of calibration gas in a third and fourth repetition with KAPPA-V.*

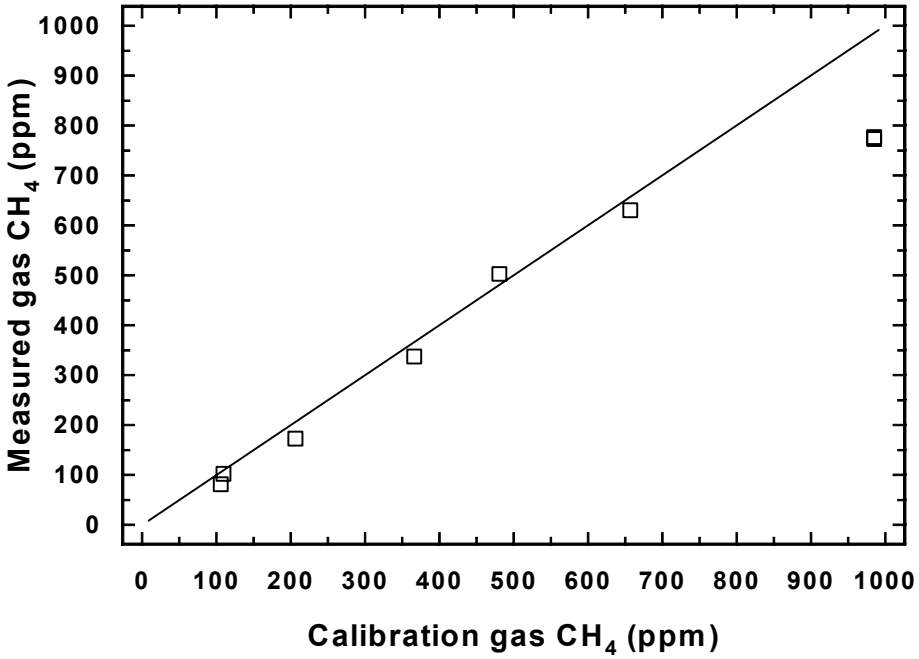

***Figure 3-4**. Linearity analysis test for methane with KAPPA-V.*

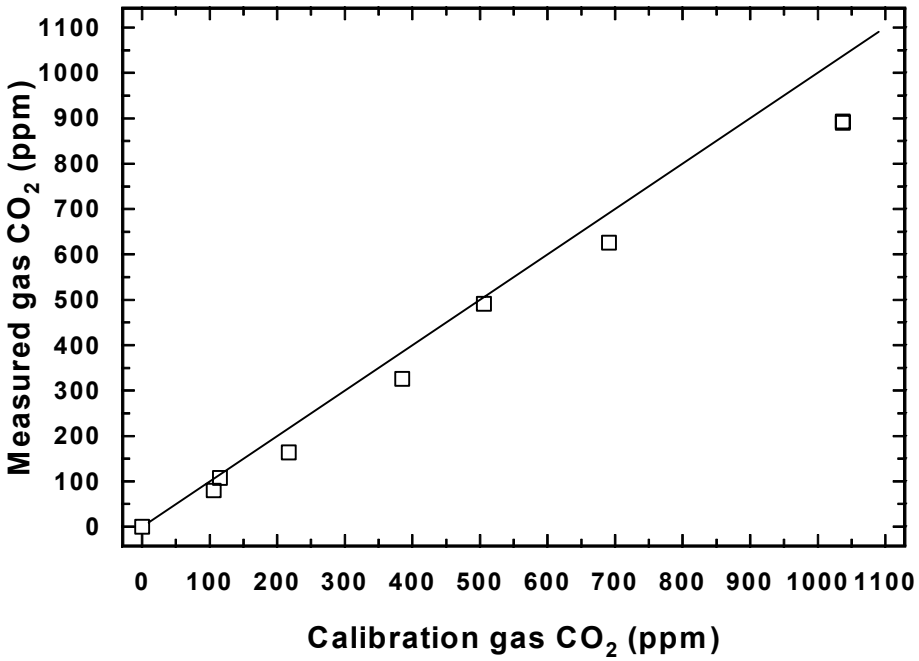

***Figure 3-5.** Linearity analysis test for carbon dioxide with KAPPA-V.*

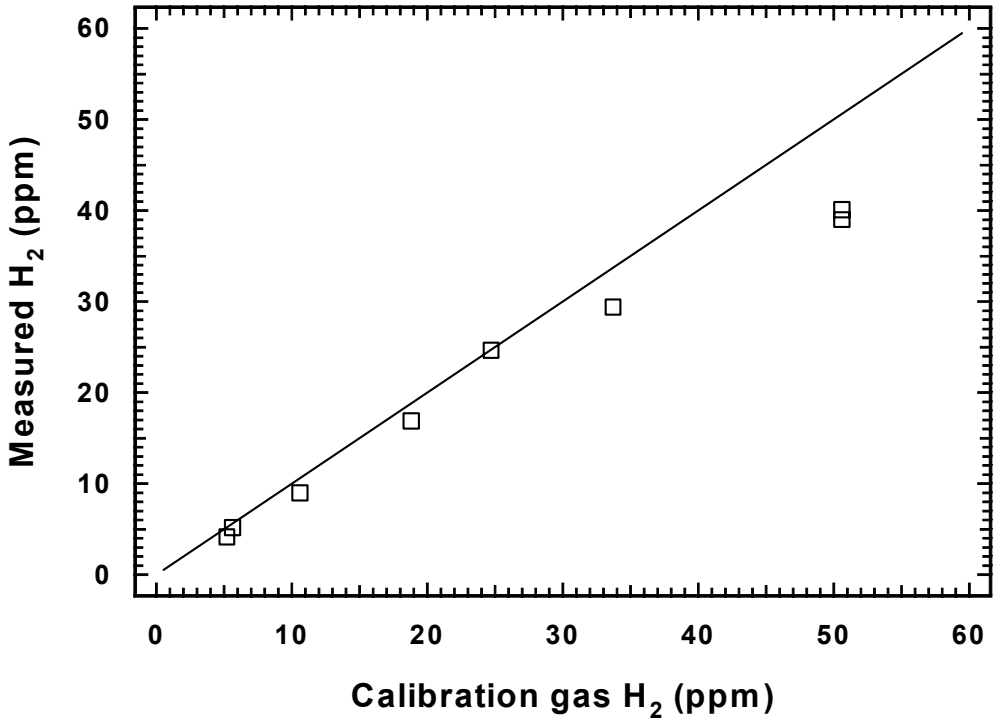

Figure 3-6. *Linearity analysis test for hydrogen with KAPPA-V.*

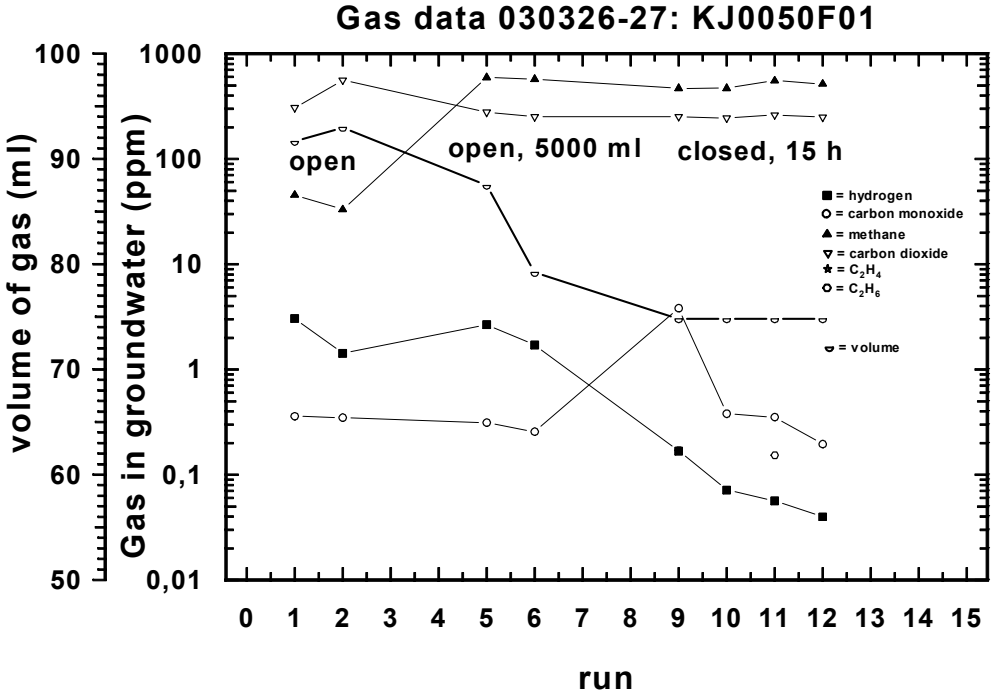

Figure 3-7. *Analysis of dissolved gas in the KJ0050F01 circulation system under various configurations. See text for details.*

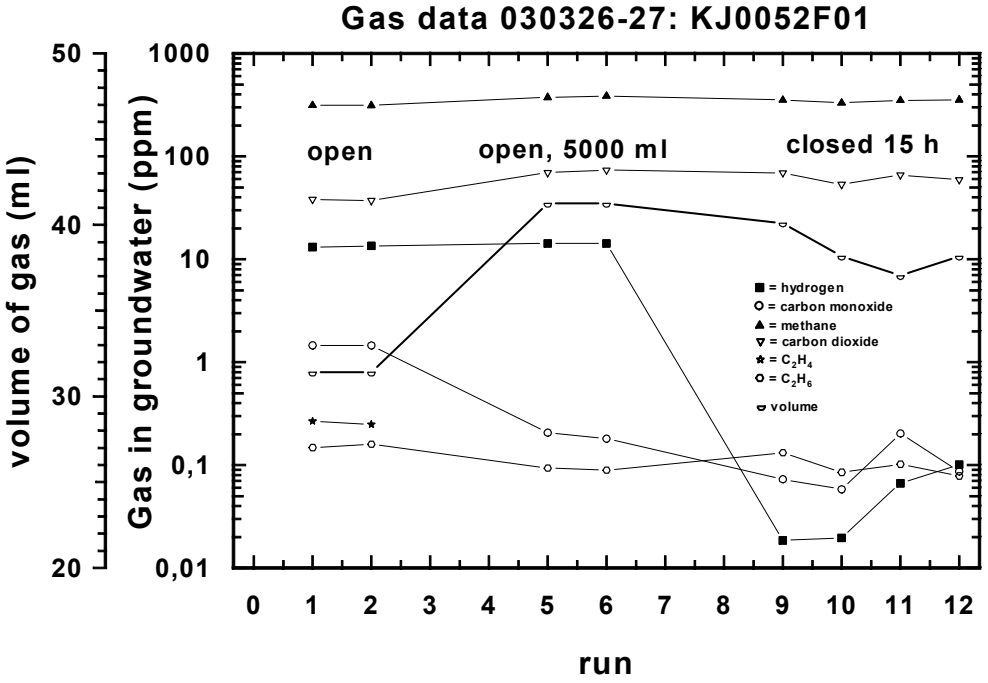

Figure 3-8. *Analysis of dissolved gas in the KJ0052F01 circulation system under various configurations. See text for details.*

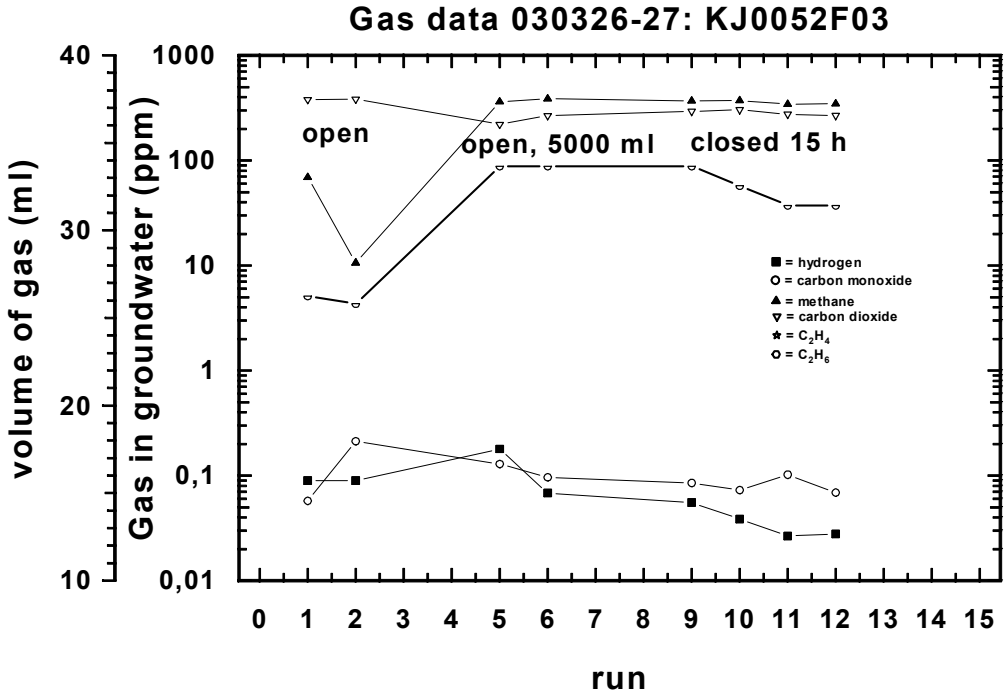

Figure 3-9. *Analysis of dissolved gas in the KJ0052F03 circulation system under various configurations. See text for details.*

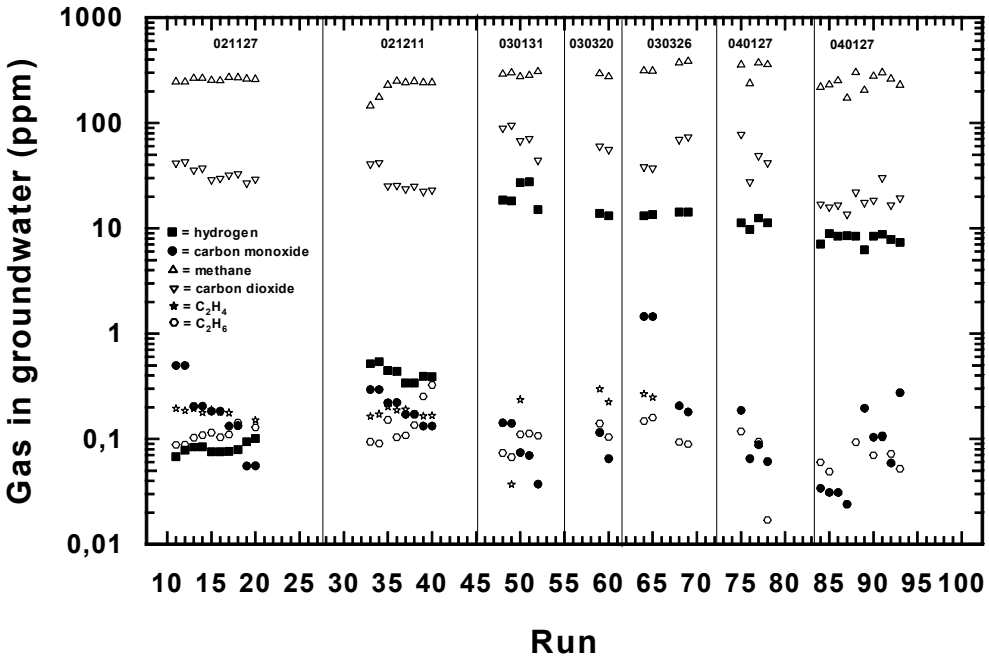

Figure 3-10. *Repeated analysis of gas in KJ0052F01 over time. Pairs of symbols indicate repeated injections from the same extraction.*

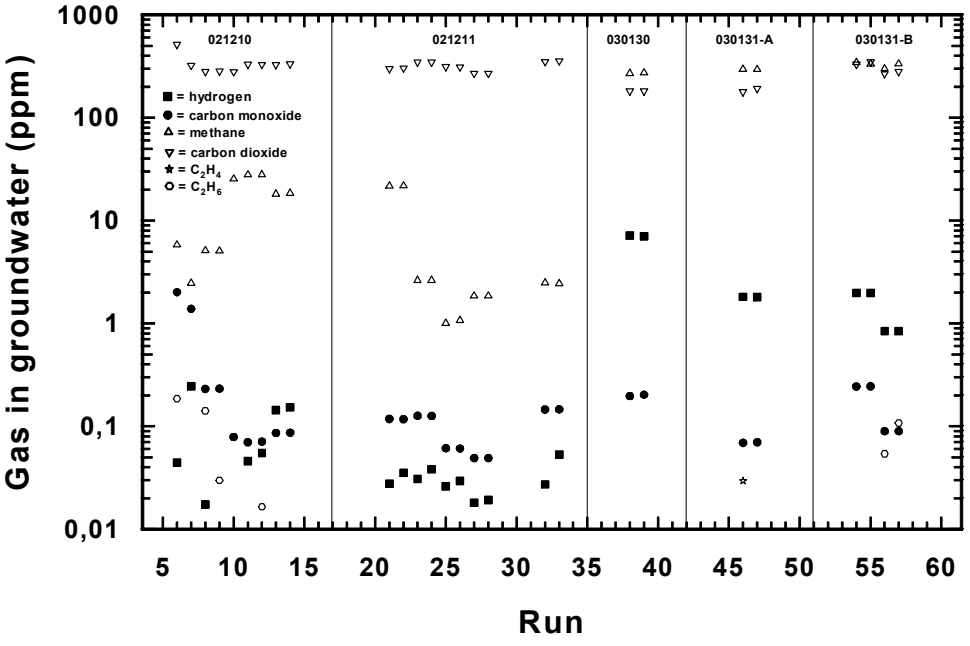

Figure 3-11. *Repeated analysis of gas in KJ0052F03 over time. Pairs of symbols indicate repeated injections from the same extraction.*

3.2 Microbiology

3.2.1 Total number of micro-organisms in groundwater

Total cell numbers were determined using the acridine orange direct count method (AODC) (Pedersen and Ekendahl, 1990). Samples were filtered onto black polycarbonate filters (0.22 µm), stained with 0.2 mL of acridine orange solution (10 µL/mL) for five minutes, and then rinsed with double-distilled water. On each filter, at least 400 cells were counted using a Zeiss epifluorescence microscope with a blue filter (530 nm). The results were calculated from an average of six filters for each sample.

3.2.2 Biomass-ATP

Water samples for ATP extraction analysis were collected in triplicate and transferred into sterile 50-mL Falcon tubes. Extraction and analysis of ATP concentrations are based on the methods of Lundin et al. (1986) and Lundin (1986). Nucleotides (ATP, ADP, and AMP) were extracted from 100-µL aliquots of groundwater within an hour of collection using 100 µL of BS buffer and charge to ATP (BioThema, ATP Biomass Kit HS, Sweden). After extraction, 100 µL of extracted ATP was mixed with 400 µL of HS buffer (BioThema, ATP Biomass Kit HS, Sweden) in a FB12/Sirius luminometer (Berthold, Germany). Prior to each sample measurement, light emission of the 400 µL of HS buffer without sample addition was allowed to diminish to fewer than 50 relative light units/second (rlu/s) in the luminometer. After addition of the ATP-extracted sample, light emission was determined using FB/Sirius PC software and a quick measurement technique was applied (Berthold, Germany). To calculate the concentration of ATP in the samples, 10 µL of internal ATP standard was added to the extracted sample in the luminometer and the light emission was measured again. All light emission measurements were performed three times. The equation used to calculate ATP concentration in the sample was:

$$\frac{(\text{average rlu/s}_{\text{sample}} - \text{average rlu/s}_{\text{HS-buffer}})}{(\text{average rlu/s}_{\text{ATP-standard}} - \text{average rlu/s}_{\text{sample}})} * 1000000 * \text{dilution} = \text{X amol ATP/mL}$$

3.2.3 Total number of micro-organisms on flow-cell surfaces

The flow cells were installed in the circulation systems on 3 July 2002; KJ0052F03 was reinstalled 18 February 2004. Sampling and counting using the AODC and ATP methods have been done, and Table 3-4 shows the results. The total numbers of cells approach between 2 and 5×10^6 cells/cm^2. These numbers seem to be typical of the MICROBE biofilms, which reach this level within 1.5 months and subsequently stay there. It may be that this is the range the groundwater system can support, and that growing to larger numbers is impossible. The circulation systems resemble chemostats, in which the cell numbers are related to the flow rate and nutrient levels (including of energy and carbon) in the flowing water (cf. 2.3.5). The ATP content gives an indication of the viability of the biofilms. On this basis KJ0052F01 is the most viable biofilm, followed by KJ0050F01; KJ0052F03 has the lowest viability, but is also much younger than the other two biofilms. Rock surfaces seem to develop biofilms with numbers similar to those of biofilms developing on glass (Table 3-4).

The typical shape, form, and distribution of biofilm organisms are displayed in Figures 3-12 to 3-14. It appears that there are significant differences in the populations on the surfaces. For instance, KJ0052F03 contained large organisms not present in the two other circulation system biofilms. The rock biofilm depicted in Figure 3-15 was obtained almost 1.5 years after the biofilm in Figure 3-14. It can still be concluded that rock and glass surfaces are colonized in a similar way (Figure 3-15) and with similar numbers (Table 3-4).

All surfaces became covered by a thin film of unknown material. Scratches in this film are visible in Figures 3-13 and 3-14. The film is, however, most visible under the scanning electron microscope (Figure 3-16), which reveals that not only the surface, but also some of the micro-organisms are partly or fully covered. It is well known that micro-organisms can produce extracellular material composed of polysaccharides and proteins that may cover a biofilm. It is currently unknown whether the observed material is of this origin, or whether it is a mixture of extracellular microbial material and surface active molecules from the groundwater.

Over time, spots of solid material developed on the surfaces, in particular in the KJ0050F01 circulation system (Figure 3-17). Growth of those deposits correlates with colonies of micro-organisms in the biofilms, as can be seen in Figure 3-16. Preliminary Electron dispersive spectroscopy (EDS) analysis identified calcium as a major component, which would suggest that calcite, a secondary fracture mineral made of CO_3^{-2} and Ca^{+2}, may be growing on surfaces in the MICROBE 450-m circulation systems. In addition, it appears as though the biofilm micro-organisms induce the growth of these deposits, as they start forming on spots where the micro-organism density is high.

Table 3-4. Total number of cells on surfaces in the flow cells and ATP.

Method	Surface	Figure	Time period	Age (months)	Cells/cm^2 (± standard deviation) $\times 10^6$		
					KJ0050F01	KJ0052F01	KJ0052F03
AODC	Glass	-	020703–020821	1.5	1.9 (±0.1)	1.8 (±0.1)	5.2 (±0.1)
AODC	Glass	3-12–3-14	020703–020918	2.5	2.1 (±0.1)	2.2 (±0.1)	3.5 (±0.1)
AODC	Glass	-	020703–031117	16.5	-	-	1.9 (±0.12)
AODC	Rock	3-15	040218–040920	7	-	-	1.5 (±0.24)
AODC	Glass	-	020703–041025	27	3.7 (±0.5)	3.1 (±0.8)	-
AODC	Glass	-	040218–041025	8	-	-	3.0 (±0.5)
ATP	Glass	-	020703–041025	27	0.026 (±0.01)	0.18 (±0.09)	
ATP	Glass	-	040218–041025	8	-	-	0.0015 (±0.0002)

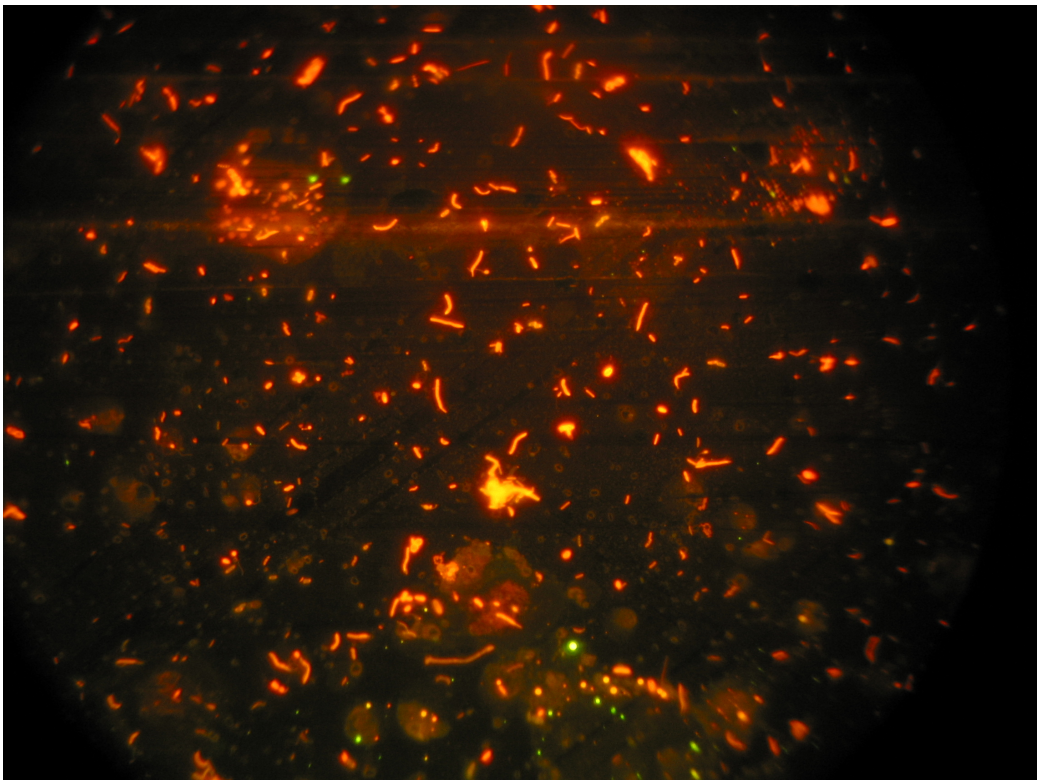

Figure 3-12. *Biofilm on glass surfaces from KJ0050F01 at an age of 2.5 months. Scale: 1 cm ≈ 10 µm.*

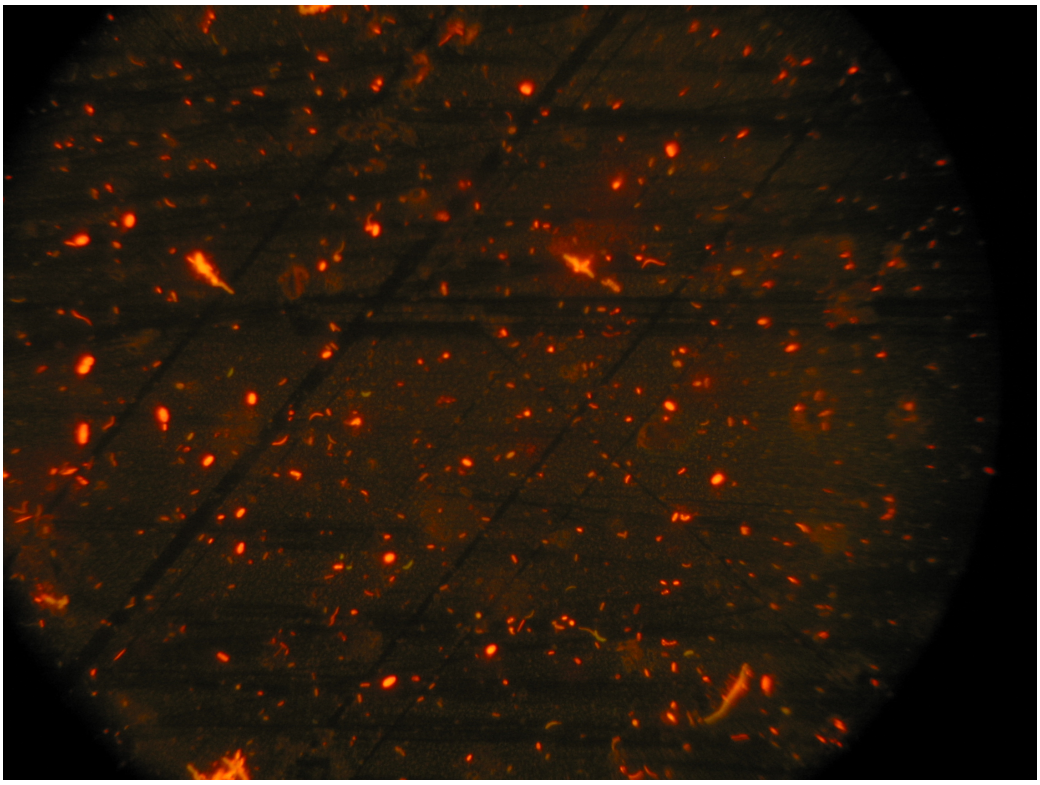

Figure 3-13. *Biofilm on glass surfaces from KJ0052F01 at an age of 2.5 months. Scale: 1 cm ≈ 10 µm.*

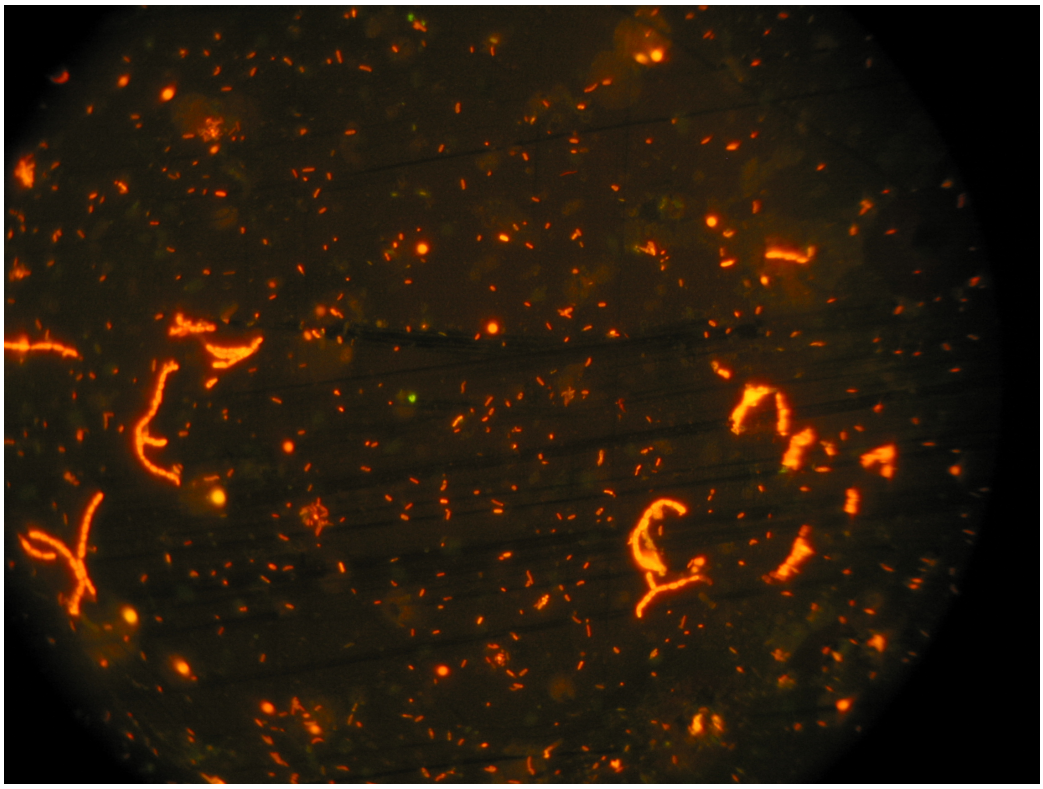

Figure 3-14. *Biofilm on glass surfaces from KJ0053F03 at an age of 2.5 months. Scale: 1 cm ≈ 10 µm.*

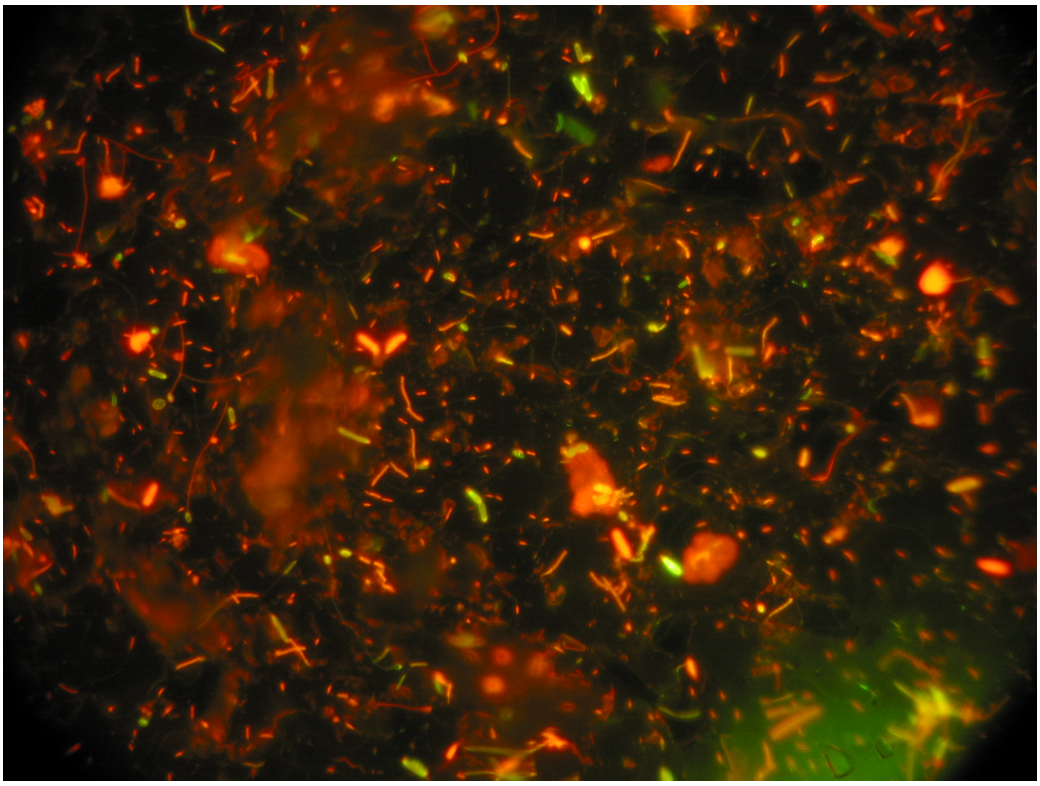

Figure 3-15. *Biofilm on rock surfaces from KJ0053F03 at an age of 7 months. Scale: 1 cm ≈ 10 µm.*

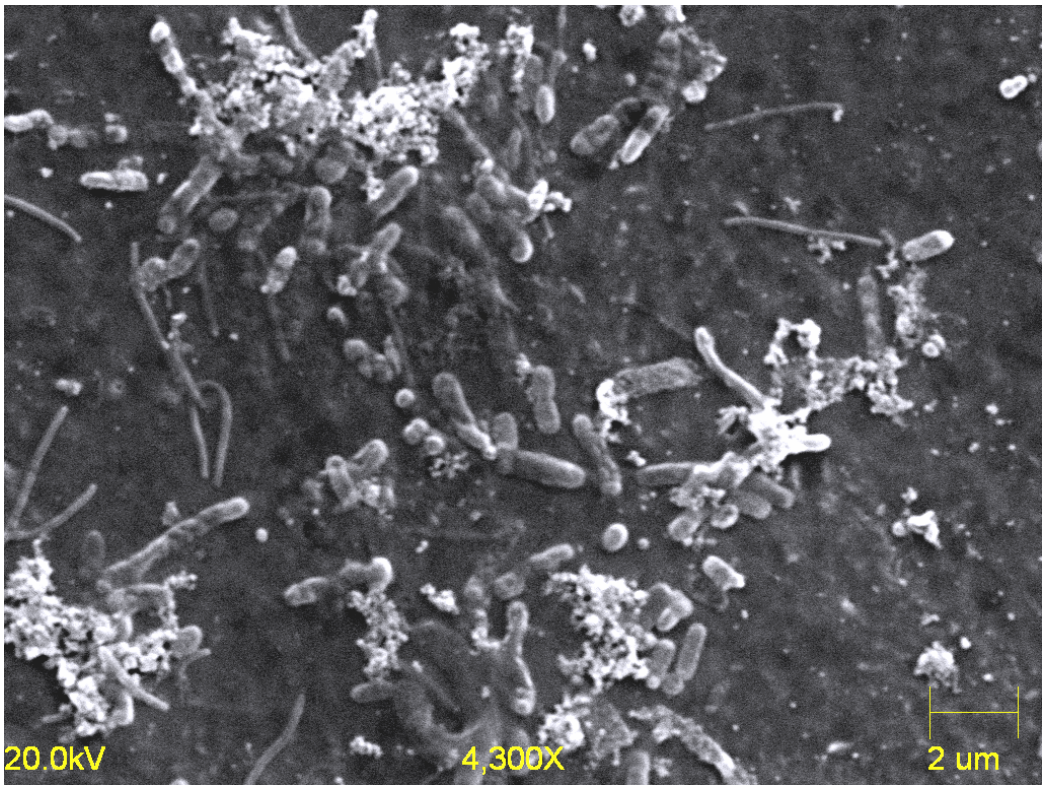

Figure 3-16. *SEM image of biofilm on glass surfaces from KJ0052F01 at an age of 24 months.*

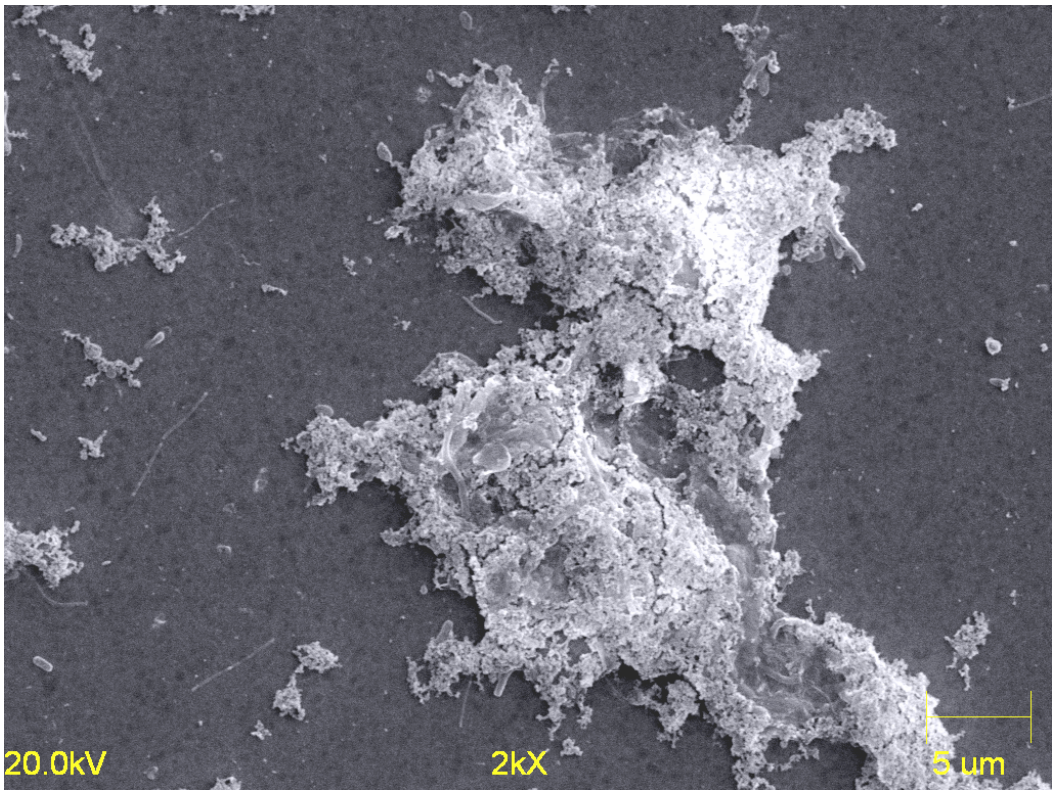

Figure 3-17. *SEM image of biofilm on glass surfaces from KJ0052F01 at an age of 24 months.*

Table 3-5A-G. Composition of anaerobic media used for MPN cultivation of different metabolic groups of anaerobic micro-organisms. All components were anoxic.

A) Ready medium	Metabolic group[a]			
Component (mL/L)	**IRB & MRB**	**SRB**	**AA & HA**	**AM & HM**
Basal medium (Table B)	940	960	860	890
Trace elements (Table C)	1.0	1.0	-	-
Trace elements (Table D)	-	-	10	10
Vitamins (Table E)	1.0	1.0	-	-
Vitamins (Table F)	-	-	10	10
$NaHCO_3$ (Table G)	30	30	60	60
$NaCH_3COO$ (Table G)	25	-	-	-
Yeast extract (Table G)	1.0	-	10	10
Thiamine stock (Table G)	1.0	1.0	1.0	1
Vitamin B_{12} stock (Table G)	1.0	1.0	1.0	1
Fe stock (Table G)	-	-	5.0	5
Resazurin (Table G)	-	1.0	2.0	2
Cysteine hydrochloride (Table G)	-	-	10	10
Bromoethansulfonic solution (BSEA) (Table G)	-	-	30	-
Selenite-tungstate (Table G)	-	1.0	-	-
Lactate (Table G)	-	5.0	-	-
Final pH	7.5	7.5	7.5	7.5

[a] IRB = iron-reducing bacteria, MRB = manganese-reducing bacteria, AM = autotrophic methanogens, HM = heterotrophic methanogens, AA = autotrophic acetogens, HA = heterotrophic acetogens.

B) Basal medium	Metabolic group[a]			
Component (g)	**IRB & MRB**	**SRB**	**AA & HA**	**AM & HM**
Double-distilled H_2O	1000	1000	1000	1000
NaCl	15	15	15	15
KCl	0.1	0.5	0.67	0.67
$MgCl_2*6H_2O$	0.1	1.2	5.5	5.5
$CaCl_2*2H_2O$	1.0	0.1	0.28	0.28
$MgSO_4*7H_2O$	0.1	-	6.9	6.9
NH_4Cl	1.5	0.25	1.0	1.0
$MnCl_2*4H_2O$	0.005	-	-	-
Na_2SO_4	-	4.0	-	-
KH_2PO_4	0.6	-	-	-
K_2HPO_4	-	0.2	0.17	0.15
$Na_2MoO_4*2H_2O$	0.001	-	-	-

[a] IRB = iron-reducing bacteria, MRB = manganese-reducing bacteria, AM = autotrophic methanogens, HM = heterotrophic methanogens, AA = autotrophic acetogens, HA = heterotrophic acetogens

C) Trace element solution	
Component	**Amount**
Double-distilled H_2O	1000 mL
Nitrilotriacetic acid	1500 mg
$Fe(NH_4)_2(SO_4)_2*6H_2O$	200 mg
Na_2SeO_3	200 mg
$CoCl_2*6H_2O$	100 mg
$MnCl_2*4H_2O$	100 mg
$Na_2MoO_4*2H_2O$	100 mg
$Na_2WO_4*2H_2O$	100 mg
$ZnSO_4*7H_2O$	100 mg
$AlCl_3$	40 mg
$NiCl_2*6H_2O$	25 mg
H_3BO_3	10 mg
$CuCl_2*2H_2O$	10 mg

D) Non-chelated trace elements	
Component	**Amount**
Double-distilled H_2O	987 mL
HCl (25% = 7.7M)	12.5 mL
$FeSO_4*7H_2O$	2.1 g
H_3BO_3	30 mg
$MnCl_2*4H_2O$	100 mg
$CoCl_2*6H_2O$	190 mg
$NiCl_2*6H_2O$	24 mg
$CuCl_2*2H_2O$	2 mg
$ZnSO_4*7H_2O$	144 mg
$Na_2MoO_4*2H_2O$	36 mg

E) Vitamin mixture for IRB, MRB, and SRB	
Component	**Amount**
Sodium phosphate buffer 10 mM pH 7.1	100 mL
4-Aminobenzoic acid	4 mg
D(+)-biotin	1 mg
Nicotinic acid	10 mg
Pyridoxine dihydrochloride	15 mg
Calcium D(+) pantothenate	5 mg

F) Vitamin mixture for AA, HA, AM, and HM	
Component	**Amount**
Sodium phosphate buffer 10 mM pH 7.1	100 mL
p-Aminobenzoic acid	10 mg
Nicotinic acid	10 mg
Calcium D(+) pantothenate	10 mg
Pyridoxine dihydrochloride	10 mg
Riboflavin	10 mg
D(+)-biotin	5 mg
Folic acid	5 mg
DL-6-8-Thiotic acid	5 mg

G) Stock solutions	
Component	**Amount**
$NaHCO_3$	84 g/L
Thiamine chloride dihydrochloride in a 25 mM sodium phosphate buffer, pH 3.4	100 mg/L
Cyanocobalamine (B_{12})	50 mg/L
$NaCH_3COO$	100g/L
Yeast extract	50 mg/L
$Fe(NH_4)_2(SO_4)_2*6H_2O$, initially dissolved in 0.1 mL concentrated HCl	20 g/L
Resazurin	500 mg/L
Cysteine-HCl	500 mg/L
Bromoethansulfonic (BESA)	35 g/L
Sodium lactate solution	50%

3.2.4 Most probable number of metabolic groups

Media preparation

Media for determining the most probable number (MPN) of metabolic groups of organisms were composed based on chemical data obtained from the boreholes during the pumping period. Synthetic media were prepared according to the scheme presented in Table 3-5. The salt concentrations of the respective circulation (Table 3-2) were adjusted with NaCl. Media for the metabolic groups of iron-reducing bacteria (IRB), manganese-reducing bacteria (MRB), sulphate-reducing bacteria (SRB), autotrophic methanogens (AM), heterotrophic methanogens (HM), autotrophic acetogens (AA), and heterotrophic acetogens (HA) were autoclaved and dispensed anaerobically into 27-mL Hungate tubes.

All culture tubes were flushed with 80/20% N_2/CO_2 gas and then each filled with 9 mL of their respective media. For IRB, 1 mL of hydrous ferric oxide (HFO) was added to each culture tube. For MRB, 2 mL of 135 mM MnO_2 solution was added. Media for the SRB contained 7.5 mL of Na_2S*9H_2O and also 1 mL of 1.0 M Na_2SO_4. Media for the acetogens and methanogens also contained 10 mL of 48 g/L Na_2S*9H_2O and no mineral substrate. For the HM, the media also contained 20 mL/L of 100 g/L NaCOOH, 3 mL/L of 6470 mM trimethylamine, 4 mL/L of methanol, and 20 mL/L of 20g/L $NaCH_3COO$. For the HA, the same procedure as was used for the HM was followed, except that $NaCH_3COO$ was not added.

MPN – inoculations and analysis for anaerobic micro-organisms

Sampling was done using the PVB sampler used for the site investigations. This sampler maintains the pressure and the anaerobic and reduced character of the sample until inoculation. The samples were transported by car to the laboratory in Göteborg and analysed the same day, within 5–6 h.

Inoculations were performed in the laboratory directly upon the arrival of the PVB sampler. After inoculation, the headspace of AA and AM tubes was flushed with 80/20% H_2/CO_2 to an overpressure of 1 bar; all MPN tubes were then incubated in the dark at 17°C for 6–8 weeks. Analysis of the MPN tubes after incubation was performed by detecting metabolic products. The presence of IRB was determined using a HACH spectrophotometer and a 1,10 phenanthroline method to detect ferrous iron concentrations in solution (Greenberg, Clesceri and Eaton, 1992). A periodate oxidation method was used with a HACH spectrophotometer to determine the amount of Mn^{2+} in solution for the estimation of MRB (Greenberg et al., 1992). Detection of SRB was assessed by measuring sulphide production using the $CuSO_4$ method described by Widdel and Bak (1992) with a UV visible spectrophotometer (Ultraspec 2000, Amersham Pharmacia Biotech). Methanogen presence was signalled by the production of CH_4 in the headspace of the culture tubes; this production was detected by gas chromatography (Varian 3400) using a flame ionization detector (column temperature, 65°C; detector temperature, 200°C), a Porapak Q column (2m × 1/8 inch diameter), and N_2 carrier gas. Acetogen presence was marked by acetic acid production, which was detected by an enzymatic UV method (enzymatic bioanalysis kit, Boehringer Mannheim, Germany) using a UV visible spectrophotometer (Ultraspec 2000, Amersham Pharmacia Biotech).

The MPN procedure results in a scheme in which tubes were graded positively or negatively for growth in comparison to a control. Three dilutions were used to calculate the most probable number of each group, according to the calculations found in Greenberg et al. (1992).

Results

Total numbers

The total numbers of cells are similar to those found in the repository site investigation programme, i.e. between 10^4 and 10^6 cell/mL (Table 3-6). Over time, KJ0052F01 was found to contain significantly more cells than the two other circulation systems. This difference was confirmed by the ATP analysis (Figure 3-18), which is presented below.

Biomass-ATP

The amount of ATP has been recalculated in the form of cells/mL using the relationship 2 amol ATP = 1 cell, which represents an upper limit for healthily growing cells. The relationship approaches 1 amol per cell in some cases. ATP was measured on two occasions as part of the MICROBE project, showing an increase in biomass from spring to fall 2004 (Table 3-6). The ATP values correlate reasonably well with the total numbers (Figure 3-18). The analysis of ATP in deep groundwater is still a new application of this method, and a separate paper (in preparation) will discuss the rationale behind ATP analysis in much greater detail.

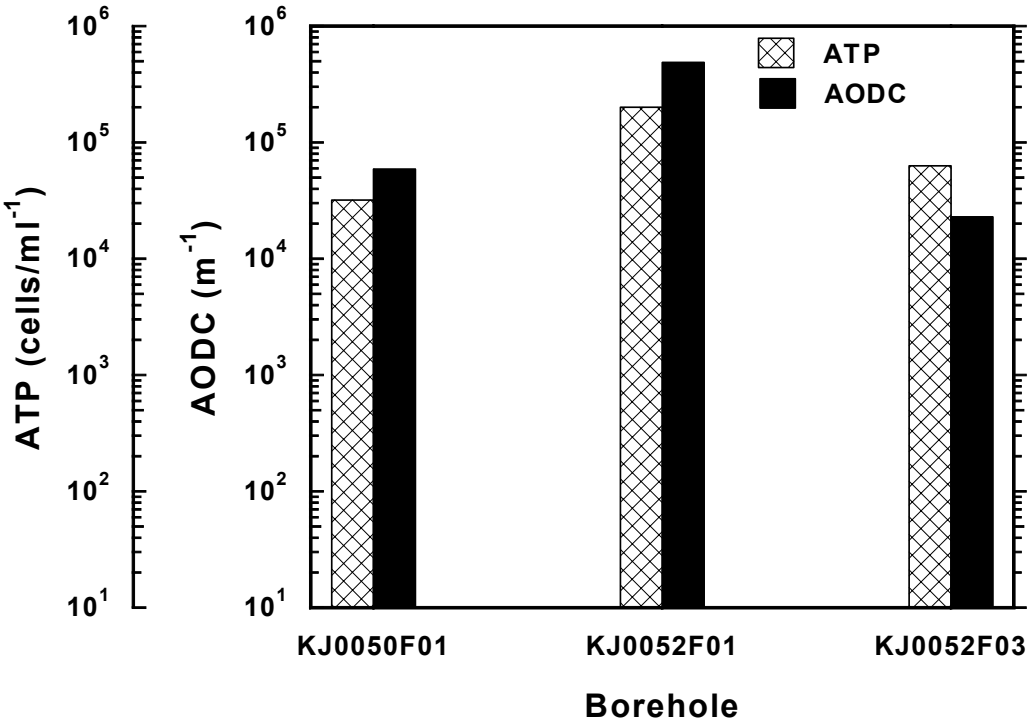

Figure 3-18. *Total number of cells measured as ATP and using microscopy (the AODC method). Table 3-6 gives the numerical data.*

Most probable numbers

Figure 3-19 and table 3-6 show the results of the MPN analysis. All groups analysed for were found, except for iron-reducing bacteria (albeit, manganese-reducing bacteria were not found in KJ0052F01). The dominant groups of micro-organisms were the acetogens followed by sulphate-reducing bacteria and methanogens. KJ0052F03 contained significantly lower numbers of microbes, generally about 100 times lower, than did the other two boreholes. This is possibly explained by the fact that the PCA signature of this borehole was shallower than the other two (Figure 3-1). All microbes analysed, except for IRB and MRB, are stimulated by a very low redox potential (–250 to –400 mV). The redox potential is usually lower in groundwater with a deep signature, than it is in shallower groundwaters.

The obtained data for acetogens and methanogens correlate excellently with the MPN data obtained from the Äspö HRL tunnel between 1994 and 1996 (cf. Figure 3 in Kotelnikova and Pedersen, 1998). At a depth of 400–450 m, acetogens averaged around 1000 cells per mL of groundwater, while methanogens averaged around 100 cells per mL groundwater.

The MPN results demonstrate the robustness of the MPN method. The data also suggest that microbial populations in deep groundwater at Äspö are stable and in a steady state with their deep aquifer environment.

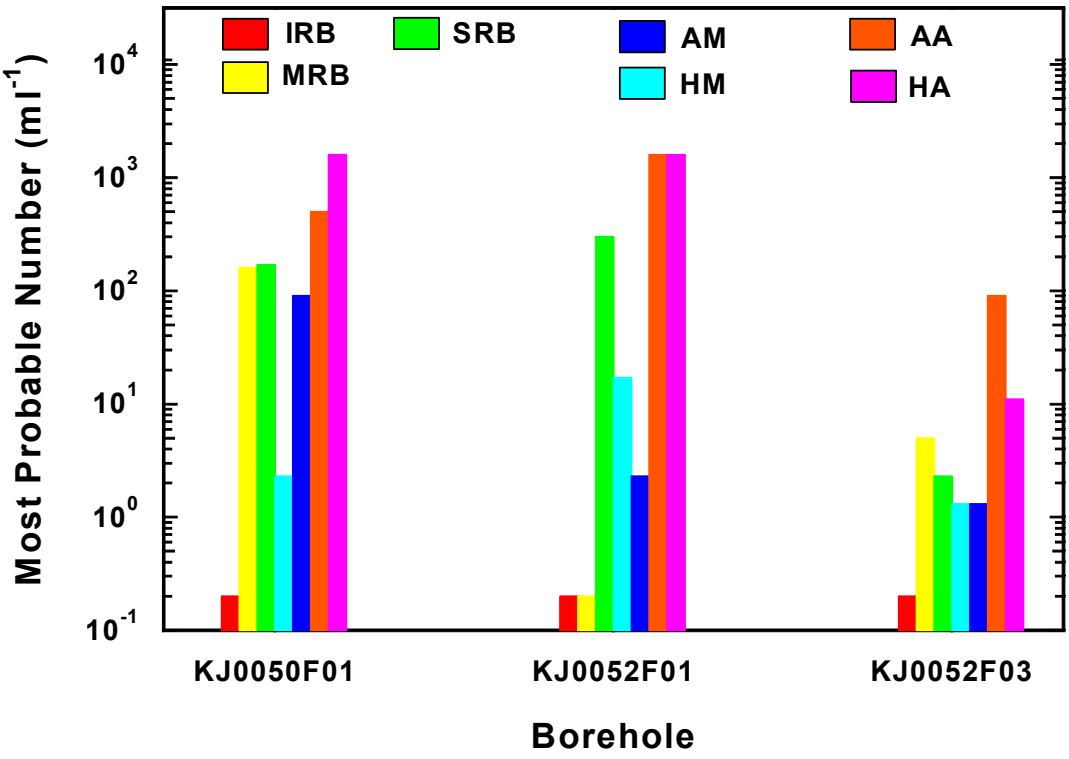

Figure 3-19. *Most probable numbers of different physiological groups of micro-organisms in the MICROBE circulations. Table 3-6 gives the numerical data.*

TABLE 3-6A-B Total number of cells and the most probable numbers of metabolic groups of micro-organisms in groundwater from deep granitic rock aquifers in Sweden, sampled with the borehole sampler PVB.

A Measurement[a]	Forsmark							MICROBE		
	KFM01	KFM01	KFM02	KFM03	KFM03	KFM03	KFM03	KJ0050F01	KJ0052F01	KJ0052F03
Depth (m)	110–121	177–184	509–516	448–453	639–646	940–947	980–1002	448.2	450.6	447.6
Total number (±SD[b]) $\times 10^4$ (cells/mL)	5.8 (2.5)	3.9 (2.3)	5.9 (2.4)	10 (1.8)	2.1 (–)	6.1 (1.6)	5.8 (0.42)	73[c] (2.0) 5.6[d] (1.6) 8.0[f] (1.5)	62[c] (10) 49[d] (19) 11[f] (0.8)	69[c] (4.0) 2.3[d] (0.3) 8.2[f] (2.1)
ATP $\times 10^4$ (cells/mL)	n.a.[e]	n.a.	n.a.	28 (0.8)	4.6 (3)	2.4 (2.5)	n.a.	3.2[c] (0.8) 46.2[f] (0.4)	20[c] (7) 135[f] (15)	6.3[c] (0.3) 28.5[f] (5.8)
IRB (cells/mL)	4000[g]	4	11	11	22	<0.2	<0.2	<0.2	<0.2	<0.2
MRB (cells/mL)	3000	<0.2	<0.2	70	1.7	1.2	<0.2	160	<0.2	5
SRB (cells/mL)	1.2	0.2	1.4	17	30	5000	24	170	300	2.3
AM (cells/mL)	n.a.	n.a.	<0.2	0.7	0.4	<0.2	<0.2	2.3	17	1.3
HM (cells/mL)	1.2	1.7	0.8	90	1.3	17	5	90	2.3	1.3
AA (cells/mL)	n.a	n.a	0.9	0.8	11	900	30	500	1600	90
HA (cells/mL)	n.a	n.a	160	90	17	23000	2.2	1600	>1600	11
Proportion of total cells cultured (%)	12	0.015	0.29	0.28	0.40	48	0.16	0.3	0.32	0.014

[a] IRB = iron-reducing bacteria, MRB = manganese-reducing bacteria, AM = autotrophic methanogens, HM = heterotrophic methanogens, AA = autotrophic acetogens, HA = heterotrophic acetogens. 2 amol ATP = 1 cell. [b] Standard deviation. [c] Sampled 020821, [d] Sampled 040322, [e] not analysed. [f] Sampled 041014. [g] Lower and upper 95% confidence limits are approximately –50% and + 100%, respectively.

B Measurement[a]	Simpevarp			MICROBE		
	KSH01A	KSH01A	KSH01A	KJ0050F01	KJ0052F01	KJ0052F03
Depth (m)	157–167	245–262	548–565	448.2	450.6	447.6
Total number (±SD[b]) × 10^4 (cells/mL)	14 (5.8)	10 (1.5)	7.2 (0.93)	73[c] (2.0) 5.6[d] (1.6) 8.0[f] (1.5)	62[c] (10) 49[d] (19) 11[f] (0.8)	69[c] (4.0) 2.3[d] (0.3) 8.2[f] (2.1)
ATP × 10^4 (cells/mL)	n.a.	n.a.	n.a.	3.2[c] (0.8) 46.2[f] (0.4)	20[c] (7) 135[f] (15)	6.3[c] (0.3) 28.5[f] (5.8)
IRB (cells/mL)	2.1	2.1	3.3	<0.2	<0.2	<0.2
MRB (cells/mL)	3.3	<0.2	<0.2	160	<0.2	5
SRB (cells/mL)	160	22	35	170	300	2.3
HM (cells/mL)	n.a	700	2.6	2.3	17	1.3
AM (cells/mL)	n.a	<0.2	<0.2	90	2.3	1.3
HA (cells/mL)	n.a	900	17	500	1600	90
AA (cells/mL)	n.a	n.a.	30	1600	>1600	11
Proportion of total cells cultured (%)	0.12	1.6	0.085	0.3	0.32	0.014

[a] IRB = iron-reducing bacteria, MRB = manganese-reducing bacteria, AM = autotrophic methanogens, HM = heterotrophic methanogens, AA = autotrophic acetogens, HA = heterotrophic acetogens. 2 amol ATP = 1 cell. [b] Standard deviation. [c] Sampled 020821, [d] Sampled 040322, [e] not analysed. [f] Sampled 041014. [g] Lower and upper 95% confidence limits are approximately –50% and + 100%, respectively.

4 References

Ekendahl, S., A.H. O'Neill, E. Thomsson and K. Pedersen. 2003. Characterisation of yeasts isolated from deep igneous rock aquifers of the Fennoscandian Shield. Microb. Ecol. **46**, 416-428.

Ferris, F.G., R.O. Hallberg, B. Lyvén and K. Pedersen. 2000. Retention of strontium, cesium, lead and uranium by bacterial iron oxides from a subterranean environment. Applied Geochemistry **15**, 1035-1042.

Ferris, F.G., K.O. Konhauser, B. Lyuvén and K. Pedersen. 1999. Accumulation of metals by bacteriogenic iron oxides in a subterranean environment. Geomicrobiol. J. **16**, 181-192.

Greenberg, A.E., L.S. Clesceri and A.D. Eaton.1992. Estimation of Bacterial DensityStandard methods for the examination of water and wastewater 18th ed, pp. 9-49. American Public Health Association, Washington.

Grenthe, I., W. Stumm, M. Laaksoharju, A.-C. Nilsson and P. Wikberg. 1992. Redox potentials and redox reactions in deep ground water systems. Chemical Geology **98**, 131-150.

Hallbeck, L. and K. Pedersen. 1990. Culture parameters regulating stalk formation and growth rate of *Gallionella ferruginea*. J. Gen. Microbiol. **136**, 1675–1680.

Hallbeck, L. and K. Pedersen. 1991. Autotrophic and mixotrophic growth of *Gallionella ferruginea*. J. Gen. Microbiol. **137**, 2657–2661.

Hallbeck, L. and K. Pedersen. 1995. Benefits associated with the stalk of *Gallionella ferruginea*, evaluated by comparison of a stalk-forming and a non-stalk-forming strain and biofilm studies in *situ*. Microb. Ecol. **30**, 257–268.

Hallbeck, L., F. Ståhl and K. Pedersen. 1993. Phylogeny and phenotypic characterization of the stalk-forming and iron-oxidizing bacterium *Gallionella ferruginea*. J. Gen. Microbiol. **139**, 1531–1535.

Haveman, S.A. and K. Pedersen. 2002. Microbially mediated redox processes in natural analogues for radioactive waste. J. Contam. Hydrol. **55**, 161–174.

Kotelnikova, S. and K. Pedersen. 1998. Distribution and activity of methanogens and homoacetogens in deep granitic aquifers at Äspö Hard Rock Laboratory, Sweden. FEMS Microbiol. Ecol. **26**, 121–134.

Laaksoharju, M., K. Pedersen, I. Rhen, C. Skårman, E.-L. Tullborg, B. Wallin and W. Wikberg. 1995. Sulphate reduction in the Äspö HRL tunnel, pp. 1–87. Swedish Nuclear Fuel and Waste Management Co., Stockholm.

Laaksoharju, M., C. Skårman and E. Skårman. 1999. Multivariate mixing and mass balance (M3) calculations, a new tool for decoding hydrogeochemical information. Applied Geochemistry **14**, 861–871.

Lundin, A.. 1986. Use of firefly luciferase in ATP-related assays of biomass, enzymes, and metabolites. Meth. Enzymol. **305**, 346–370.

Lundin, A., M. Hasenson, J. Persson and Å. Pousette. 1986. Estimation of biomass in growing cell lines by adenosine triphosphate assay. Meth. Enzymol. **133**, 27–42.

Pedersen, K.. 1982. Method for studying microbial biofilms in flowing-water systems. Appl. Environ. Microbiol. **43**, 6–13.

Pedersen, K.. 2000. The microbe site. Drilling, instrumentation and characterisation. SKB International Progress Report, IPR-00-36 **IPR-00-36**, 1–25.

Pedersen, K. 2001. Diversity and activity of microorganisms in deep igneous rock aquifers of the Fennoscandian Shield, pp 97–139. *In* J.K. Fredrickson and M. Fletcher (eds.), Subsurface microbiology and biogeochemistry. Wiley-Liss Inc., New York.

Pedersen, K. 2002. Microbial processes in the disposal of high level radioactive waste 500 m underground in Fennoscandian shield rocks, pp 279–311. *In* M.J. Keith-Roach and F.R. Livens (eds.), Interactions of microorganisms with radionuclides. Elsevier, Amsterdam.

Pedersen, K. 2003. Past and present biofilm formation in deep Fennoscandian shield groundwater, pp 371–380. *In* W. Krumbein, D.M. Paterson and G.A. Zavarzin (eds.), Fossil and recent Biofilms. A natural history of life on earth. Kluwer Academic Publishers, Dordrecht.

Pedersen, K. and S. Ekendahl. 1990. Distribution and activity of bacteria in deep granitic groundwaters of southeastern Sweden. Microb. Ecol. **20**, 37–52.

Pedersen, K., C. Holmström, A.-K. Olsson and A. Pedersen. 1986. Statistic evaluation of the influence of species variation, culture conditions, surface wettability and fluid shear on attachment and biofilm development of marine bacteria. Arch. Microbiol. **145**, 1–8.

Pedersen, K., M. Motamedi, O. Karnland and T. Sandén. 2000a. Cultivability of microorganisms introduced into a compacted bentonite clay buffer under high-level radioactive waste repository conditions. Engineering Geology **58**, 149–161.

Pedersen, K., M. Motamedi, O. Karnland and T. Sandén. 2000b. Mixing and sulphate-reducing activity of bacteria in swelling compacted bentonite clay under high-level radioactive waste repository conditions. J. Appl. Microbiol. **89**, 1038–1047.

Taylor, C.D. and C.O. Wirsen. 1997. Microbiology and ecology of filamentous sulfur formation. Science **277**, 1483–1485.

Widdel, F. and F. Bak 1992. Gram-negative, mesophilic sulphate-reducing bacteria, pp 3352–3378. *In* A. Balows, H.G. Truper, M. Dworkin, W. Harder and K.-Z. Schleifer (eds.), The prokaryotes. Springer-Verlag, New York.

5 Appendix 1: Expansion vessel

5.1 Schematic drawing

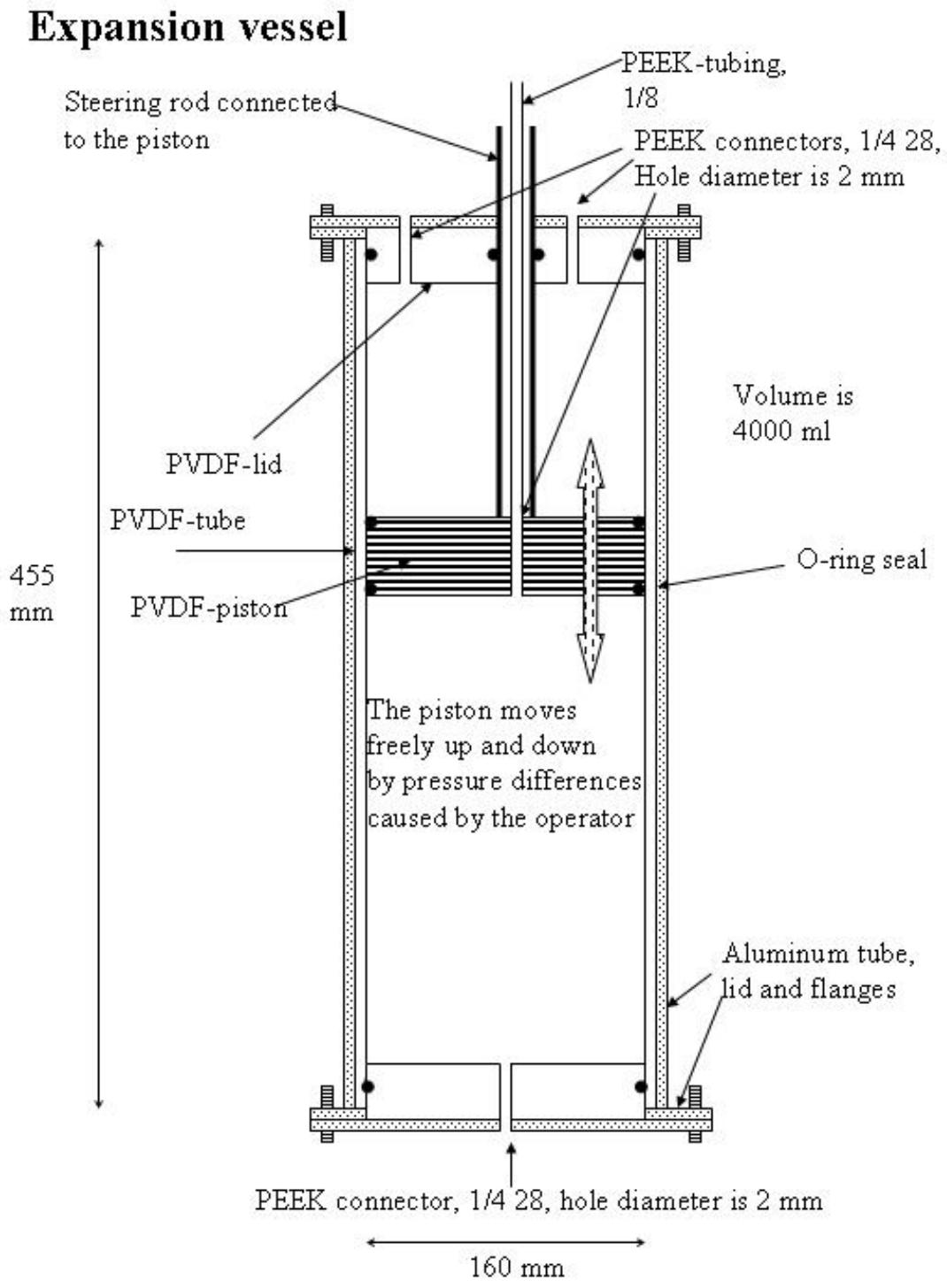

5.2 Construction drawing, dimensions in mm.

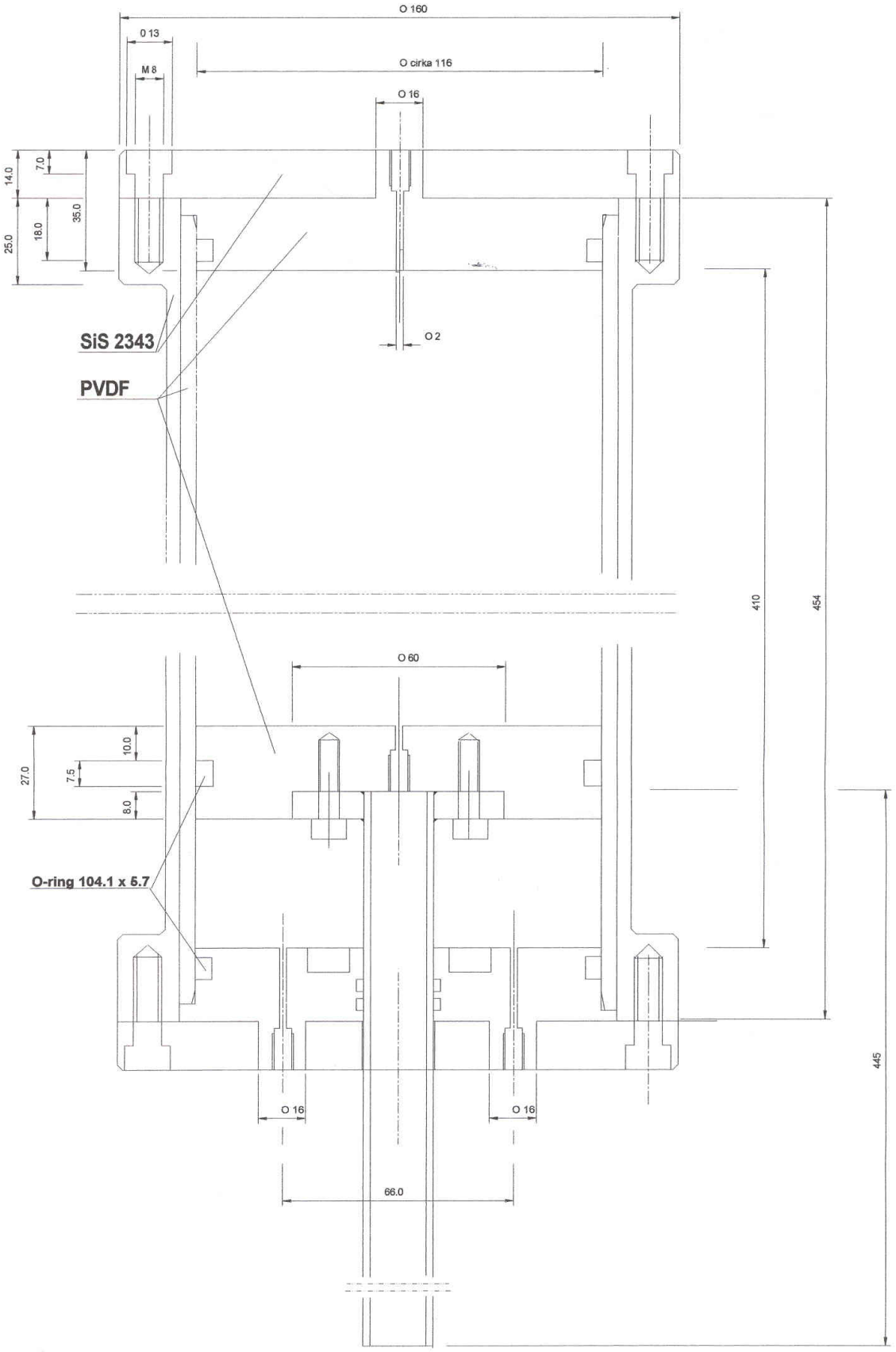

6 Appendix 2: Flow cell

6.1 The flow-cell tube and diffusers, dimensions in mm.

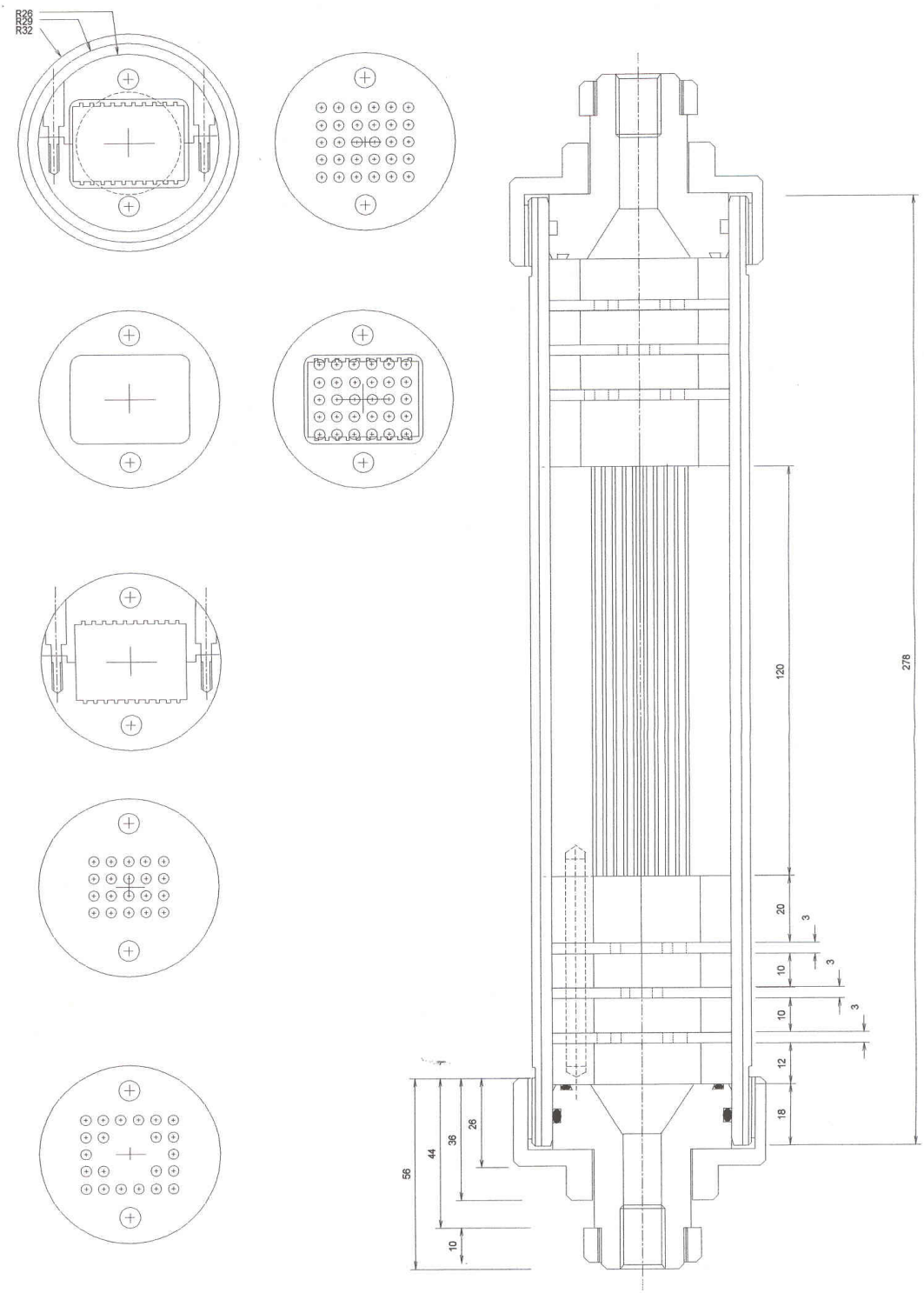

6.2 Holders for diffusers, dimensions in mm.

Typ 1

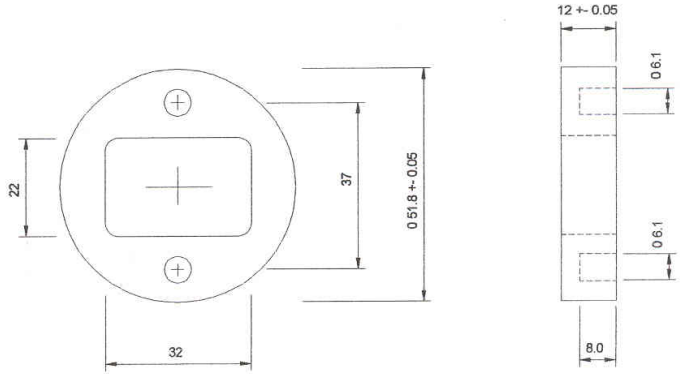

Typ 2

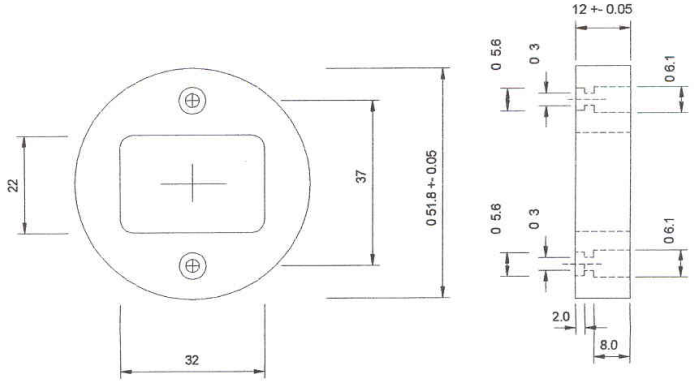

Typ 3

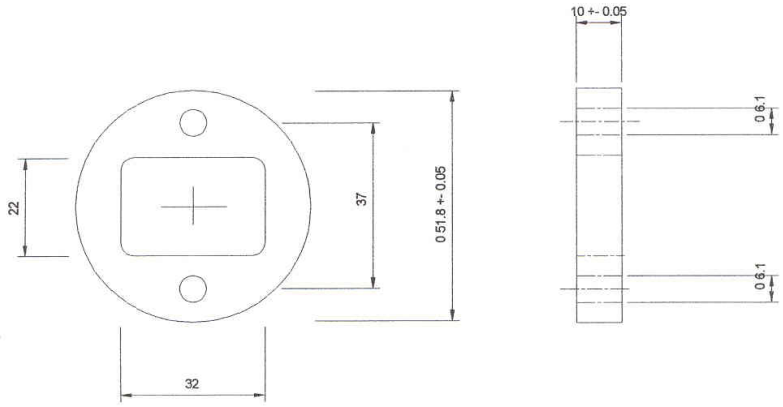

Typ 4

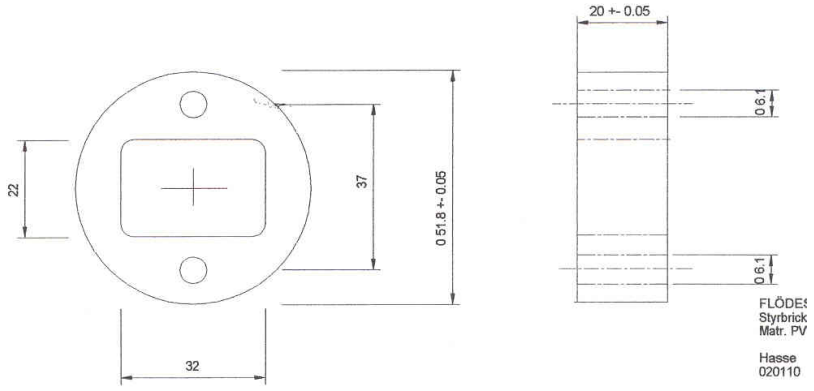

6.3 Diffusers, dimensions in mm.

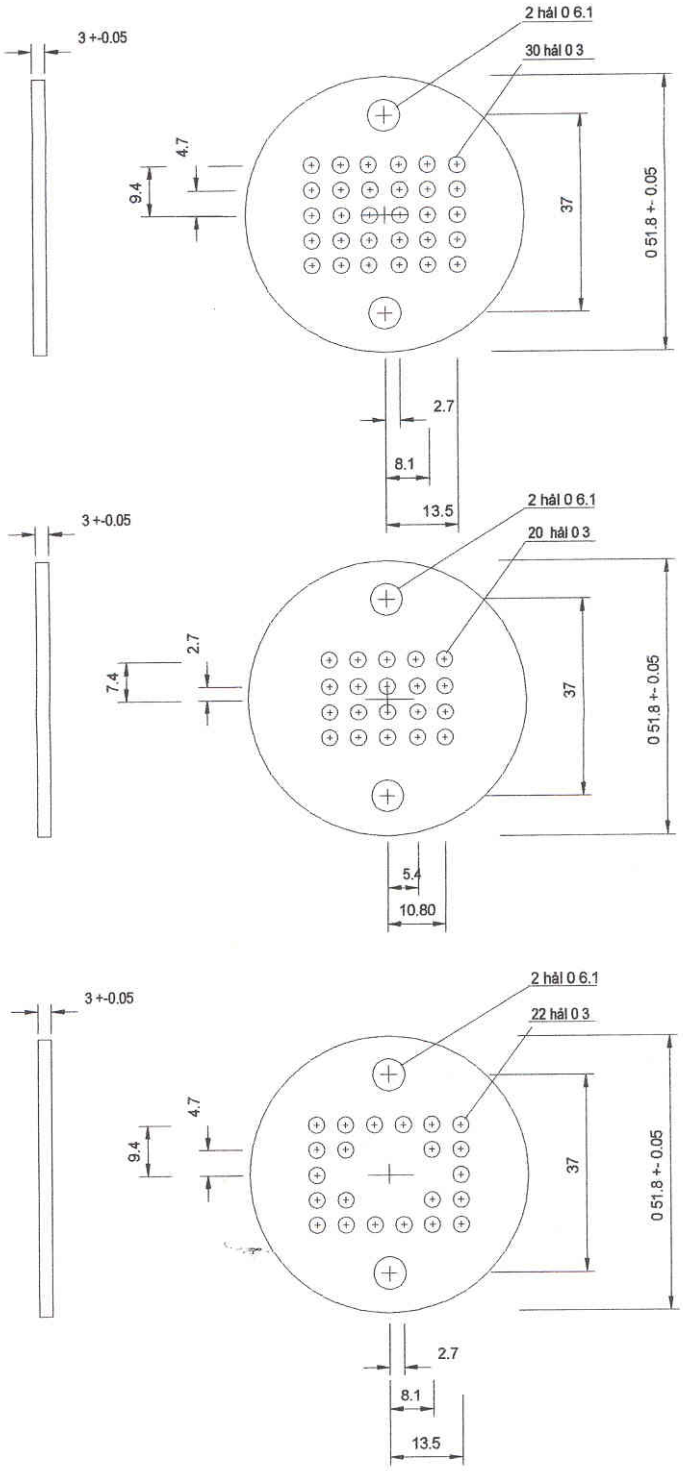

6.4 Inlet/outlet of flow cell, dimensions in mm.

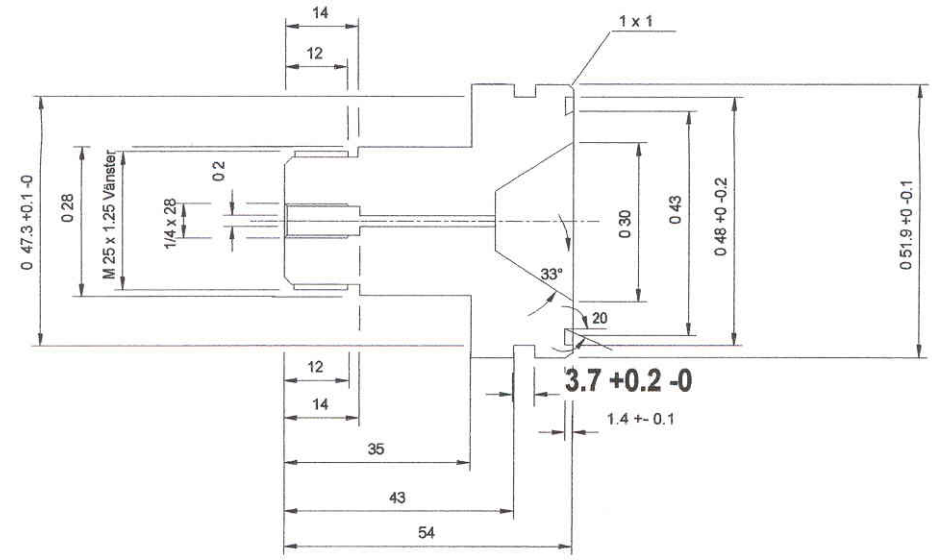

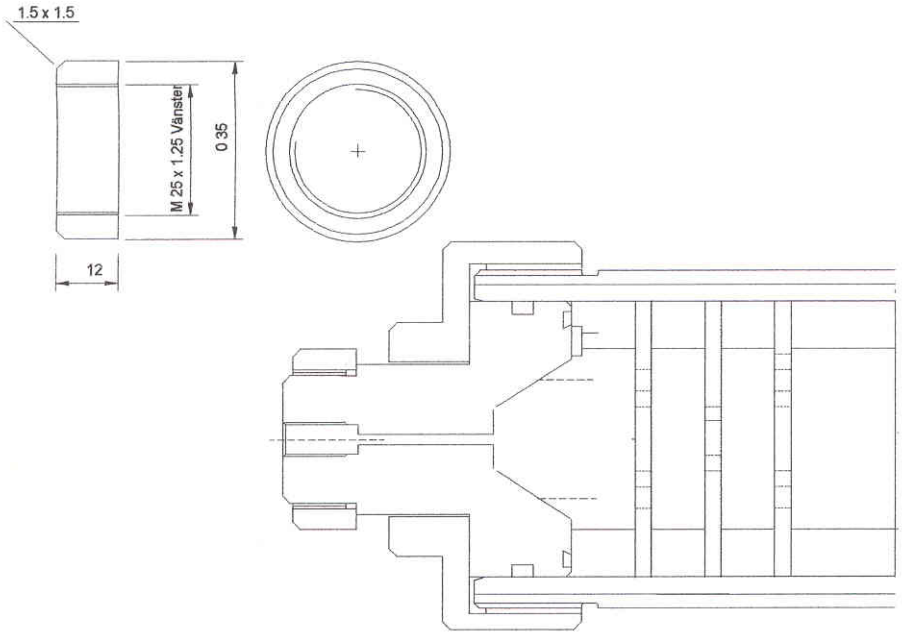

6.5 Test pile with the u-shaped lock tool for sampling (lower right) , dimensions in mm.

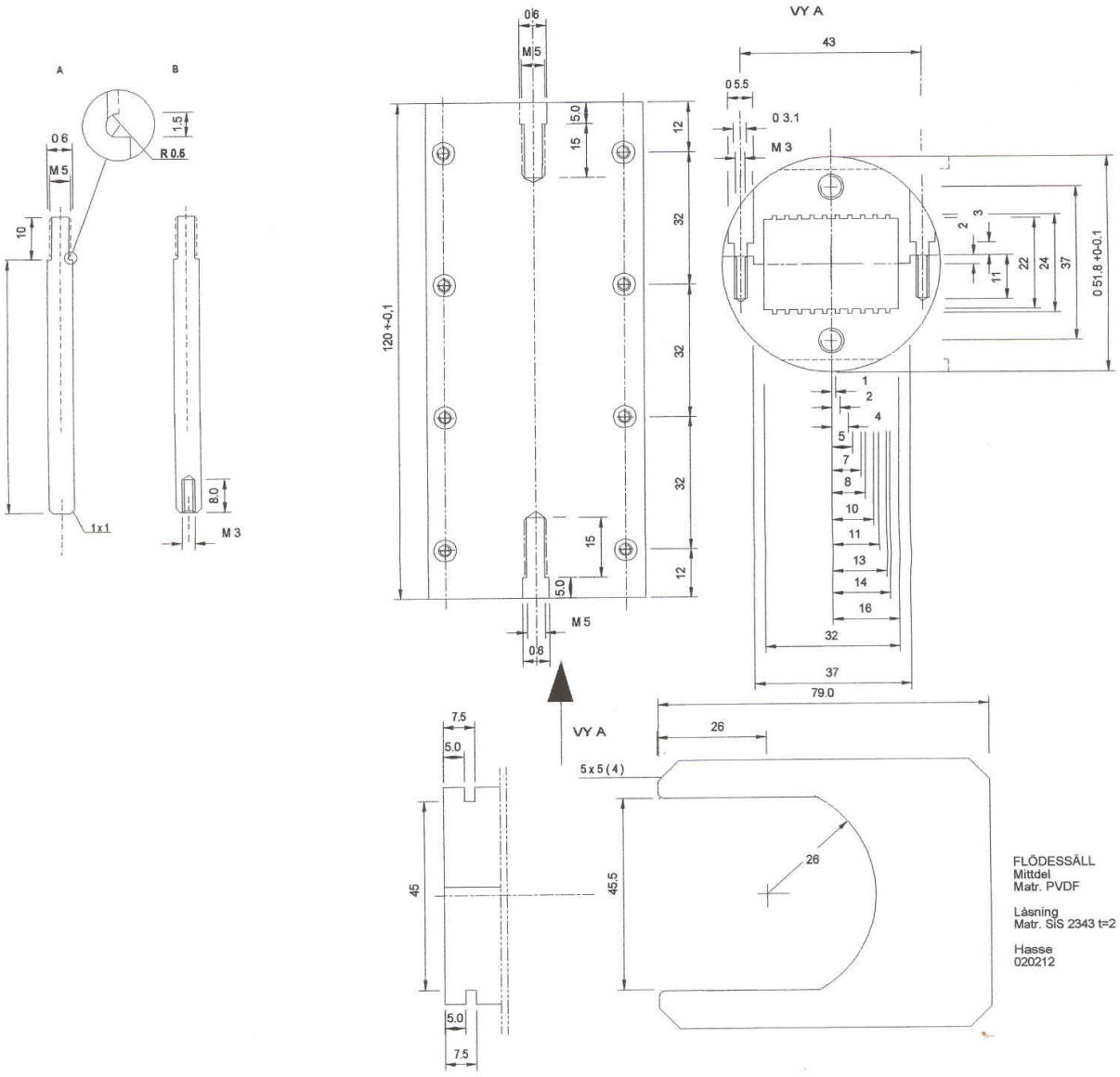

6.6 Check list for sampling cabinet flow cells at MICROBE

Materials:

Sterile Petri dishes
Formaldehyde
Forceps, must be long and thin if sampling from the lower glass level
Lift instrument
U-clamp sterilized with 99.5% vEtOH and flame, one per flow cell
99% EtOH
Small gas bottle with flame
Replacement test surfaces
Sterile gloves

1. Open bypass valve in the cabinet the circulation of which you will sample.
2. Close the valves of the flow cell (FC) to be sampled.
3. Slide out the FC cabinet holders about 15–20 cm.
4. Place a trough under the FC to be sampled.
5. Remove the PEEK tube from the top of the FC to be sampled.
6. Open top lid of FC and place face down on a sterile plastic Petri dish.
7. Sterilise the lift instrument (LI) by dipping the brass part in 99.5% EtOH and flame; let cool. Leave LI standing in a sterile Petri dish.
8. Lift up the first ring with LI and place it in a sterile Petri dish.
9. Flood the FC via the lower FC valve.
10. Lift up the FC package with LI and lock it with the sterile U-clamp, keeping the slide surfaces under water at all times. If prolonged opening is needed (more than 4–5 minutes) make extra floods.
11. Remove the diffuser package by hand while wearing sterile gloves; place the diffuser standing upright in a sterile Petri dish.
12. Use 99.5% EtOH and flame (let cool) sterilized forceps to sample test surfaces. Replace sampled surface. Take careful notes regarding which surfaces you have sampled.
13. Reverse 11 → 10 → 8 → 6 → 5 → 3 → 2 → 1.
14. Wash exterior of FCs with tap water and dry.
15. Check an extra time that all valves are in their original positions; check that all flows are running properly.
16. Take note of the flow rates, circulated volumes, and cabinet temperatures.
17. Fill in a daily log.

7 Appendix 3: Gas extractor

7.1 Schematic drawing

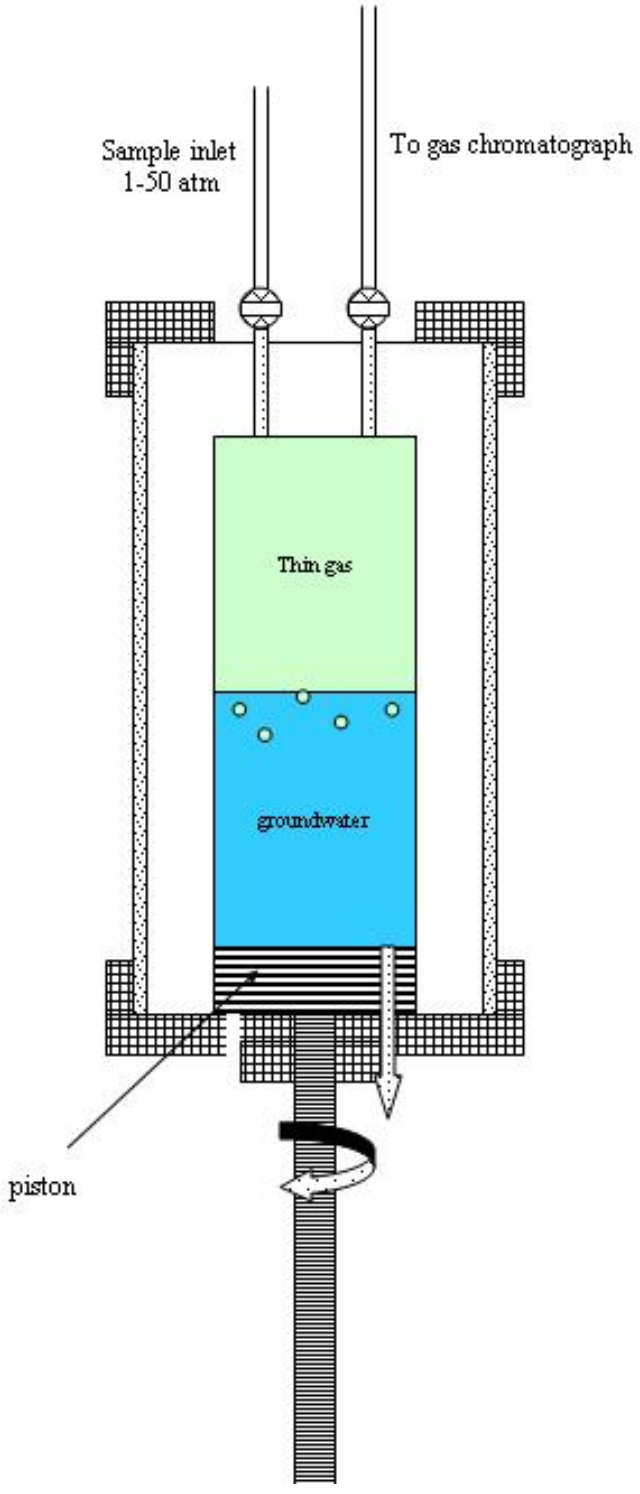

7.2 Extractor cylinder, dimensions in mm.

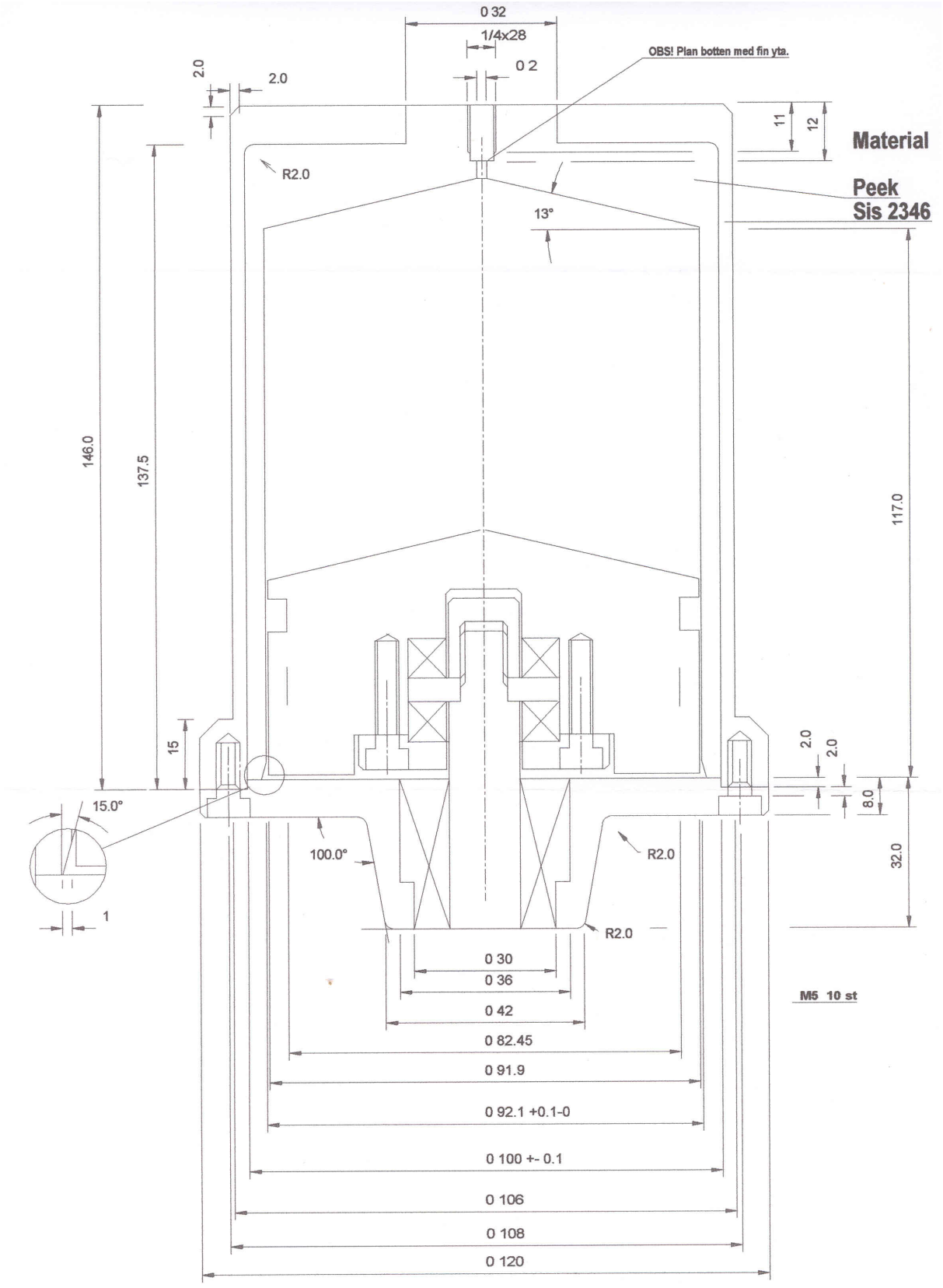

7.3 Extractor piston, dimensions in mm.

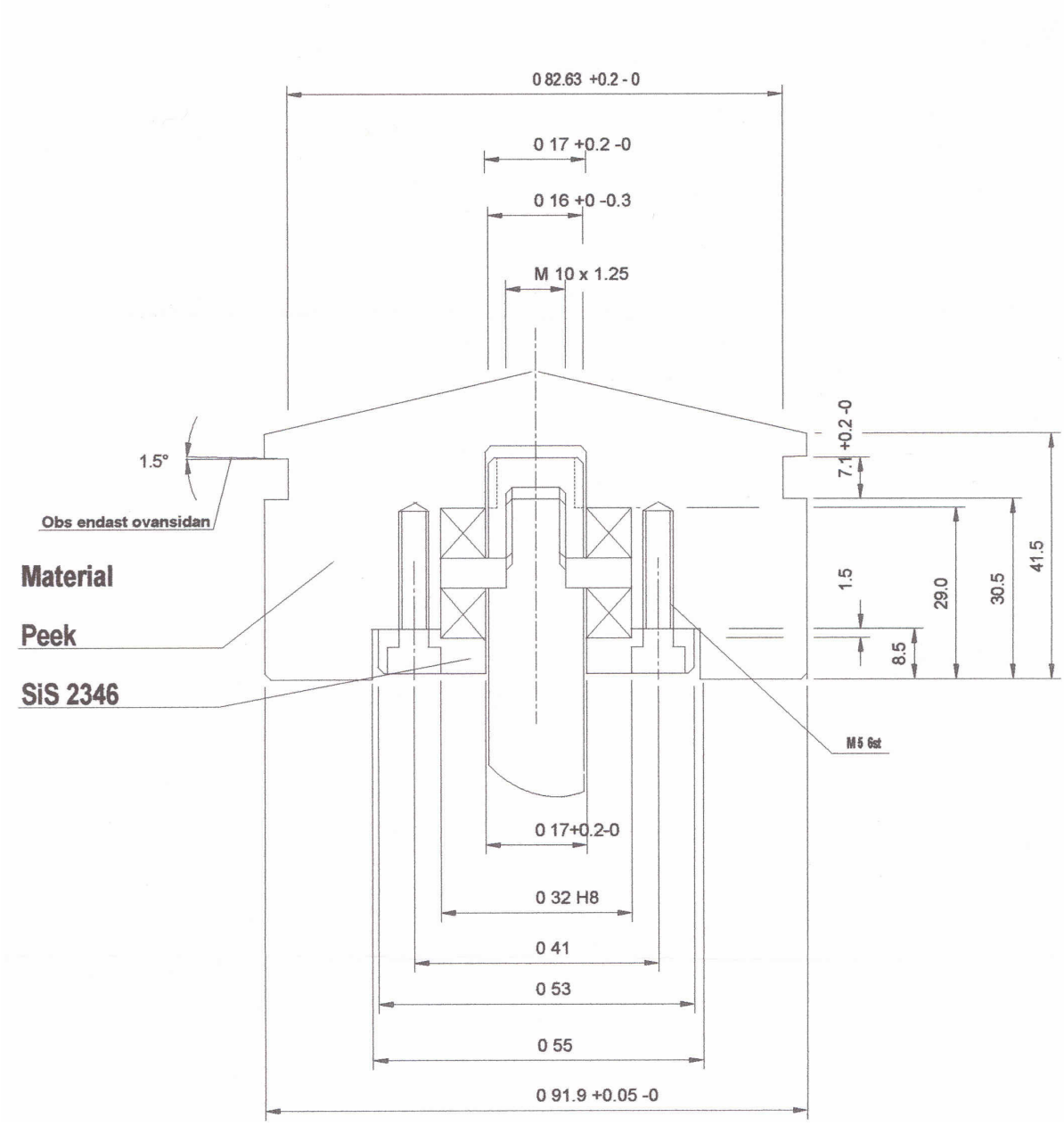

7.4 Cryo trap, CO_2 container.

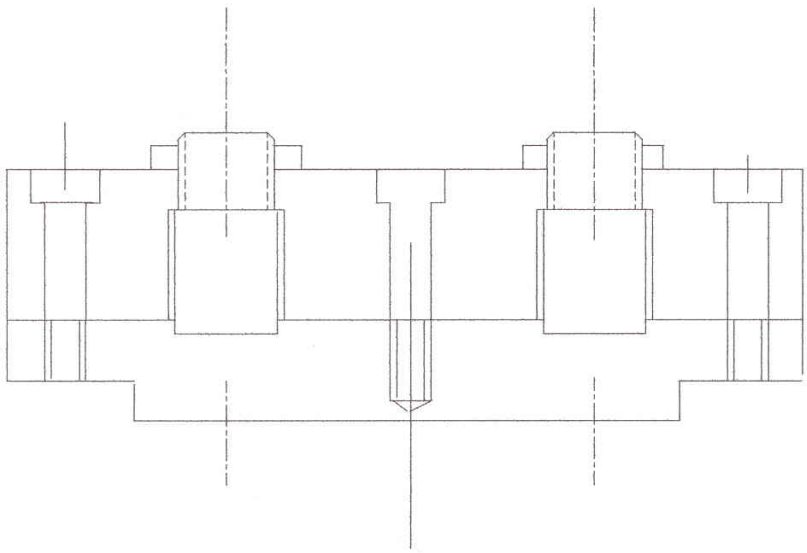

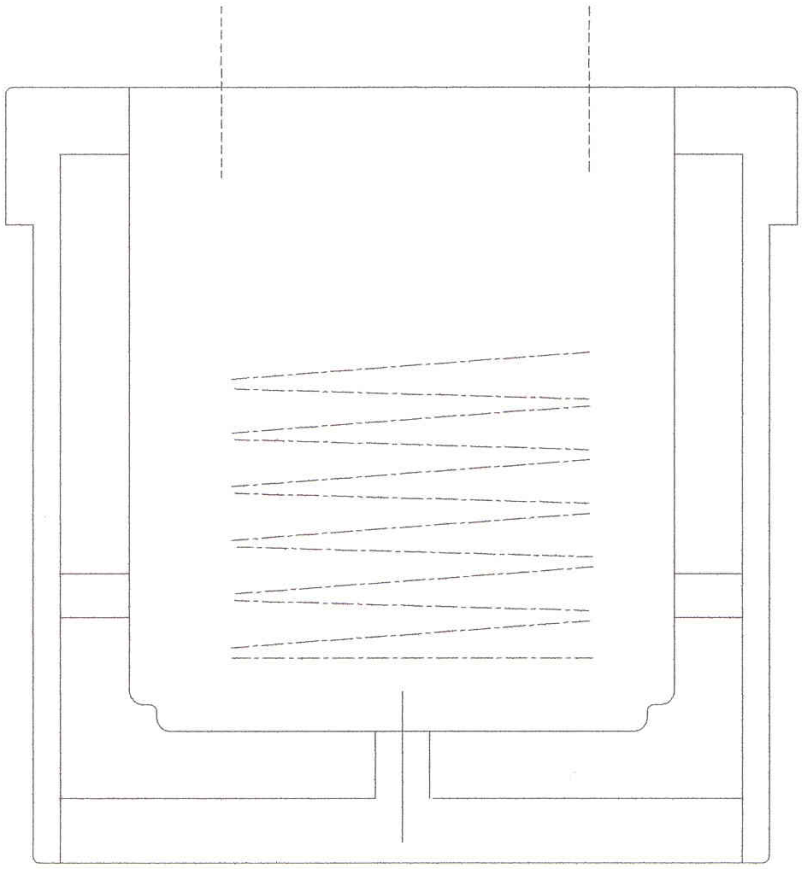

7.5 Cryo trap, lid, dimensions in mm.